CHAPTER 4 DOSIMETRY OF PARTICULATE MATTER

Overall Conclusions regarding the Dosimetry of Particulate Matter (PM)

- Our basic understanding of the mechanisms of particle deposition and clearance has not changed since the last PM ISA (U.S. EPA, 2009). However, comparisons of deposition across species have improved. Evidence in this review also better quantifies the fraction of inhaled particles reaching the lungs and particle translocation from the respiratory tract.
- Evidence included in this review shows a smaller fraction of inhaled air enters though the nose of children relative to adults. This, in combination with lower nasal particle deposition efficiency in children compared to adults, results in a greater fraction of inhaled PM reaching and potentially depositing in the lungs of children relative to adults.
- New dosimetric information shows that PM_{10} overestimates the size of particles likely to enter the human lung. New dosimetric information that improves interspecies extrapolations, quantifies the fraction of inhaled PM entering the lungs of humans and rodents.
- New information, altering a conclusion in the last PM ISA, shows that particle translocation from the olfactory mucosa via axons to the olfactory bulb may be important in humans.
- New data show translocation of gold nanoparticles from the human lung into circulation. Of deposited particles, a small fraction (0.05%) eliminated via urine is quantitively similar between humans and rodents. New rodent data show that the fraction (≤0.2% for particles 5–200 nm) of nanoparticle translocation from the lungs is particle size dependent and that gastrointestinal tract absorption of particles is a minor route into circulation.

4.1 Introduction

Particle dosimetry refers to the characterization of deposition, translocation, clearance, and retention of particles and their components within the respiratory tract and extrapulmonary tissues. This chapter summarizes basic concepts presented in dosimetry chapters of more recent PM AQCDs (U.S. EPA, 2004, 1996) and the PM ISA (U.S. EPA, 2009), and updates the state of the science based upon new literature appearing since publication of these PM assessments. Although the basic understanding of the mechanisms governing deposition and clearance of inhaled particles has not changed, there is significant additional information on the role of certain biological determinants such as sex, age, and lung disease on deposition and clearance.

Relative to the last PM ISA (U.S. EPA, 2009), extra emphasis is placed on differences between children and adults. In general, children breathe less through the nose and have less deposition in the extrathoracic airways than adults. This leads to a relatively higher concentration of PM reaching the lower airways of children than adults. Much of the literature described in this chapter supporting differences in route of breath as a function of age and sex comes from older literature that was not included in prior reviews. Additionally, substantially more particle translocation data have become available on the extent of inhaled material is detected in organs. Some studies have evaluated whether translocation is due to direct air-blood barrier translocation from the lung versus gastrointestinal uptake of particles or solubilization with subsequent movement to organs. There are also limited data on transplacental

movement of particles. Although only a small portion of insoluble particles translocate to extrapulmonary organs, their translocation can be rapid (<1 hour) and is size dependent. Translocation of particles depositing on the olfactory epithelium to the olfactory bulb is also now recognized as a potentially important route of movement to the brain for insoluble particles (<200 nm) or soluble components of any sized particle in humans as well as rodents.

The dose from inhaled particles deposited and retained in the respiratory tract is governed by a number of factors. These include exposure concentration and duration, activity and breathing conditions (e.g., nasal vs. oronasal and minute ventilation), and particle properties (e.g., particle size, hygroscopicity, and solubility in airway fluids and cellular components). The basic characteristics of particles as they relate to deposition and retention, as well as anatomical and physiological factors influencing particle deposition and retention, were discussed in depth in CHAPTER 10 of 1996 PM AQCD and updated in CHAPTER 6 of the 2004 PM AQCD. Species differences between humans and rats in particle exposures, deposition patterns, and pulmonary retention were also reviewed by Brown et al. (2005). New to this review, similarities in particle deposition among several species are provided. Other than a brief overview in this introductory section, the disposition (i.e., deposition, absorption, distribution, metabolism, and elimination) of fibers and unique nano-objects (e.g., hollow spheres, rods, fibers, tubes) is not reviewed herein (see Section P.3.1). Substantial exposures to fibers and unique nano-objects generally occur in the occupational settings rather than the ambient environment.

The deposition by interception of micro-sized fibers was briefly discussed in the 1996 and 2004 PM AQCD, but fiber retention in the respiratory tract was not addressed. Airborne fibers (length/diameter ratio ≥3), can exceed 150 μm in length and appear to be relatively stable in air. This is because their aerodynamic size is determined predominantly by their diameter, not their length. Fibers longer than 10 μm can deposit by interception and when aligned with the direction of airflow may penetrate deep into the respiratory tract. Once deposited, macrophage mediated clearance is the primary mechanism of removing micro-sized particles from the pulmonary region. The length of fibers can, however, affect their phagocytosis and clearance. For example, fibers of >17 μm in length are too long to be fully engulfed by rat alveolar macrophages and can protrude from macrophages (i.e., macrophage frustration) (Zeidler-Erdely et al., 2006). The ability of fibers, particularly small ones (<5 μm length and <0.25 μm diameter), to translocate from the lungs to the parietal pleura, liver, and kidney is reviewed by Miserocchi et al. (2008). Further discussion of the fiber disposition in the respiratory tract is beyond the scope of this chapter.

The term "ultrafine particle" has traditionally been used by the aerosol research and inhalation toxicology communities to describe airborne particles or other laboratory generated aerosols used in toxicological studies that are ≤100 nm in size (based on physical size, diffusivity, or electrical mobility). Generally consistent with the definition of an ultrafine particle (UFP), the International Organization for Standardization (ISO) define a nanoparticle as an object with all three external dimensions in the nanoscale, i.e., from approximately 1 to 100 nm (ISO, 2008). The ISO also defined a nano-object as a

material with one or more external dimensions in the nanoscale. The terms, nanoparticle and UFP, have been used rather synonymously in the toxicological literature. Within this chapter the usage of UFP or nanoparticle is restricted to particles have physical diameter or mobility diameter (the size of a sphere having the same diffusivity or movement in an electrical field as the particle of interest) less than or equal 100 nm, whereas other chapters may extend the definition to <0.30 μm (Section P.3.1 and Section 2.4.3.1).

4.1.1 Size Characterization of Inhaled Particles

Particle size is a major determinant of the fraction of inhaled particles depositing in and cleared from various regions of the respiratory tract. The distribution of particle sizes in an aerosol is typically described by the lognormal distribution (i.e., the situation in which the logarithms of particle diameter are distributed normally). The geometric mean is the median of the distribution, and the variability around the median is the geometric standard deviation (GSD or σ_g).

The particle size associated with any percentile of the distribution, d_i, is given by:

$$d_i = d_{50\%}\,\sigma_g^{z(P)}$$

Equation 4-1

where: z(P) is the normal standard deviate for a given probability. In most cases, the aerosols to which people are naturally exposed are polydisperse. By contrast, most experimental studies of particle deposition and clearance in the lung use monodisperse particles (GSD <1.15). Ambient aerosols may also be composed of multiple size modes, each mode should be described by its specific median diameter and GSD.

Aerosol size distributions may be measured and described in various ways. When a distribution is described by counting particles, the median is called the count median diameter (CMD). On the other hand, the median of a distribution based on particle mass in an aerosol is the mass median diameter (MMD). Impaction and sedimentation of particles in the respiratory tract depend on a particle's aerodynamic diameter (d_{ae}), which is the size of a sphere of unit density that has the same terminal settling velocity as the particle of interest. The size distribution is frequently described in terms of d_{ae} as the mass median aerodynamic diameter (MMAD), which is the median of the distribution of mass with respect to aerodynamic equivalent diameter. Alternative descriptions should be used for particles with actual physical sizes below ≈0.5 μm because, for those sized particles, aerodynamic properties become less important and diffusion becomes ever more important. For these smaller particles, their physical diameter or CMD are typically used since diffusivity is not a function of particle density. For small irregular shaped particles and aggregates, the diameter of a spherical particle that has the same diffusion coefficient in air as the particle in question is appropriate, i.e., a thermodynamic diameter. Unless stated otherwise, all particle diameters in the text of this chapter that are ≥0.5 μm are aerodynamic diameters.

All particle diameters ≤0.1 μm are a thermodynamic diameter. A few studies provide UFP deposition data and continue to monitor deposition to diameters of 0.2 to 0.3 μm. Those larger 0.2 to 0.3 μm particles should be assumed to be thermodynamic diameters. Within this chapter, plots of predicted particle deposition with particles between 0.1 and 0.5 μm were simulated assuming unit density spheres so that the physical, thermodynamic, and aerodynamic diameters are the same.

A number of papers have become available that assess the deposition and translocation of very small nanoparticles below 10 nm in diameter (see Section 4.3.3). Calculation of particle surface area for micron sized particles have are general calculated as πd^2. Specific surface area (i.e., normalized to particle mass) is $6/(\rho d)$, where ρ is particle density. However, when particle diameter is below 10 nm, this means of estimating surface area become imprecise. Below 10 nm, it becomes necessary to consider the angularity of the surface in particles consisting of a small number of atoms (Janz et al., 2010). It is also interesting to consider the number of atoms in some of the newer nanoparticle literature. For instance, considering gold nanoparticles, a 1.2 nm particles contain 35 gold atoms, a 1.4 nm particle has 55 gold atoms, and a 1.8 nm particle has 150 gold atoms (Pan et al., 2007).

4.1.2 Structure and Function of the Respiratory Tract

4.1.2.1 Anatomy

The basic structure of the human respiratory tract is illustrated in Figure 4-1. In the literature, the terms extrathoracic (ET) region and upper airways or upper respiratory tract are used synonymously. The terms lower airways and lower respiratory tract are used to refer to the thoracic airways, i.e., the combination of the tracheobronchial (TB) region which is the conducting airways and the alveolar region which is the functional part or parenchyma of the lung. A review of interspecies similarities and differences in the structure and function of the respiratory tract is provided by Phalen et al. (2008). Although the structure varies, the illustrated anatomic regions are common to all mammalian species with the exception of the respiratory bronchioles. Respiratory bronchioles, the transition region between ciliated and fully alveolated airways (i.e., alveolar ducts and sacs), are found in humans, dogs, ferrets, cats, goats, and monkeys (Phalen et al., 2008; Phalen and Oldham, 1983). Respiratory bronchioles are absent in rats and mice and abbreviated in hamsters, guinea pigs, rabbits, oxen, sheep, and pigs (Phalen et al., 2008; Phalen and Oldham, 1983). The branching structure of the ciliated bronchi and bronchioles also differs between species from being a rather symmetric and dichotomous branching network of airways in humans to a more monopodial branching network in other mammals including monkeys.

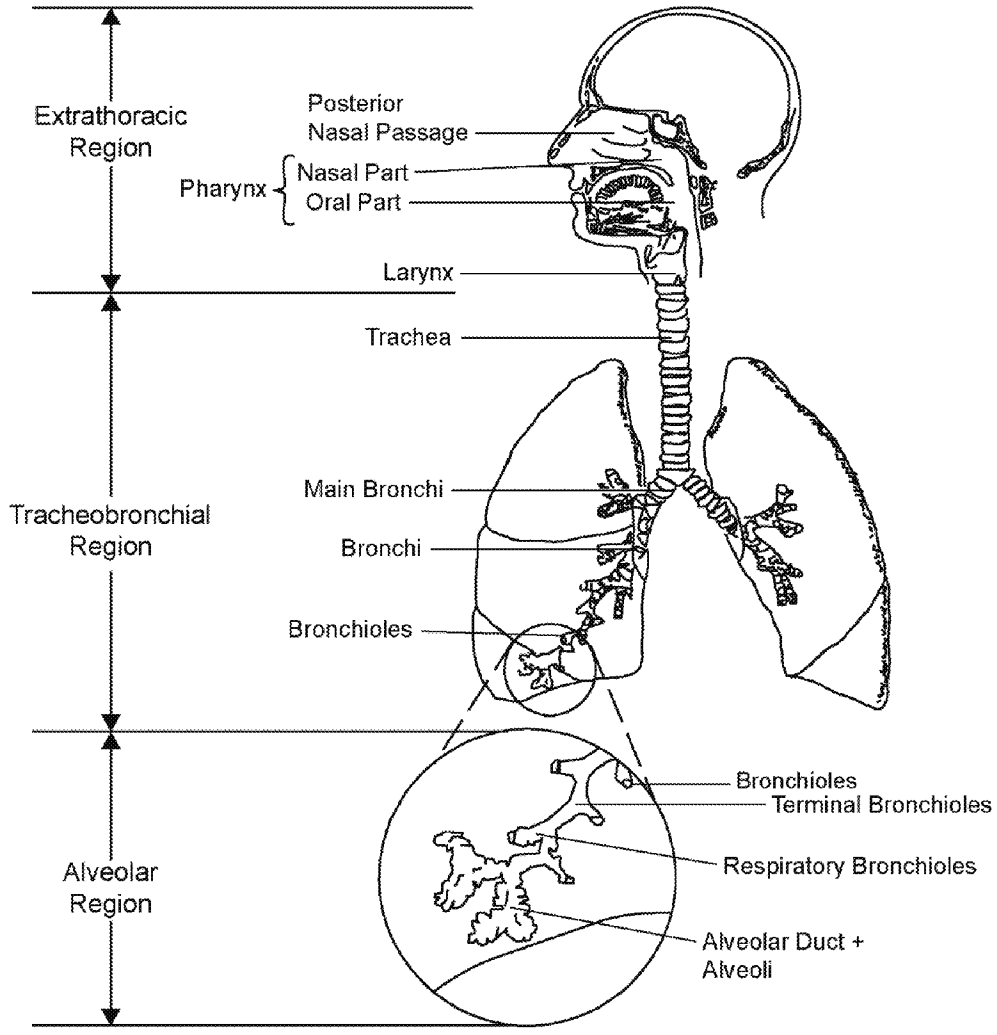

Source: Permission pending, Based on ICRP (1994) and U.S. EPA (1996).

Figure 4-1. Diagrammatic representation of human respiratory tract regions.

The development of the lung is not complete at birth. Prior to the work of Dunnill (1962), there were two competing opinions as to whether the lung was: (1) fully developed at birth and simply increased in volume by increasing dimensions of the airways and alveoli or (2) increased in volume by the creation of new units (alveoli and alveolar sacs) within the distal lung. Based on postmortem morphometric analysis of 20 lungs from 10 children, Dunnill (1962) concluded there was continued creation of new alveolar sacs and alveoli from birth to 8 years of age. This conclusion, in part, was based on the observation that the number of alveoli in the 8-year-old child was close to that observed in an adult male. After about 8 years of age, the continued increase in lung volume was presumed due to increased airway and alveolar dimensions. In a larger study 36 boys and 20 girls ranging from 6 weeks to 14 years of age, Thurlbeck (1982) concluded that the creation of new alveoli continued until at least 2 years of age,

but that there is considerable variability in the number of alveoli among individuals and a considerably larger number of alveoli than observed by Dunnill (1962). This variability and larger number of alveoli lead Thurlbeck (1982) to question whether the lungs of 8 year old child in the Dunnill (1962) study would have continued to grow with creation of additional alveoli. Although it was clear from these studies that new alveoli were created in humans postnatally, it was unclear when this process ceased.

Recent work shows postnatal creation of alveoli into young adulthood occurs in multiple mammalian species. The prenatal and postnatal creation of alveoli is synonymously termed alveogenesis, alveologenesis, and alveolarization in the literature (Bourbon et al., 2005). Lewin and Hurtt (2017) review six stages of lung development (i.e., embryonic, pseudoglandular, canlicular, saccular, alveolar, and microvascular maturation) across several mammalian species as well as some aspects of immune function development and some causes of impaired lung development. Here, a few points related to the structural development of the lung are noted based largely on Lewin and Hurtt (2017). The canlicular stage is completed about 25 gestational weeks in humans and is marked by the completion of tracheobronchial airways branching structure. Alveolar cells become identifiable during the saccular stage at about 24 weeks in human fetus and about 19 days in rat fetus. Subsequently, terminal bronchioles end in sac-like structures. Rats and mice are born at this stage of respiratory development, whereas alveolarization begins prenatally with 10–20% of adult alveoli found at birth in humans, rabbits, and sheep. Rapid alveolarization occurs during the first 3 weeks of life in rats and first 2–3 years in humans (Herring et al., 2014). Following the period of rapid alveolarization there is evidence for a more gradual increase that may occur to until young adulthood for multiple species including rodents, dogs, monkeys, and humans (Lewin and Hurtt, 2017; Herring et al., 2014; Narayanan et al., 2012; Hyde et al., 2007). This is consistent with the period of increasing in lung volume in humans with age (and height) until around 18 years of age in females and 20 years of age in males (Hankinson et al., 1999).

4.1.2.2 Breathing Rates

Some general species information relevant to particle dosimetry (e.g., breathing parameters and respiratory surface areas) is provided in Table 4-1. The data in this table are for gross comparison among resting adults since specific strains are not individually characterized nor are changes with animal age characterized. Additional data for rats on respiratory tract volumes and breathing rates as a function of animal weight are available from Miller et al. (2014). Across species, ventilation rates increase with increases in activity. Within species, there are also differences among strains in breathing patterns and rates. Furthermore, stress due to experimental protocols may alter breathing patterns differentially among species. In rats, Mauderly and Kritchevsky (1979) reported restraint to cause increased breathing frequency (f) and decreased tidal volume (V_T), while minimally affecting overall minute ventilation. In mice, Mendez et al. (2010) reported restrained animals to have approximately 2.4 times the minute ventilation of unrestrained animals (27 and 64 mL/min, respectively). Most of this increase in minute ventilation came from a doubling of f from 145 min^{-1} to 290 min^{-1}. However, in a study of four mouse

strains, DeLorme and Moss (2002) consistently observed decreased breathing frequency and minute ventilation in restrained mice (f, 335 min^{-1}; minute ventilation, 70 mL/min) relative to unrestrained mice (f, 520 min^{-1}; minute ventilation, 120 mL/min). These findings are consistent with Alessandrini et al. (2008), who reported a breathing frequency of 500 min^{-1} and minute ventilation of 106 mL/min in unrestrained mice. Thus, even within one species there can be large differences in breathing conditions between studies. Breathing patterns and minute ventilation must both be considered to accurately assess particle deposition fractions and dose rates.

Table 4-1. Typical respiratory parameters and body weights among animals and humans.

Species	Breathing Frequency min^{-1}	Tidal Volume mL	Minute Ventilation mL/min	Functional Residual Capacity mL	Alveolar surface Area m^2	Body Weight kg
Mouse (restrained)	290[a]	0.22[a]	64[a]	0.5[e]	0.05[f]	0.02[f]
Mouse (unrestrained)	145[a]	0.19[a]	27[a]	0.5[e]	0.05[f]	0.02[f]
Rat	102[b]	2.1[b]	214[b]	3.5[e]	0.4[f]	0.4[f]
Dog	22[c]	175[c]	3,600[c]	500[c]	52[f]	16[f]
Human (male)	12[d]	625[d]	7,500[d]	3,300[d]	140[d]	73[d]
Human (female)	12[d]	444[d]	5,330[d]	2,700[d]	100[g]	60[d]

[a]Mendez et al. (2010).
[b]de Winter-Sorkina and Cassee (2002).
[c]Mauderly (1979).
[d]ICRP (1994).
[e]Takezawa et al. (1980), anesthetized animals.
[f]Stone et al. (1992).
[g]Alveolar surface area of male scaled by ratio of total lung capacity, i.e., 4.97 ÷ 6.98.

Table 4-1 shows considerable variation among species in adults. The effect of activity on ventilation rates is discussed in Section 4.2.4.1 in relation to the effect of activity in adults on particle deposition. Minute ventilation changes with age and growth [for humans see U.S. EPA (2011)]. Breathing patterns of humans are well recognized to change with increasing age, i.e., V_T increase and respiratory rates decrease (Tobin et al., 1983a; Tabachnik et al., 1981). Some guidance for humans with regard to changing breathing patterns with age and activity are provided by ICRP (1994). Recent data show median f decreases linearly from 44 min^{-1} in infants to 30 min^{-1} at 2 years of age and linearly from 22 min^{-1} at 6 years to 15.5 min^{-1} at 18 years (Fleming et al., 2011). Allometric scaling can be used to adjust breathing

patterns of immature animals as a function body weight (BW, kg). Breathing frequency (min^{-1}) from Piccione et al. (2005) is $82*BW^{-0.287}$ and aligns well with breathing frequency for rats, but for mice provides a value between that of restrained and unrestrained animals. Minute ventilation (L/min) from Bide et al. (2000) is $0.499*BW^{0.809}$ and aligns well with minute ventilation for rats, but for mice provides a value lower than that of unrestrained animals. Allometric predictions for mice can be scaled (observed ÷ predicted value) to match those of adults in Table 4-1 and tidal volume may be estimated as minute ventilation divided by breathing frequency.

The ICRP indicated a 3-month-old infant might be expected to breathe with a minute ventilation of 1.5 L/min (V_T, 39 mL; *f*, 38 min^{-1}) at rest/sleep and 3.2 L/min (V_T, 66 mL; *f*, 48 min^{-1}) during light activity/exercise. Some more recent data suggest higher respiratory rates for 3-month-olds with a median *f* of 42 min^{-1} with 10th to 90th percentiles of 34 and 56 min^{-1}, respectively (Fleming et al., 2011). For their in vitro investigation of nasal versus oral particle penetration into the lower respiratory tract, Amirav et al. (2014) used minute ventilations of 2.0 and 3.2 L/min (50 and 80 mL V_T at 40 min^{-1}) for 5month-olds as well as for 14-month-olds and minute ventilations of 2.4 and 3.6 L/min (80 and 120 mL V_T at 30 min^{-1}) for 20-month-olds based on the recent literature. Normalized to body mass, median daily ventilation rates (m^3/kg-day) decrease over the course of life (Brochu et al., 2011). This decrease in ventilation relative to body mass is rapid and nearly linear from infancy through early adulthood. Relative to normal-weight male and female adults (25−45 years of age; 0.271 m^3/kg-day), ventilation rates normalized to body mass are increased 1.5 times in normal-weight children (7−10 years of age; 0.402 m^3/kg-day) and doubled in normal-weight infants (0.22−0.5 years of age; 0.538 m^3/kg-day).

4.1.2.3 Epithelial Lining Fluid

The site of particle deposition within the respiratory tract has implications related to lung retention and surface dose of particles as well as potential systemic distribution of particles or solubilized components. There are progressive changes in airway anatomy with distal progression into the lower respiratory tract. In the bronchi there is a thick liquid lining and mucociliary clearance rapidly moves deposited particles toward the mouth. In general, in the bronchi, only highly soluble materials moving from the air into the liquid layer will have systemic access via the blood. With distal progression, the protective liquid lining diminishes and mucus clearance rates slow. Soluble compounds and some poorly soluble UFPs may potentially cross the air-liquid interface to enter the tissues and the blood, especially in the alveolar region.

The epithelial lining fluid (ELF) over most of the tracheobronchial region may generally be described as consisting of two layers: an upper mucus layer and a periciliary layer, which surrounds the cilia (Button et al., 2012; Widdicombe, 2002; Widdicombe and Widdicombe, 1995; Van As, 1977). The length of motile human cilia is about 7 μm in the distal nasal airways, trachea, and bronchi and around 5 μm in the bronchioles (Yaghi et al., 2012; Song et al., 2009; Clary-Meinesz et al., 1997; Widdicombe

and Widdicombe, 1995). In the healthy lung, the thickness of the periciliary layer is roughly the length of the cilia (Song et al., 2009; Widdicombe and Widdicombe, 1995). This periciliary layer forms a continuous liquid lining over the tracheobronchial airways; whereas the upper mucus layer is discontinuous and diminishes or is absent in smaller bronchioles (Widdicombe, 2002; Van As, 1977). The periciliary layer may be the only ELF layer (i.e., there is little to no overlaying mucus) in the ciliated airways of infants and healthy adults who are unaffected by pathology related to disease, infection, or other stimuli (Bhaskar et al., 1985).

The ELF covering the alveolar surface is considerably thinner than the periciliary layer found in the tracheobronchial region. The alveolar ELF consists of two layers: an upper surfactant layer and a subphase fluid (Ng et al., 2004). Bastacky et al. (1995) conducted a low temperature scanning electron microscopy analysis of rapidly frozen samples (9 animals; 9,339 measurements) of rat lungs inflated to approximately 80% total lung capacity. The alveolar ELF was found to be continuous, but of varied depth. Three distinct ELF areas were described: (1) a thin layer (0.1 μm median depth, GSD ~ 2.16; GSDs were calculated from 25th, 50th, and 75th percentiles of the distributions) over relatively flat areas and comprising 80% of the alveolar surface, (2) a slightly thinner layer (0.08 μm, GSD ~ 1.79) over protruding features and accounting for 10% of the surface, and (3) a thick layer (0.66 μm, GSD ~ 2.18) occurring at alveolar junctions and accounting for 10% of the surface. Based on these distributions of thicknesses, 10% of the alveolar region is covered by an ELF layer of 0.04 μm or less. Presuming that these depths would also occur in humans at 80% total lung capacity and assuming isotropic expansion and contraction, depths should be expected to be 20–40% greater during normal tidal breathing (rest and light exercise) when the lung is inflated to between 50–60% total lung capacity averaged across the respiratory cycle. During tidal breathing, a median ELF depth of 0.12–0.14 μm would be expected over 80% of the alveolar surface with 10% of the alveolar surface having a median depth of around 0.05 μm or less. Considering the entire distribution of depths during tidal breathing, about 30, 60, and 90% of the alveolar surface would be estimated to have a lining layer thickness of less than or equal to 0.1, 0.2, and 0.5 μm, respectively.

4.1.3 Route of Breathing

As humans, we breathe oronasally, i.e., through both our nose and mouth. In general, we breathe through our nose when at rest and increasingly through the mouth with increasing activity level. Few people breathe solely through their mouth. In contrast to humans, rodents are obligate nose breathers. Brown et al. (2013) found that the penetration of particles greater than 1 μm into the lower respiratory tract of humans was more affected by route of breathing than age, sex, activity level, or breathing pattern (i.e., V_T and f). This section describes how route of breathing, also referred to as "respiratory mode" or "breathing habit" in the literature, is affected by age, sex, activity level, and upper respiratory tract anomalies. Based on literature that is decades old but that has not been included in prior PM ISA or

AQCDs, this section will show that children breathe more though the mouth than adults and that across all ages, males breathe more through their mouth than females.

One of the more commonly referenced studies in dosimetric papers is Niinimaa et al. (1981). This paper is referenced in all prior PM reviews back to 1982 PM AQCD (U.S. EPA, 1982) as the primary data source on route of breathing. Niinimaa et al. (1981) examined route of breathing in a group of healthy individuals (15–35 years of age; 14 M, 21.6 ± 3.8 years; 16 F, 22.9 ± 5.4 years) recruited via advertisements posted on the University of Toronto campus. The investigators found that most individuals, 87% (26 of 30) in the study, breathed through their nose until an activity level was reached where they switched to oronasal breathing. Thirteen percent (4 of 30) of the subjects, however, were oronasal breathers even at rest. These two subject groups (i.e., the 87 and 13% of subjects) are commonly referred to in the literature [e.g., ICRP (1994)] as "normal augmenters" and "mouth breathers," respectively. More recently, Bennett et al. (2003) reported a more gradual increase in oronasal breathing with males (n = 11; 22 ± 4 years) tending to have a greater oral contribution than females (n = 11; 22 ± 2 years) at rest (87 vs. 100% nasal, respectively) and during exercise (45 vs. 63% nasal at 60% maximum workload, respectively).

Consistent with this trend for women to have a greater nasal contribution (Bennett et al., 2003), in a large study of children (63 M, 57 F; 4–19 years), Leiberman et al. (1990) reported a statistically greater nasal fraction during inspiration in girls relative to boys (77 and 62%, respectively; $p = 0.03$) and a marginally significant difference during expiration (78 and 66%, respectively; $p = 0.052$). Another large study (88 M, 109 F; 5–73 years) also reported females as having a significantly greater fraction of nasal breathing than males (Vig and Zajac, 1993). This effect was largest in children (5–12 years) with an inspiratory nasal fraction of 66% in males and 86% in females during resting breathing. This study also reported that the partitioning between the nose and mouth was almost identical between inspiration and expiration. In children and adults, sex explains some interindividual variability in route of breathing with females breathing more through the nose than males.

A few studies have attempted to measure oronasal breathing in children as compared to adults (Bennett et al., 2008; Becquemin et al., 1999; James et al., 1997; Vig and Zajac, 1993). James et al. (1997) found that children (n = 10; 7–16 years) displayed more variability than older age groups (n = 27; 17–72 years) with respect to their oronasal pattern of breathing with exercise. Becquemin et al. (1999) found that children (n = 10; 8–16 years) tended to display more oral breathing both at rest and during exercise than adults (n = 10; 27–56 years). The highest oral fractions were also found in the youngest children. Similarly, Bennett et al. (2008) reported children (n = 12; 6–10 years) tended to have a greater oral contribution than adults (n = 11; 18–27 years) at rest (68 vs. 88% nasal, respectively) and during exercise (47 vs. 59% nasal at 40% maximum workload, respectively). Vig and Zajac (1993) reported a statistically significant effect of age on route of breathing which was most apparent in males with the fraction of nasal breathing increasing from 67% in children (5–12-year-olds) to 82% in teens (13–19-year-olds), and 86% in adults (20–73 years). Females had a nasal fraction of 86% in children and

teens and 93% in adults. Based on these studies, the nasal fraction appears to increase with age until adulthood.

Several large studies have reported an inverse correlation ($r = -0.3$ to -0.6) between nasal resistance and nasal breathing fraction (Vig and Zajac, 1993; Leiberman et al., 1990; Leiter and Baker, 1989). However, neither pharmaceutical constriction nor dilation of the nasal passages affected the nasal fraction (Leiberman et al., 1990; Leiter and Baker, 1989). Nasal resistance decreases with age and is lower in females than males (Vig and Zajac, 1993; Becquemin et al., 1991). These differences in nasal resistance may account for larger nasal fractions in adults than children and females than males. Smaller studies (n = 37) have not found a significant correlation between nasal resistance and nasal fraction but have noted that those having high resistance breathe less through the nose (James et al., 1997). Bennett et al. (2003) reported a tendency for lower nasal resistance in African-American blacks (5 M,6 F; 22 ± 4 years) relative to Caucasians (6 M, 5 F; 22 ± 3 years). The nasal fraction in blacks tended to be greater at rest and 40% maximum workload and achieved statistical significance relative to Caucasians at 20 and 60% maximum workload. Leiter and Baker (1989) reported that of the 15 mouth-breathing children as identified by a dentist, pediatrician, or otolaryngologist in their study, the three having greatest nasal resistance breathed 100% through the mouth. These investigators also reported that the nasal fraction was negatively correlated ($p \leq 0.004$) with nasal resistance during both inspiration and expiration. However, the correlation appears driven by the three individuals with 100% mouth breathing. In a study of 102 children (evenly divided by sex) aged 6 to 14 years, Warren et al. (1990) reported that both nasal cross-sectional area and the fraction of nasal breath both increased with age, but did not report the association between these parameters or assess the effect of sex. The average nasal breathing fraction increased linearly from about 47% at 6 years of age to 86% at 14 years of age. Overall, breathing habit appears related to nasal resistance, which may explain some of the effects of age and sex on breathing habit.

Diseases affecting nasal resistance may also affect breathing route. Chadha et al. (1987) found that the majority (11 of 12) of patients with asthma or allergic rhinitis breathe oronasally even at rest. James et al. (1997) also reported the subjects (n = 37; 7–72 years) having hay fever, sinus disease, or recent upper respiratory tract symptoms tended to the have a greater oral contribution relative to those absent upper respiratory tract symptoms. James et al. (1997) additionally observed that two subjects (5.4%) breathed solely through the mouth but provided no other characteristics of these individuals. Greater oral breathing may occur due to upper respiratory tract infection and inflammation.

Some studies of children suggest obesity also affects breathing habit. Using MRI, Schwab et al. (2015) examined anatomic risk factors of obstructive sleep apnea in children (n = 49 obese with sleep apnea, 38 obese control, 50 lean controls; 11–16 years of age). In obese children with sleep apnea, adenoid size was increased relative to both obese and lean controls not having sleep apnea. The size of the adenoid was also increased in male obese controls (n = 24) relative to male lean controls (n = 35), whereas adenoid size was similar between female obese controls (n = 14) and female lean controls

(n = 15). Both nasopharyngeal cross-sectional area and minimum area were similar between lean and obese controls, but decreased in obese children with obstructive sleep apnea. In a longitudinal study of children (n = 47 F, 35 M) assessed annually from 9 to 13 years of age, Crouse et al. (1999) found nasal cross-section was minimal at 10 years of age. The authors speculated this may be due to prepubertal enlargement of the adenoids. In a 5 year longitudinal study of children (n = 17 M, 9 F) following adenoidectomy, Kerr et al. (1989) reported a change in mode of breathing from oral to nasal. These studies suggest the obese children, especially boys, may have increased oral breathing relative to normal weight children.

In summary, breathing habit is affected by age, sex, nasal resistance, and possibly obesity. Numerous studies show children to inhale a larger fraction of air through their mouth than adults. Across all ages, males also inhale a larger fraction of air through their mouth than females. Other factors that increase nasal resistance such as allergies or acute upper respiratory infections can also increase the fraction of oral breathing. Obesity, especially in boys, may also contribute to increased nasal resistance and an increased oral fraction of breathing relative to normal weight children.

4.1.4 Ventilation Distribution

Ventilation distribution refers to how an inhaled breath becomes divided in the lung. Ventilation distribution affects the partitioning or mass transport of inhaled aerosols between lung regions and the residence time within these regions. The effects of ventilation distribution on particle deposition are discussed in Section 4.2.4.6. In large mammals such as humans, there is a gravity induced gradient which causes the volume of alveoli in dependent lung regions (i.e., the lowest areas in the lungs) to be smaller than those in nondependent lung regions. During normal tidal breathing, dependent regions may have somewhat increased ventilation relative to nondependent regions. As a breath is distributed, so too may be associated airborne particles. Some experimental data are available on the association between regional deposition of ultrafine, fine, and coarse particles and regional ventilation in the healthy and diseased lung. Ventilatory inhomogeneity due to obstructive disease generally exceeds normal gravity induced gradients.

The distribution of ventilation has been studied in a number of animal species. There is a pronounced gravitation gradient in the ventilation distribution of standing horses with the dependent (ventral) regions receiving more of each breath than the nondependent (dorsal) regions (Amis et al., 1984). In standing Shetland ponies, late-term pregnancy has been reported to increase ventilation to the nondependent regions possibly due to intra-abdominal pressure on the dependent (ventral) regions (Schramel et al., 2012). In contrast to horses, data out to 20 days postpartum showed equal ventral-dorsal ventilation in these ponies. In the supine position, dogs and sloths show increased ventilation of the dependent (dorsal) regions relative to the nondependent (ventral) regions (Hoffman and Ritman, 1985). However, in the prone position there is essentially uniform ventral-dorsal ventilation in both the dogs and sloths. Thus, the position in which rats are exposed may influence the regional delivery and deposition of

inhaled aerosols. In rats, the nondependent region of the lung has been reported to be better ventilated, whether positioned supine, prone, or on either side (Dunster et al., 2012; Rooney et al., 2009). In humans, ventilation patterns are affected by both body position and lung inflation.

Milic-Emili et al. (1966) showed apical (nondependent) to basal (dependent) differences in pleural pressure can affect ventilation distribution in healthy individuals. In upright humans, the apical lung receives the majority of an inhaled air at low lung volumes (less than 20% vital capacity). Above this volume, the vertical proportioning of ventilation is relatively constant across a breath with basal regions (dependent part) having somewhat increased ventilation relative to apical regions (Milic-Emili et al., 1966). The effect of gravity is shifted by changes in body position. For instance, while lying on the left side, aerosols inhaled at low lung volumes will be preferentially transported into and deposited in the right lung (Bennett et al., 2002). In upright individuals at high lung volumes (70% or more of total lung capacity), particles are transported preferentially into and deposit in the left lung (Bennett et al., 2002). A more uniform left-right distribution of particle deposition is observed for inhalations closer to functional residual capacity (FRC). Left-right asymmetry in particle deposition at high lung volumes is primarily due to differences in ventilation between the lungs (Möller et al., 2009). The effect of gravity-induced gradients on ventilation and left-right asymmetry in upright individuals described here for healthy individuals, however, are small relative to the ventilatory heterogeneity caused by obstructive lung disease (Suga et al., 1995).

4.1.5 Particle Inhalability

In order to potentially become deposited in the respiratory tract, particles must first be inhaled. The inspirable particulate mass fraction of an aerosol is that fraction of the ambient airborne particles that can enter the uppermost respiratory tract compartment, the head (Soderholm, 1985). The American Conference of Governmental Industrial Hygienists (ACGIH) and the International Commission on Radiological Protection (ICRP) have established inhalability criteria for humans (ACGIH, 2005; ICRP, 1994). These criteria are indifferent to route of breathing and assume random orientation with respect to wind direction. They are based on experimental inhalability data for $d_{ae} \leq 100$ μm at wind speeds of between 1 and 8 m/s. For the ACGIH criterion, inhalability is 97% for 1 μm particles, 87% for 5 μm, 77% for 10 μm, and plateaus at 50% for particles above ~40 μm. The ICRP criterion, which also plateaus at 50% for very large d_{ae}, does not become of real importance until 5 μm where inhalability is 97%. Dai et al. (2006) reported slightly lower nasal particle inhalability in humans during moderate exercise than rest (e.g., 89.2 vs. 98.1% for 13 μm particles, respectively). Nasal particle inhalability is similar between an adult and 7-year old child (Hsu and Swift, 1999). Inhalability into the mouth from calm air in humans also becomes important for d_{ae} >10 μm (Anthony and Flynn, 2006; Brown, 2005). Unlike the inhalability from high wind speeds which plateaus at 50% for d_{ae} greater than ~40 μm, particle inhalability from calm air continues to decrease toward zero with increasing d_{ae} and is affected by route of breathing.

Inhalability data in laboratory animals, such as rats, are only available for breathing from relatively calm air (velocity ≤ 0.3 m/s). For nasal breathing, inhalability becomes an important consideration for particles larger than 1 μm in rodents and 10 μm in humans (Ménache et al., 1995). The inhalability of particles of 2.5, 5, and 10 μm is 80, 65, and 44% in rats, respectively, whereas it only decreases to 96% for an d_{ae} of 10 μm in humans during nasal breathing (Ménache et al., 1995). Asgharian et al. (2003) suggested that an even more rapid decrease in inhalability with increasing d_{ae} may occur in rats, particularly for faster breathing rates. Asgharian et al. (2014) extended his model to calculate inhalability for mice which had a slightly more rapid decline in inhalability with increasing particle size than rats. Inhalability and nasal deposition are particularly important considerations influencing how much PM makes it into the lower respiratory tract of rodents relative to humans.

Kim et al. (2014) provide some computational fluid dynamics (CFD) simulations of inhalability for a 7-month old. Although the simulations were for an infant under a hood for drug delivery, these simulations may reasonably approximate inhalability from calm air. For a child sitting while quietly breathing (Q, 5 L/min), nasal inhalability decreased from 83% for 1 μm to 63% for 5 μm particles. For oronasal breathing, with 65% of air entering the mouth, inhalability was about 93% for 1 to 5 μm particles. These data suggest that particle inhalability of infants is much less than expected in adults.

4.1.6 Thoracic and Respirable Particles

This section describes sampling conventions that are used by in ambient and occupational settings. The particle sampling conventions are compared to demonstrate their similarities and differences. Finally, modeling is used to illustrate how the size of particles entering the lower respiratory tract (i.e., the thorax) is affected by route of breathing (see Section 4.1.3) and differs among species.

The terms thoracic particles and respirable particles refer to the fraction of particles that are able to enter the thoracic and gas exchange region of the lung, respectively. The European Committee for Standardization (CEN) specifically defines the thoracic fraction as the mass fraction of inhaled particles penetrating beyond the larynx (CEN, 1993). They further define the respirable fraction as the mass fraction of inhaled particles penetrating into the unciliated airways. More typically, the literature has defined the respirable fraction in relation to the fraction of particles entering the gas-exchange region or the fraction penetrating through the tracheobronchial region, the ciliated airways, or conducting airways. Relative to total airborne particles, the particle size having 50% penetration for the thoracic and respirable fractions are 10 μm and 4.0 μm (aerodynamic diameters), respectively (CEN, 1993). These criteria were specifically developed for workplace atmospheres. In 1987, the EPA adopted PM_{10} as the indicator of PM for the National Ambient Air Quality Standards (NAAQS) to delineate the subset of inhalable particles (referred to as thoracic particles) that were thought small enough to penetrate to the thoracic region (including the tracheobronchial and alveolar regions) of the respiratory tract.

Figure 4-2 illustrates the thoracic fraction and EPA's PM_{10} sampler collection efficiencies discussed above. These criteria are similar for particles smaller than 10 μm. However, the curves diverge between 12−13 μm, with a dramatic drop in collection efficiency for EPA's PM_{10} versus a more gradual decrease in sampler collection efficiency for the thoracic fraction criterion. The occupational respirable particle sampling convention and EPA's $PM_{2.5}$ are also illustrated in Figure 4-2. In 1997, EPA extended size-selective sampling to include fine particles indicated by $PM_{2.5}$ and retained PM_{10} as an indicator for the purposes of regulating the thoracic coarse particles or coarse fraction particles (i.e., the inhalable particles that remain if $PM_{2.5}$ particles are removed from a sample of PM_{10}). The selection of $PM_{2.5}$ by the EPA was mainly to delineate the atmospheric fine (combustion derived, aggregates, acid condensates, secondary aerosols) and coarse (crustal, soil-derived dusts) PM modes and for consistency with community epidemiologic health studies reporting various health effects associated with $PM_{2.5}$ (U.S. EPA, 1997). Although Miller et al. (1979) recommended a particle size cut-point of ≤2.5 μm as an indicator for fine PM based on consideration of particle penetration into the gas-exchange region, the selection of $PM_{2.5}$ was not based on dosimetric considerations and was not intended to represent a respirable particle sampling convention. The thoracic sampling convention intentionally over represents the true penetration of particles into the thoracic region (compare Figure 4-1 and Figure 4-3). The American Conference of Governmental Industrial Hygienist (ACGIH) committee that recommended a 50% cut-point at 10 μm for the thoracic fraction considering uncertainty related to individual biological variability in respiratory health status, breathing patterns (rate and route), and airways structure as well as differences in work rates, all of which can cause differences in inhaled aerosol deposition and dose. Facing those uncertainties, the committee afforded extra protection to exposed workers by choosing a 50% cut-point at 10 μm rather than in the range of 5−7 μm where experimental studies showed 50% penetration of particles into the lower respiratory tract during oral breathing at ventilation rates equivalent to light exercise (ACGIH, 1985).

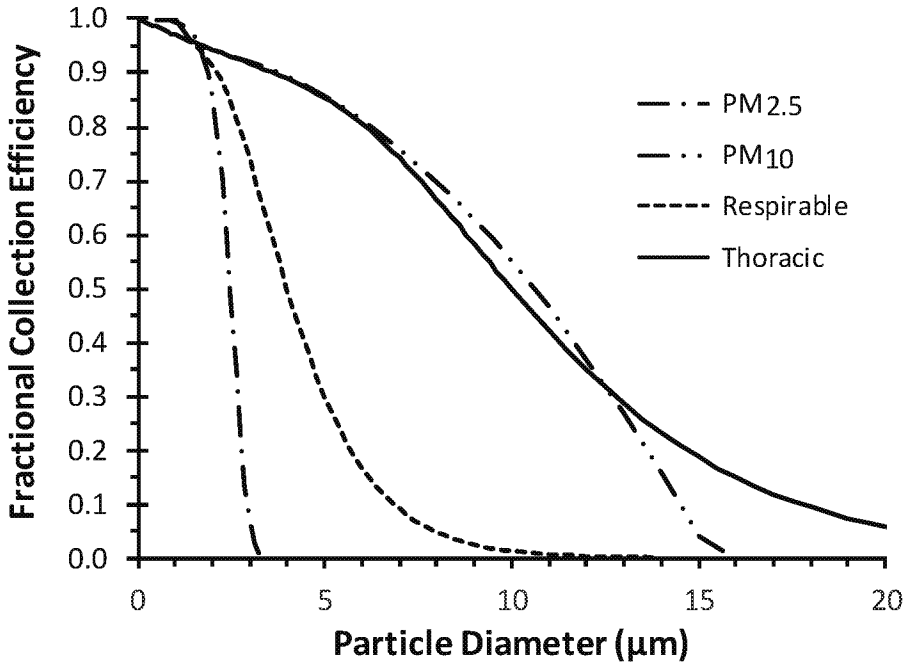

Source: Permission pending, $PM_{2.5}$ from Equation 1 of Peters et al. (2001) and/or 40CFR53, Subpart F, Table F-5; PM_{10} from Equation 11.19 of Hinds (1999) and/or 40CFR53.43 Table D-3; Respirable and Thoracic fractions are from Appendix C of ACGIH (2005).

Figure 4-2 Sampling conventions for U.S. EPA's $PM_{2.5}$ and PM_{10} and occupational criteria for thoracic and respirable fractions.

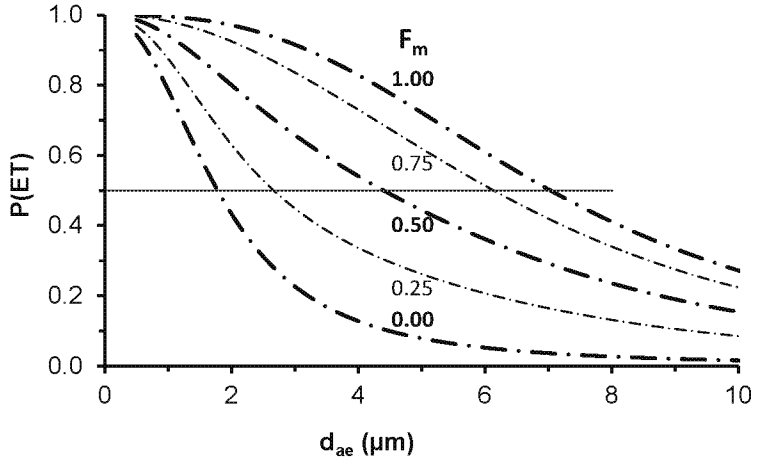

Source: Permission pending, Brown et al. (2013).

Figure 4-3 Thoracic fraction, i.e., particle penetration through the extrathoracic region, P(ET), as a function of breathing route in adult male during light exercise (V_T, 1,250 mL; *f*, 20 min^{-1}). F_m is the fraction of breath passing through mouth.

Brown et al. (2013) provide estimates of the thoracic and respirable fractions for healthy adult males, females, and a 10-year old child. The penetration of particles greater than 1 μm into the lower respiratory tract of humans was more affected by route of breathing than age, sex, activity level, or breathing pattern (i.e., V_T and *f*). Figure 4-3 illustrates this effect of route of breathing on the thoracic fraction. For typical activity levels and route of breathing, they estimated a 50% cut-size for the thoracic fraction at an aerodynamic diameter of around 3 μm in adults and 5 μm in children. The fraction of 10 μm particles entering the thorax was <20% for most activity levels and breathing habits. The penetration of 10 μm particles into the thorax was greatest, around 40%, for low levels of activity and purely oral breathing. Regardless of the breathing habit or activity level, the differences in the 50% cut-points for the thoracic and respirable fractions were far less than those used for occupational sampling. For oral breathing the 50% cut-point for the respirable fraction during oral breathing was within about 2 μm of the thoracic fraction cut-point, whereas it differs by 6 μm for occupational sampling criteria. For more typical breathing habits, the cut-points for the respirable and thoracic fractions were within about 0.5 μm. Two primary conclusions based on this study are: (1) PM_{10} over estimates the penetration of particles into the lower respiratory tract and (2) children are predicted to have greater particle penetration into the lower respiratory tract than adults.

Asgharian et al. (2014) recently provided estimates of the thoracic fraction in mice and rats as well as humans. The 50% cut-points for the thoracic fraction were roughly 1.1 μm in mice, 1.5 μm in rats,

and 3.7 μm in humans [see Figure 4 of Asgharian et al. (2014)]. The larger thoracic 50% cut-point for humans reported by Asgharian et al. (2014) relative to Brown et al. (2013) is, in part, due to the lower ventilation rate of 7.5 L/min used by the former versus average daily ventilation rates of 9 L/min and greater by the latter. One of the critical points that Asgharian et al. (2014) provide is that only a small fraction (2−5%) of particles greater than 3 μm reach the lower respiratory tract of the rodents. Thus, an appreciable fraction of inhaled thoracic coarse particles (i.e., $PM_{10-2.5}$) should not be expected to reach the lower respiratory tract of rodents during inhalation exposures.

Figure 4-4 illustrates the thoracic fraction in humans, rats, and mice calculated using the Multi-Path Particle Dosimetry model (MPPD; Version 3.04, ©2016).[42] For 50% cut-points are 3.4 μm (human, rest), 2.2 μm (human, light exercise), 1.6 μm (mouse, unrestrained), 1.1 μm (mouse, restrained), 1.6 μm (rat, rest). Note that although Table 4-1 shows increased breathing frequency and ventilation rates in restrained mice based on the review by Mendez et al. (2010), DeLorme and Moss (2002) consistently observed a lower breathing frequency and minute ventilation in restrained mice (f, 335 min^{-1}; minute ventilation, 70 mL/min) relative to unrestrained mice (f, 520 min^{-1}; minute ventilation, 120 mL/min). Regardless, with an increase in minute ventilation there is a decrease in the 50% cut-point for the thoracic fraction in both humans and mice.

[42]The MPPD model can be used to calculate particle deposition and clearance in multiple species. A description of the model, recent model improvements, and advancements incorporated into the MPPD model are provided by Miller et al. (2016). For additional information about the MPPD model (Version 3.04) or to obtain a copy, the reader is referred to: http://www.ara.com/products/mppd.htm.

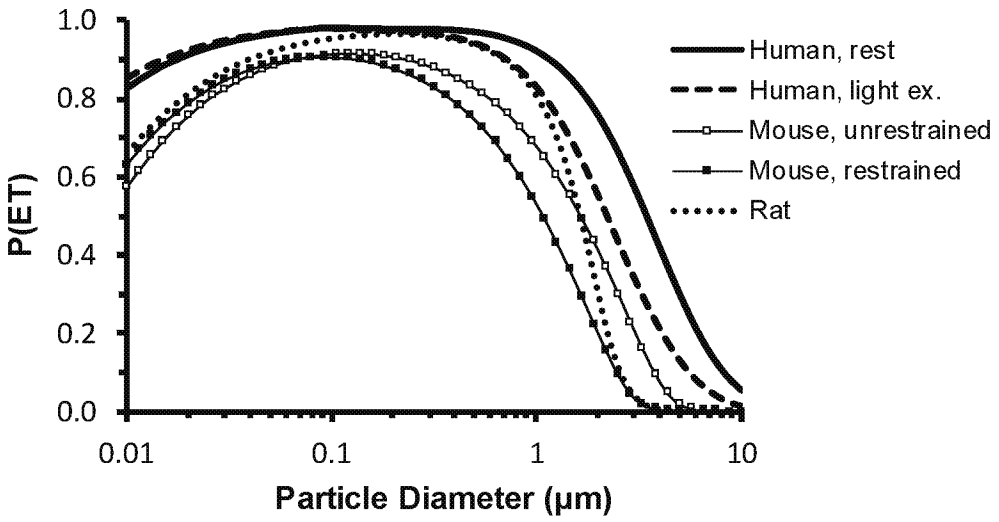

Source: Permission pending, Estimates obtained using MPPD (Version 3.04).

Figure 4-4. Multispecies comparison of the thoracic fraction for nasal breathing with consideration for inhalability, i.e., particle penetration through the extrathoracic region, P(ET). Human, rest (V_T, 625 mL; *f*, 12 min^{-1}); Human, light exercise (V_T, 1,000 mL; *f*, 19 min^{-1}); Mouse, unrestrained (V_T, 0.19 mL; *f*, 145 min^{-1}); Mouse, restrained (V_T, 0.22 mL; *f*, 290 min^{-1}); Rat (V_T, 2.1 mL; *f*, 102 min^{-1}).

4.1.7 Dose and Dose Metrics

Assuming a constant exposure concentration, breathing rate, and aerosol particle size distribution, the total particle exposure or intake dose (ID) is given by:

$$ID = C \times f \times V_T \times I(d_{50\%}, \sigma_g) \times t$$

Equation 4-2

where: C is the mass concentration of the aerosol, *f* is breathing frequency, V_T is tidal volume, I(d50%, σ_g) is aerosol inhalability, and *t* is the duration of exposure. As discussed in Section 4.1.5, I(d50%, σ_g) should be considered for comparisons across species (e.g., human vs. rat), although this parameter should be negligible for particles under 1 µm. Intake doses characterized by Equation 4-2 are commonly normalized to body mass (Alexander et al., 2008). This may be particularly appropriate for soluble particles or materials expected to have systemic effects. Although C was specified as having units of particle mass per unit volume, other metrics such as particle surface area or number of particles per unit volume may be desired, especially for smaller particle sizes (e.g., <0.1 µm). Equation 4-2 is limited

in that it does not recognize that there are within-species differences as a function of particle size in total deposition (whole lung) and regional deposition (e.g., between TB and alveolar region) of particles.

The particle mass dose in a specific region (D_r) of the respiratory tract resulting from the particle inhalation may be given as:

$$D_r = ID \times DF_r$$

Equation 4-3

where: ID is the intake dose from Equation 4-2 and DF_r is the fraction of inhaled particles depositing in region *r* of the respiratory tract. The DF_r in Equation 4-3 can be calculated for a polydisperse aerosol by estimating the deposition fractions for a series of monodisperse aerosols as:

$$DF_r(d_{50\%}, \sigma_g) \approx \frac{1}{100} \sum_{P=0.01}^{0.99} DF_r(d_i)$$

Equation 4-4

where: $DF_r(d_i)$ in the summation is the deposition fraction in a region of the particle size associated with a given percentile, P, of the size distribution as calculated by Equation 4-1. Depending on health endpoints and particle size, the most appropriate dose metric choice for D_r may be mass, particle surface area, or number of particles deposited. The D_r may also be normalized to factors such as lung weight or surface area of specific regions of the respiratory tract. Because all of the variables potentially change over time, Equation 4-3 and Equation 4-4 are most appropriate for short duration exposures. Within an individual, the variability in DF_r over time is largely attributable to variations in inhaled particle size, *f*, V_T, and route of breathing (ICRP, 1994). Inter-subject and inter-species variability in DF_r is additionally affected by morphologic differences in the size and structure of the respiratory tract.

For chronic exposures, it is necessary to consider the retained dose. The particle dose retained in a region of the lung is determined by the balance between rate of input and the rate of removal. The particle burden (Br) in a region of lung may be expressed as:

$$B_r(t) = \dot{D}_r(t - \Delta t)\Delta t + B_r(t - \Delta t)[\exp(-\lambda_r \Delta t)]$$

Equation 4-5

where: $\dot{D}_r$ is the rate of deposition per unit time in region *r*, *t* is time, and λ_r is the clearance rate constant for region *r*, Δt is the time increment for the calculations (~1% [or less] of the clearance halftime [i.e., $0.693/\lambda_r$] of the region). $\dot{D}_r$ is calculated as D_r in Equation 4-3 except it is calculated for discrete Δt where parameters (namely, *f*, V_T, route of breathing, and DF_r) are relatively constant.

Under the premise that health effects from UFP are more associated with particle surface area of deposited particles than particle number or mass, some companies have started producing instruments to measure Lung Deposited Surface Area (LDSA). For a monodisperse ultrafine aerosol containing spherical

particles, the LDSA ($\mu m^2/cm^3$) is simply calculated as the particle surface area (μm^2) times particle number concentration ($\#/cm^3$) times the DF_r, where the DF_r is predicted for an adult male using the ICRP (1994) model under conditions of light exercise (V_T = 1.25 L and f = 20 min^{-1}) and nasal breathing (Asbach et al., 2009; Fissan et al., 2007). For a polydisperse aerosol, the estimated LDSA for specified particle size bins would be summed across aerosol distribution to obtain the total LDSA. Todea et al. (2015) assessed the accuracy of four types of commercially available devices available for the measurement of LDSA in the alveolar region.[43] The principle of operation is similar among the commercial devices with each imparting a unipolar charge on the incoming aerosol and subsequent measurement of electrical current from particles collected on a filter. Some conditioning of the incoming aerosol is typical, such as use of an impactor to remove large particles (roughly >1 μm) and/or an ion trap to remove small particles (generally <20 nm). The instruments do not actually measure the surface area of the particles, rather they provide an estimate of the particle surface area that is predicted to be deposited in the alveolar region of the lung. Theoretically, the measured LDSA most accurately matches predicted lung deposition for particles between 40 and 300 nm. However, measured values should be within ±30% from 20 to 400 nm. Studies characterizing LDSA in urban and microenvironments are becoming available [e.g., (Geiss et al., 2016; Kuuluvainen et al., 2016)] as are studies of health effects studies using LDSA [e.g., (Endes et al., 2017; Soppa et al., 2017)].

It should be noted that transfer into region *r* from another region may also occur. Such situations in which a region receives a portion of its burden from another region are common in the lung, for example, mucus clearance of the segmental bronchi into the lobar bronchi, which clear into the main bronchi, which in turn clear into the trachea. In addition, the clearance from one region can transfer burden into more than one other compartment, e.g., soluble particles in the airways may be cleared into the blood as well as via the mucus. Multiple pathways for clearance of insoluble particles exist. The main alveolar particle clearance pathway is macrophage mediated clearance with macrophage migration to the ciliated airways, but macrophage or particles themselves may also move from the alveoli into the lymph and remerge in the ciliated airways or blood. There are also considerable species differences in rates of clearance that should be considered for interspecies extrapolations evaluating chronic exposure scenarios.

4.2 Particle Deposition

Inhaled particles may be either exhaled or deposited in the ET, TB, or alveolar region. A particle becomes deposited when it moves from the airway lumen to the wall of an airway. The deposition of particles in the respiratory tract depends primarily on inhaled particle size, route of breathing (nasal or oronasal), tidal volume (V_T), breathing frequency (f), and respiratory tract morphology. The distinction between air passing through the nose versus the mouth is important since the nasal passages more effectively remove inhaled particles than the oral passage. Respiratory tract morphology, which affects

[43] One instrument offered the option of measuring LDSA for either the alveolar or the tracheobronchial region.

particle transport and deposition, varies between species, the size of an animal or human, and health status.

The fraction of inhaled aerosol becoming deposited in the human respiratory tract has been measured experimentally. Studies, using light scattering or particle counting techniques to quantify the amount of aerosol in inspired and expired breaths, have characterized total particle deposition for varied breathing conditions and particle sizes. The vast majority of in vivo data on the regional particle deposition has been obtained by scintigraphic methods where external monitors are used to measure gamma emissions from radiolabeled particles. These scintigraphic data have shown highly variable regional deposition with sites of highly localized deposition or "hot spots" in the obstructed lung relative to the healthy lung. Even in the healthy lung, "hot spots" occur in the region of airway bifurcations. Mathematical models aid in predicting the mixed effects of particle size, breathing conditions, and lung volume on total and regional deposition. Experimentally, however, there is considerable interindividual variability in total and regional deposition even when inhaled particle size and breathing conditions are strictly controlled. Section 4.2.4 on Biological Factors Modulating Deposition provides more detailed information on factors affecting deposition among individuals.

4.2.1 Mechanisms of Deposition

Particle deposition in the lung is predominantly governed by diffusion, impaction, and sedimentation. Most discussion herein focuses on these three dominant mechanisms of deposition. Simple interception, which is an important mechanism of fiber deposition, is not discussed in this chapter. Electrostatic and thermophoretic forces as mechanisms of deposition have not been thoroughly evaluated and receive limited discussion. Some generalizations with regard to deposition by these mechanisms follows, but should not be viewed as definitive rules. Both experimental studies and mathematical models have demonstrated that breathing patterns can dramatically alter regional and total deposition for all sized particles. The combined processes of aerodynamic and diffusive (or thermodynamic) deposition are important for particles in the range of 0.1 μm to 1 μm. Aerodynamic processes predominate above and thermodynamic processes predominate below this range. For detailed equations related to particle behavior in air and deposition in the human respiratory tract, the reader is referred to Annex D of ICRP (1994). Equations for calculation of deposition in the MPPD model are mostly summarized in Anjilvel and Asgharian (1995) and Asgharian and Price (2007) with physiological parameters summarized in Miller et al. (2016).

Diffusive deposition, by the process of Brownian diffusion, is the primary mechanism of deposition for particles having physical diameters of less than 0.1 μm. For particles having physical diameters of roughly between 0.05 and 0.1 μm, diffusive deposition occurs mainly in the small distal bronchioles and the pulmonary region of the lung. However, with further decreases in particle diameter

below ~0.05 μm, increases in particle diffusivity shift more deposition proximally to the bronchi and ET regions.

Governed by inertial or aerodynamic properties, impaction, and sedimentation increase with d_{ae}. When a particle has sufficient inertia, it is unable to follow changes in flow direction and strikes a surface thus depositing by the process of impaction. Impaction occurs predominantly at bifurcations in the proximal airways, where linear velocities are at their highest and secondary eddies form. Sedimentation, caused by the gravitational settling of a particle, is most important in the distal airways and pulmonary region of the lung. In these regions, residence time is the greatest and the distances that a particle must travel to reach the wall of an airway are minimal.

The electrical charge on some particles may result in an enhanced deposition over what would be expected based on size alone. With an estimated charge of 10−50 negative ions per particle, Scheuch et al. (1990) found deposition of 0.5 μm particles in humans (V_T = 500 mL, f = 15 min^{-1}) to increase from 13.4% (no charge) to 17.8% (charged). This increase in deposition is thought to result from image charges induced on the surface of the airway by charged particles. Yu (1985) estimated a charge threshold level above which deposition fractions would be increased of about 12, 30, and 54% for 0.3, 0.6, and 1.0 μm diameter particles, respectively. Electrostatic deposition is generally considered negligible for particles below 0.01 μm because so few of these particles carry a charge at Boltzmann equilibrium. This mechanism is also thought to be a minor contributor to overall particle deposition, but it may be important in some laboratory studies due to specific aerosol generation techniques such as nebulization. Laboratory methods such as passage of aerosols through a Kr-85 charge neutralizer prior to inhalation are commonly used to mitigate this effect.

The National Radiological Protection Board (NRPB) evaluated the potential for corona discharges from high voltage power lines to charge particles and enhance particulate doses (NRPB, 2004). They concluded that electrostatic effects would be the most important for particles in the size range from about 0.1−1 μm, where deposition may theoretically increase by a factor of three to ten. However, given that only a small fraction of ambient particles would pass through the corona to become charged, the small range of relevant particle sizes (0.1−1 μm), and the subsequent required transport of charged particles to expose individuals; the NRPB concluded that effects, if any, of electric fields on particle deposition in the human respiratory tract would likely be minimal.

When assessing particle behavior in the lower respiratory tract, it is important to consider how temperature affects their behavior. The mean free path of particles in air (i.e., the distance that particle travel in a given direction before colliding with an air molecule) and the dynamic viscosity of inhaled air are affected by the increased temperature in the lower respiratory tract relative to standard temperature and pressure. The mean free path increases from 66.4 nm at 20°C to 71.2 nm at 37°C (Briant, 1990). The dynamic viscosity of air increases from 1.82×10^{-4} poise at 20°C to 1.90×10^{-4} poise at 37°C (Briant, 1990). Due to these two parameters, the diffusivity of particles <0.1 μm is 1.08 times higher at 37 than 20°C. For micron sized particles, the time that it takes particles to change directions in response to a

change in the direction of airflow as well as the settling velocity of particles are decreased by about 4% at 37°C relative to 20°C. Thus, diffusive deposition is increased, whereas aerodynamic deposition is decreased at 37°C relative to 20°C.

There is less of an effect of body temperature on the particle behavior in the upper respiratory tract. Nasal mucosal temperatures decrease during inspiration and increase during expiration (Bailey et al., 2017; Lindemann et al., 2002). During inhalation of room temperature air (23−25°C), anterior mucosal temperatures can cycle 3−6°C between inspiration and expiration. More distally, 1°C fluctuations are observed at the nasopharynx, with average expiratory mucosal temperatures of 34°C (Lindemann et al., 2002). This indicates the temperature of inhaled air cannot achieve body temperature until it reaches the lower respiratory tract.

Thermophoretic forces on particles occur due to temperature differences between respired air and respiratory tract surfaces. Temperature gradients of around 20°C are thought to produce sufficient thermophoretic force to oppose diffusive and electrostatic deposition during inspiration and to perhaps augment deposition by these mechanisms during expiration (Jeffers, 2005). Thermophoresis is only relevant in the extrathoracic and large bronchi airways and reduces to zero as the temperature gradient decreases deeper in the lung. Theoretical analysis of thermophoresis has been done for smooth walled tubes and is important over distances that are several orders of magnitude smaller than the diameter of the trachea. The alteration of the flow patterns by airway surface features such as cartilaginous rings may affect particle transport and deposition over far greater distances than thermophoretic force.

4.2.2 Deposition Patterns

Knowledge of sites where particles of different sizes deposit in the respiratory tract and the amount of deposition therein is necessary for understanding and interpreting the health effects associated with exposure to particles. Particles deposited in the various respiratory tract regions are subjected to large differences in clearance mechanisms and pathways and, consequently, retention times. Deposition patterns in the human respiratory tract were described in considerable detail in dosimetry chapters of prior PM AQCD (U.S. EPA, 2004, 1996); as such, they are only briefly described here.

Predicted total and regional particle deposition in several mammalian species are illustrated in Figure 4-5. For all the species illustrated in Figure 4-5, ET deposition was based on experimental data at specific particle sizes or empirical fits to experimental data, while TB and pulmonary deposition were based on theoretical losses by diffusion, sedimentation, and impaction in species specific models of lower airways morphology. The predicted deposition for the human (male), mouse (unrestrained), and rat are for respiratory parameters in Table 4-1 using the MPPD model (Version 3.04, ©2016). Miller et al. (2016) reviews recent additions to the MPPD model that contribute to the ability to conduct cross-species extrapolations of both deposition and clearance. The effects of physiologic parameters on deposition in humans and rats free of respiratory disease are also described by de Winter-Sorkina and Cassee (2002).

The predicted deposition for the dog (V_T = 170 mL, f = 11.7 min^{-1}) and hamster (V_T = 0.72 mL, f = 59 min^{-1}) are based on Yeh (1980). The trends and magnitude of particle deposition are quite similar between the illustrated species. In the mouse and rat, due to particle inhalability, there is a gradual decrease in total and ET deposition for particles greater than about 2.5 to 3 μm. In the human, a similar decline in total deposition due to particle inhalability starts becoming apparent for particles above 7 to 8 μm.

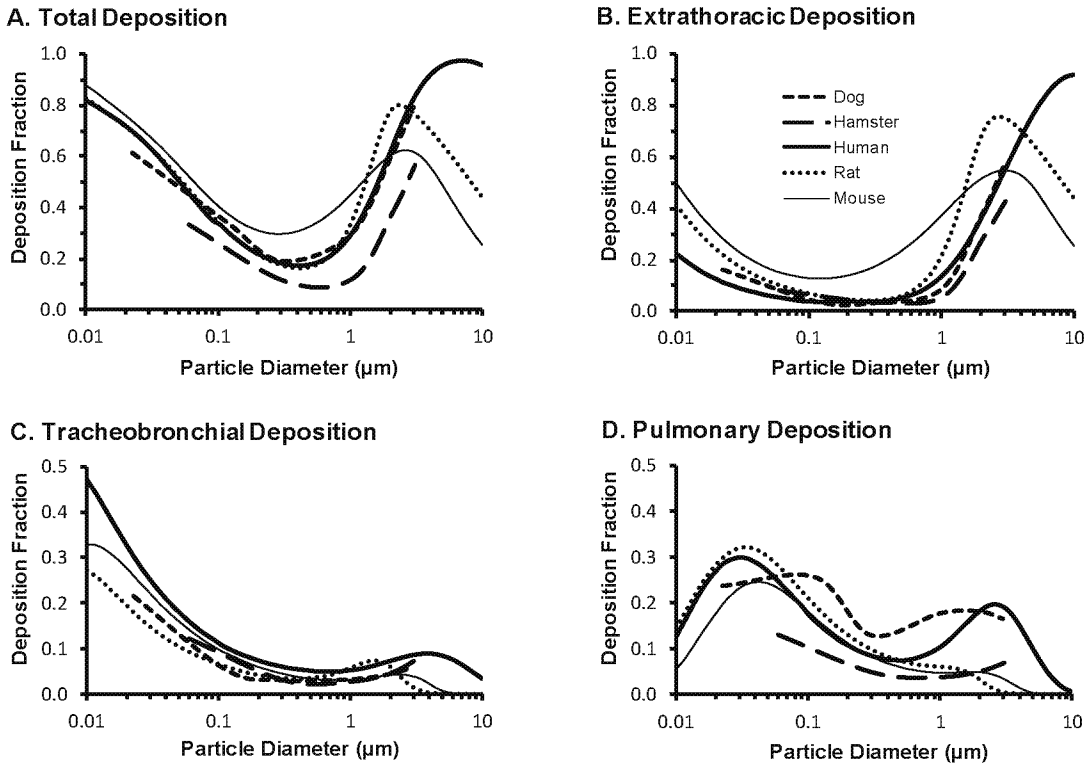

Source: Permission pending, Adapted and updated from Brown (2015).

Figure 4-5. Predicted total and regional particle deposition adjusted for particle inhalability in select mammalian species. (A) Total deposition, (B) Extrathoracic deposition, (C) Tracheobronchial deposition, (D) Pulmonary deposition.

4.2.2.1 Total Respiratory Tract Deposition

Across mammalian species, the efficiency of deposition in the respiratory tract may generally be described as a "U shaped" curve on a plot of deposition efficiency versus the of log particle diameter as illustrated in Figure 4-5. Total deposition shows a minimum for particle diameters in the range of 0.1 to 1.0 μm, where particles are small enough to have minimal sedimentation or impaction and sufficiently

large so as to have minimal diffusive deposition. Total deposition does not decrease to zero for any sized particle, in part, because of mixing between particle laden tidal air and residual lung air. The particles mixed into residual air remain in the lung following a breath and are removed on subsequent breaths or gradually deposited. Total deposition approaches 100% for particles of roughly 0.01 μm due to diffusive deposition and for particles of around 10 μm due to the efficiency of sedimentation and impaction.

Total human lung deposition, as a function of particle size, is depicted in Figure 4-6. These experimental data were obtained by using monodisperse spherical test particles in healthy adults during controlled tidal breathing (V_T, 500 mL; *f*, 15 min^{-1}) on a mouthpiece. The experimental ultrafine data are for 11 males (age, 31 ± 4 years; FRC, 3,911 mL) and 11 females (age, 31 ± 4 years; FRC, 3,314 mL) from Jaques and Kim (2000). The fine and coarse data are for eight males (age, 31 ± 7 years; FRC, 3,730 mL) and seven females (age, 31 ± 6 years; FRC, 3,050 mL) from Kim and Hu (2006). The MPPD (Version 3.04) model used an upper airway volume of 40 mL and 50 mL for males and females, respectively, and the FRC from studies to predict particle deposition. Assuming isotropic expansion and contraction of the airways, scaling the airway morphology (length and diameters) to the cube root of volume, the model predictions are in good agreement with the mean experimental data.

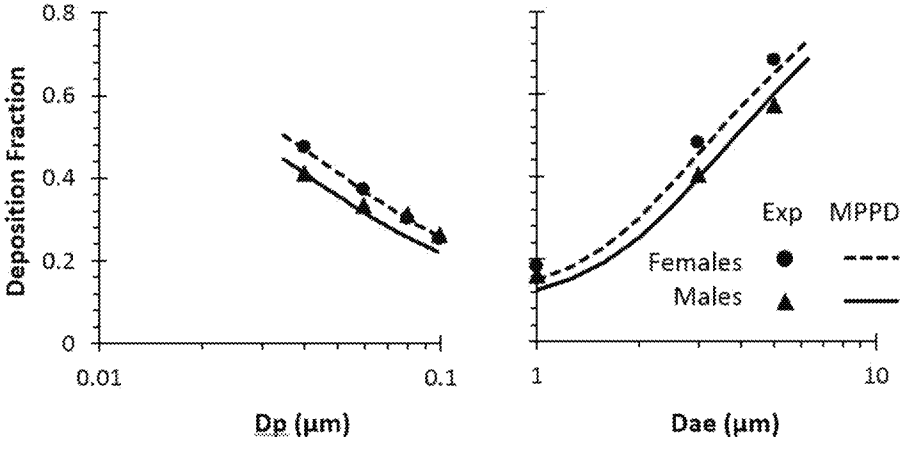

Note: See text for more detail.

Source: Permission pending, Human data from Jaques and Kim (2000) and Kim and Hu (2006) with predicted deposition obtained from the MPPD model (Version 3.04).

Figure 4-6. Experimental (Exp) and predicted (MPPD) total lung deposition for controlled tidal breathing on a mouthpiece.

4.2.2.2 Extrathoracic Region

The first line of defense for protecting the lower respiratory tract from inhaled particles is the nose and mouth. Particle deposition in the ET region, especially the nasal passages, reduces the amount available for deposition in the TB and alveolar regions. Most of the new studies in the last PM ISA (U.S. EPA, 2009) were largely derived from computational fluid dynamics (CFD) modeling and experimental measurements in casts. Those studies generally reported that for particles >1 μm, deposition efficiency in the oral and nasal passages is a function of an impaction parameter (Stokes number) with the addition of a flow regime parameter (Reynolds number) for the oral passages. New studies are again largely derived from CFD modeling and experimental measurements in casts. Only a few new studies are discussed here, these were generally selected as those providing data for infants and children.

Several new papers from the same group describe nasal airway growth and particle deposition based on studies of nasal casts (Xi et al., 2014; Zhou et al., 2014; Zhou et al., 2013; Xi et al., 2012). The casts are for a 10-day old girl, 7-month old girl, a 5-year old boy, and a 53-year old man. The papers provide morphological data and total and regional deposition data (in vitro and CFD) for ultrafine and larger-sized particles (2−28 μm). For UFP, CFD simulations showed good agreement with other published studies of deposition in nasal casts for adults, infants, and children. Predicted ultrafine deposition was low (<10%) for particles larger than 10 nm, but rose rapidly to between 70 and 90% as particle size decreased to 1 nm (Xi et al., 2012). For particles ≤5 nm (not larger sizes), deposition also increased with decreasing flow (3 to 45 L/min), but this effect was less marked than the increase in deposition with decreasing particle size. Overall, the nasal deposition fractions of among the casts were rather similar when assessed as a function of a diffusion factor ($D^{0.5}Q^{-0.28}$; where, D is the particle diffusion coefficient and Q is flow rate). As a function of this diffusion factor, the deposition fractions were nearly identical for the 5-year old boy and 53-year old man with these two casts having greater deposition than those for the two younger girls' casts. For larger particles (monodisperse, 2−28 μm) delivered under resting breathing conditions, deposition data were well predicted and similar among all five casts as a function of a modified-impaction factor ($d_{ae}^2\Delta p^{2/3}$; where, Δp is the pressure drop across the nasal cast).

Another group has also recently published a series of experimental and CFD simulations of particle deposition in casts (Garcia et al., 2015; Schroeter et al., 2015; Garcia et al., 2009). The modified-impaction factor used by Zhou et al. (2014) was adopted from Garcia et al. (2009), who found that this factor better collapsed deposition factions among five adult nasal casts than several definitions of the Stokes number for nasal casts. More recently, Garcia et al. (2015) provided simulations of total ultrafine nasal deposition as well as that on the olfactory mucosa of humans and rats. Similar to Xi et al. (2012), these authors found that total nasal deposition in humans was low (<10%) for particles above about 10 nm, below which size deposition increased rapidly with decreasing particle size. Rats were predicted to have greater total and olfactory deposition than humans. However, due the much higher ventilation rate of humans than rats, humans were predicted to experience greater dose per olfactory

surface area for particles between 1 and 7 nm; above this size the dose per surface area was slightly greater in rats than humans. Figure 4-7 illustrates the olfactory dose rate of particles in humans and rats not normalized to olfactory surface area. Schroeter et al. (2015) provided experimental and CFD simulations for total and regional deposition of particles between 2.6 and 14.3 μm. For 5 to 14.3 μm particles inhaled during rest (Q, 16.5 L/min) about 2−5.5% deposition in the olfactory region was measured experimentally. In general, the CFD predicted pattern of deposition shifted proximally in the nose with increasing inspiratory flow and particle size. Nasal deposition was minimal for particles below 3 μm and 100% for the 14.3 μm particles.

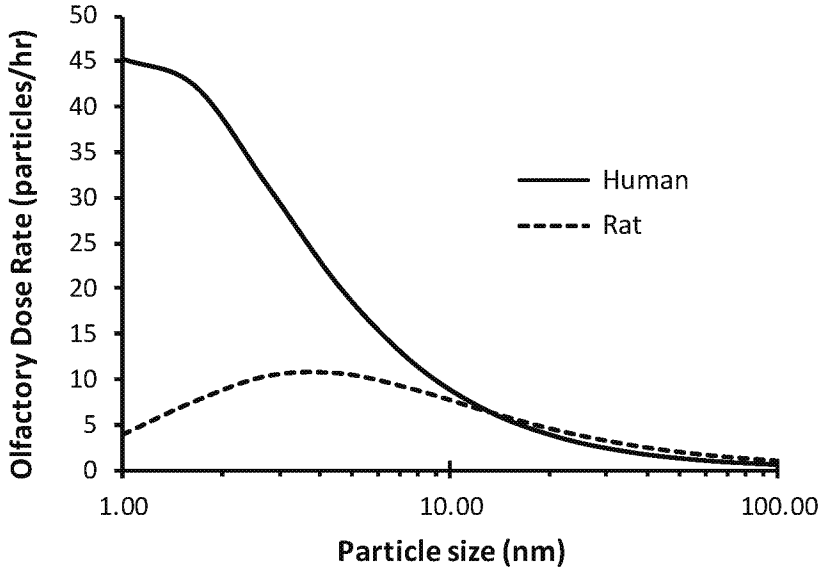

Source: Permission pending, Based on empirical equations in Garcia et al. (2009) and Garcia et al. (2015).

Figure 4-7. Predicted nanoparticle olfactory dose rate (particles/hour) for resting ventilation (human, 7.5 L/min; rat, 0.288 L/min) and a concentration of one particle/cm^3 at any given particle size.

Some other recently published studies have used in vitro and in silico models to examine oral and nasal particle deposition in infants. Kim et al. (2014) used CFD simulations to evaluate particle inhalability (see Section 4.1.5) and penetration into the lower respiratory tract of a 7-month old. For quiet nasal breathing (Q, 5 L/min), the authors reported about 13.8% deposition of 2.5 μm particles in the nose, 0.4% in the lower-pharynx, and 11.8% in the larynx. As a point of clarification, the authors provided data separately for the nasopharynx which is the upper-pharynx and the pharynx.[44] For quiet oronasal

[44] Based on Figure 1a of Kim et al. (2014), it appears that the "pharynx" as used in the paper is the lower-pharynx or oropharynx which begins at the soft palate and extends to the openings of the larynx and esophagus.

breathing (Q, 5 L/min; 35% nasal, 65% oral), the authors reported about 3.9% deposition of 2.5 μm particles in the nose, 2.2% in the mouth, 6.9% in the lower-pharynx, and 17.2% in the larynx. Counter to studies in adults, oronasal breathing increased particle losses in the head by greatly increased deposition in the lower-pharynx and larynx. Amirav et al. (2014) also provide data suggesting greater ET removal of particles during oral than nasal breathing at typical breathing rates for 5-, 14-, and 20-month-olds. Aerosols were generated using a Respimat® soft mist inhaler which produces an aqueous aerosol with a mode in the range of 1.1–2.1 μm, although almost 50% of the aerosol mass associated with particles >3.3 μm (Zierenberg, 1999). Amirav et al. (2014) found for the 5- and 14-month-olds that the amount of aerosol penetrating the upper respiratory tract was significantly greater through the oral passages than the nose. At 20-months of age, the particle loses in the nasal and oral passages were equivalent. In contrast with adults, these studies suggest that the nasal airways of infants may have lower particle removal efficiency than the oral airway.

While these in silco (CFD) and in vitro (casts) data are informative, they are not in agreement with existing experimental data. Figure 4-8 illustrates experimental human nasal deposition data for adults and children (Bennett et al., 2008; Becquemin et al., 1991) and predictive equation fitting four children's' and an adult cast deposition data (Zhou et al., 2014). Becquemin et al. (1991) provide data for 20 children (6 M, 14 F; 5–15 years, mean 10 years) and 10 adults (5 M, 5 F; 21–54 years, mean 36 years) who inhaled 1, 2, and 3 μm particles under breathing conditions simulating rest and moderate exercise. Bennett et al. (2008) provide data for 12 children (9 M, 3 F; 6–10 years) and 11 adults (6 M, 5 F; 18–27 years) who inhaled 1 and 2 μm particles under breathing conditions simulating rest and light exercise. For Figure 4-8, mean total nasal deposition (η_{total}) data for particles were extracted from Table 2 of Becquemin et al. (1991) and Table 3 of Bennett et al. (2008). Assuming inspiratory and expiratory deposition efficiency were equivalent, inspiratory nasal deposition efficiency (η_{insp}) was calculated as:

$$\eta_{insp} = 1 - \sqrt{1 - \eta_{total}}$$

Equation 4-6

The pressure drop (Δp) across the nose was calculated as the product of nasal resistance and inspiratory flow provided in the papers. The equation fitting deposition and in five nasal casts (4 children, 1 adult) of is not predictive of mean nasal deposition either in children or adults. The mean deposition for adults tends to exceed that of children.

Figure 4-9 illustrates experimental human nasal deposition data for 2 μm particles in adults and children (Bennett et al., 2008) with the predictive equation fitting nasal cast deposition data (Zhou et al., 2014). The predictive equation fits the data for children fairly well ($r = 0.67$, $p = 0.024$). However, the fit of adults provides a negative r^2, showing that the mean is a better predictor or nasal deposition efficiency in adults than the Zhou et al. (2014) model. Bennett et al. (2008) used linear regression to examine the relationship between total nasal deposition and pressure drop and found that the intercept was significantly increased in adults relative to children. That is, as illustrated in Figure 4-9, there was overlap in $d_{ae}^2 \Delta p^{2/3}$ between adults and children, but adults had greater nasal deposition than children. Similarly,

Becquemin et al. (1991) provided plots of total nasal deposition against the modified-impaction factor, $d_{ae}^2\Delta p^{2/3}$. Although there was considerable overlap in $d_{ae}^2\Delta p^{2/3}$ between children and adults, nasal deposition again tended to be greater in adults than in children.

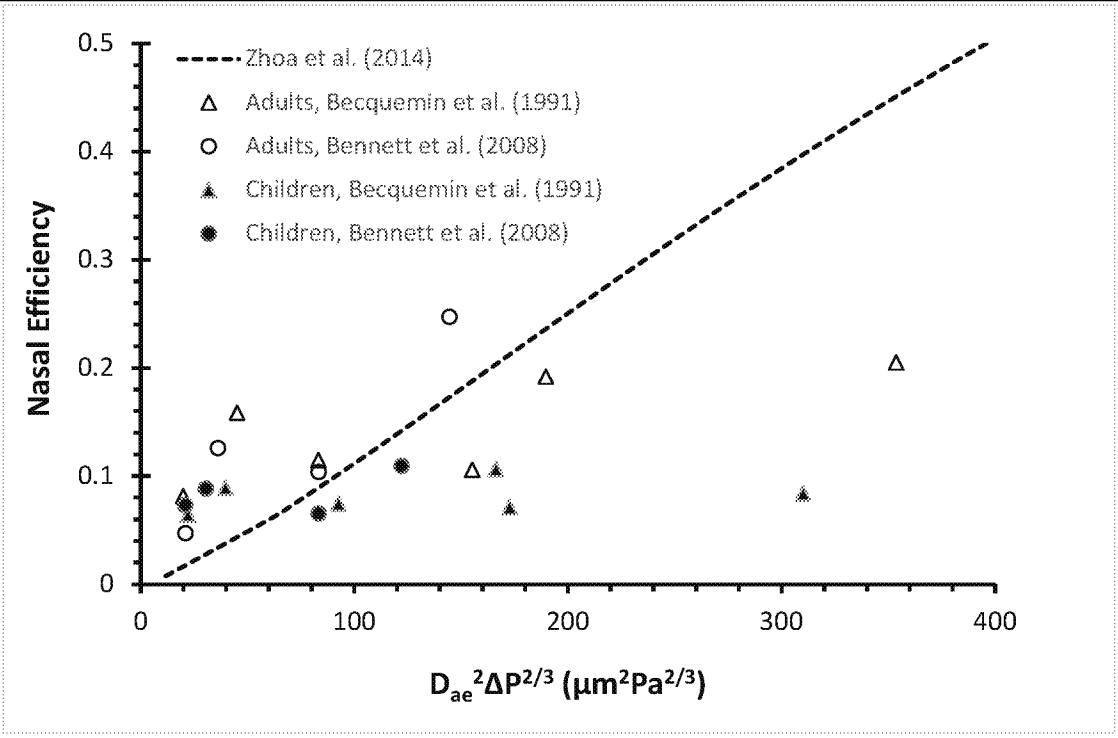

Source: Permission pending, Human data from Becquemin et al. (1991) and Bennett et al. (2008) with inspiratory nasal deposition efficiency estimated using Equation 4-6.

Figure 4-8. Comparison of group mean human nasal deposition data with nasal cast deposition data. Nasal efficiency during inspiration is plotted as a function of the modified impaction parameter. See text for more details.

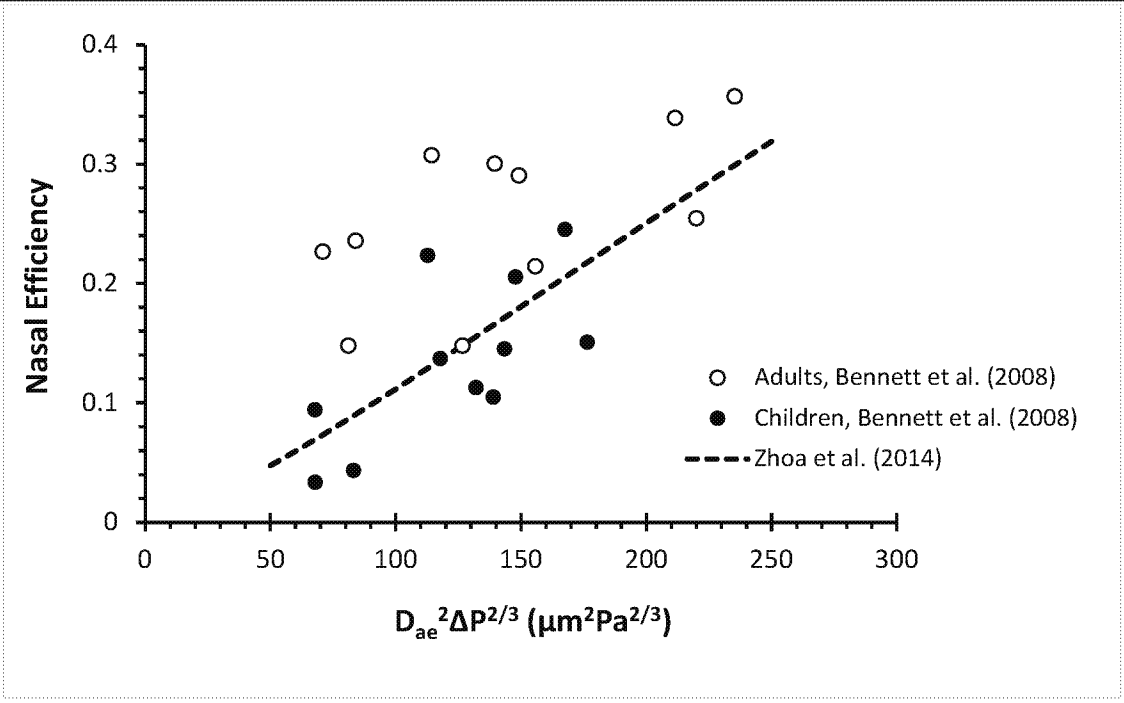

Source: Permission pending, Human data extracted from Figure 5B of Bennett et al. (2008) with inspiratory nasal deposition efficiency estimated using Equation 4-6.

Figure 4-9. Comparison of individual level data for 2 μm inspiratory nasal deposition efficiency in during light exercise in adults and children with nasal cast model efficiency. Individual level deposition data are for 11 children and 11 adults. See text for more details.

Theory, CFD modeling, and research measuring deposition in nasal casts show that nasal deposition efficiency increases with increasing particle size and Δp across the cast. Consistent with that evidence, the ICRP (1994) Human Respiratory Tract Model recommends the use of scaling factors to increase nasal deposition in children relative to adults. For the children (V_T, 478 mL; f, 28 min^{-1}; 6–10 years of age) and adults (V_T, 940 mL; f, 20 min^{-1}) in Figure 4-9, the ICRP model predicts a η_{insp} for 2 μm particles of 0.275–0.338 (scaling factor of 1.26 for 10 year olds and 1.58 for 6 year-olds) and η_{insp} of 0.217 (scaling factor of 1.0 for adults). The mean experimental η_{insp} were 0.136 and 0.257 in children and adults, respectively. Recognizing that experimental data showed lower nasal deposition in children than adults, Brown et al. (2013) recommended using a scaling factor of one for estimates of nasal efficiency in children. Using a scaling factor of one for children (V_T, 478 mL; f, 28 min^{-1}), the ICRP model predicts η_{insp} of 0.173 for 2 μm particles. The scaling factor needs to be reduced to 0.89 to match the experimental η_{insp} of 0.136 for 2 μm particles in the Bennett et al. (2008) study. Although theory and studies using casts suggest increase nasal deposition efficiency with increasing Δp across the nose, experimental data show less nasal deposition in children than adults.

4.2.2.3 Tracheobronchial and Alveolar Region

Inhaled particles passing the ET region enter and may become deposited in the lungs. For any given particle size, the pattern of particle deposition influences clearance by partitioning deposited material among lung regions. Deposition in the tracheobronchial airways and alveolar region cannot be directly measured in vivo. Much of the available deposition data for the TB and alveolar regions have been obtained from experiments with radioactively labeled, poorly soluble particles (U.S. EPA, 1996) or by use of aerosol bolus techniques (U.S. EPA, 2004). In general, the ability of these experimental data to define specific sites of particle deposition is limited to anatomically large regions of the respiratory tract such as the head, larynx, bronchi, bronchioles, and alveolar region. Mathematical modeling can provide more refined predictions of deposition sites. Highly localized sites of deposition within the bronchi are described in Section 4.2.2.4. Both experimental and modeling techniques are based on many assumptions that may be relatively good for the healthy lung but not for the diseased lung. For discussion of these issues, the reader is referred to Section 4.2.4.4 and Section 4.2.4.5.

The ICRP (1994) relied on scintigraphic and aerosol bolus techniques to estimate TB deposition. Due to concern that these methods may have led to an overestimation of deposition in the TB airways, Brown et al. (2013) used the MPPD model to determine particle penetration through the TB airways. That is, in ascertaining regional lung deposition, there are uncertainties in the ICRP (1994) assessment of TB deposition due to slow particle clearance from the TB airways and the penetration of even shallowly inhaled aerosol boluses into the alveolar region. These would lend toward an overestimation of TB particle deposition and likewise an underestimation of alveolar deposition using ICRP (1994) formulas. However, the ICRP (1994) model might be preferable since it was based on human experimental data, whereas the MPPD model is a deterministic model based on theoretical deposition in a series of tubes. Accordingly, a comparison of the models was provided by Brown et al. (2013). Most apparent for oral breathing due to low ET particle removal, the 50% cut points were between 0.5 and 1 μm smaller using the ICRP (1994) versus the MPPD model. This finding is consistent with the supposition that the ICRP (1994) model overestimates TB deposition.

4.2.2.4 Sites of Localized Deposition

From a toxicological perspective, it is important to realize that not all epithelial cells in an airway will receive the same dose of deposited particles. Localized deposition in the vicinity of airway bifurcations has been analyzed using experimental and mathematical modeling techniques as described in prior reviews (U.S. EPA, 2009, 2004, 1996). Although there are a couple of new papers describing localized ultrafine, fine, and coarse particle deposition in the olfactory region of humans (see Section 4.3.3.1, Olfactory Delivery), there do not appear to be recent papers describing localized deposition in the tracheobronchial airways.

In the 1996 PM AQCD (U.S. EPA, 1996), experimental data were available illustrating the peak deposition of coarse particles (3, 5, and 7 μm d_{ae}) in daughter airways during inspiration and the parent airway during expiration, but always near the carinal ridge (Kim and Iglesias, 1989). In the 2004 PM AQCD (U.S. EPA, 2004), mathematical models predicted distinct "hot spots" of deposition in the vicinity of the carinal ridge for both coarse (10 μm) and ultrafine (0.01 μm) particles (Heistracher and Hofmann, 1997; Hofmann et al., 1996). In a model of lung Generations 4–5 during inspiration, hot spots occurred at the carinal ridge for 10 μm d_{ae} particles due to inertial impaction and for 0.01 μm particles due to secondary flow patterns formed at the bifurcation. During expiration, preferential sites of deposition for both particle sizes occurred (1) approaching the juncture of daughter airways on the walls forming and across the lumen from the carinal ridge; and (2) the top and bottom (visualizing the Y-shaped geometry laying horizontal) of the parent airway downstream of the bifurcation.

Studies reviewed in the 2009 ISA (U.S. EPA, 2009) further support these findings. Most of these studies quantified localized deposition in terms of an enhancement factor. Typically, the enhancement factor was the ratio of the deposition in a prespecified surface area (e.g., 100 × 100 μm which corresponds to ~10 × 10 epithelial cells) to the average deposition density for the whole airway geometry. Enhancement factors are very sensitive to the size of the surface considered (Balashazy et al., 1999). The deposition of 0.001 μm is rather uniform, however, the deposition pattern became increasingly less uniform with increasing particle size (Farkas and Balásházy, 2008; Farkas et al., 2006). For particles greater than ~0.01 μm, some cells located near the carinal ridge of bronchial bifurcations may receive hundreds to thousands of times the average dose (particles per unit surface area) of the parent and daughter airways. The inertial impaction of particles ≥1 μm d_{ae} at the carinal ridge of large bronchi also increases with increasing inspiratory flows.

4.2.3 Interspecies Patterns of Deposition

Across species comparisons of the modeling of total, extrathoracic, tracheobronchial, and alveolar deposition were provided in Figure 4-5. In general, there are consistent patterns in predicted deposition among species with the exception of rodents having lower deposition of particles larger than 2.5–3 μm due to lower inhalability of rodents relative to larger mammals. Figure 4-10 illustrates the experimental regional deposition in mice, rats, dogs, and humans. Regional deposition is the fraction of particles found in each compartment relative to total respiratory tract deposition.

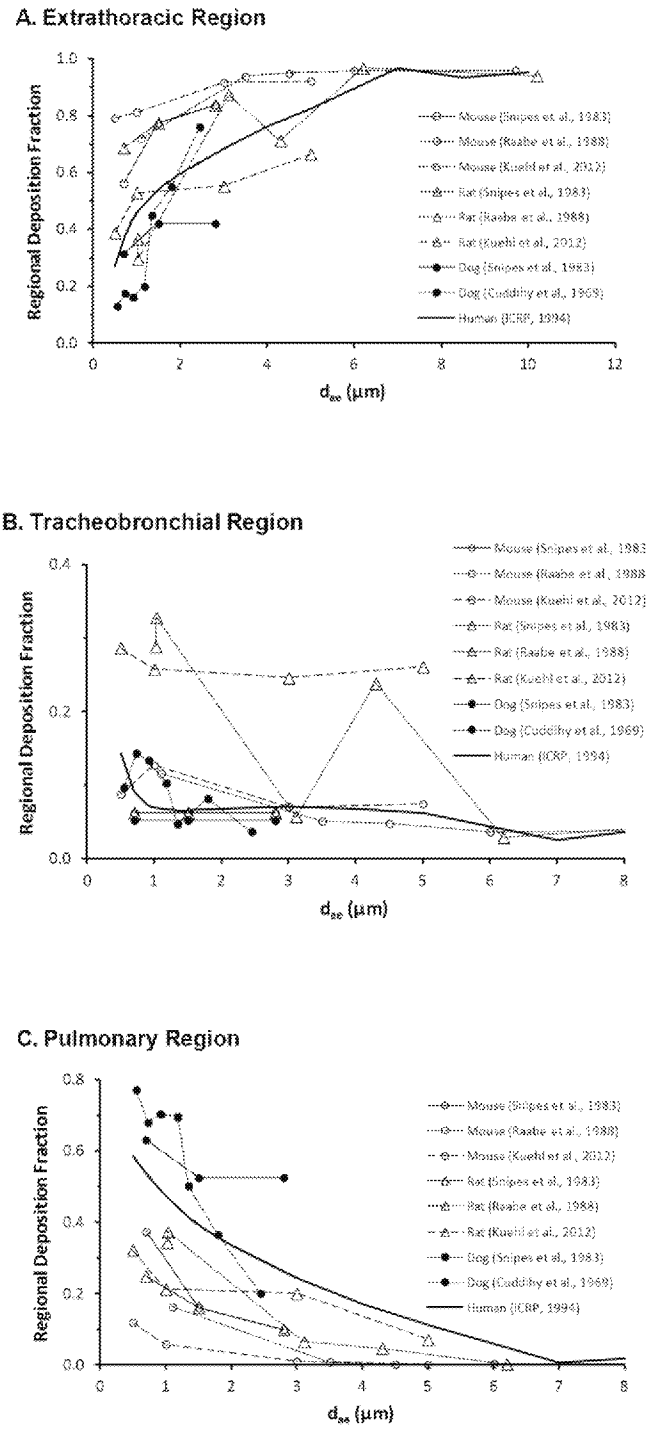

Source: Permission pending, Brown (2015).

Figure 4-10. Experimental regional particle deposition (normalized to total deposition) in select mammalian species. (A) extrathoracic deposition (nasal breathing); (B) tracheobronchial deposition; and (C) pulmonary deposition.

Within a given species, considerable between study variability is apparent (see Figure 4-10). Some of the within species variability may be attributable to breathing pattern. Kuehl et al. (2012) reported breathing patterns for mice (V_T = 0.20 mL, f = 275 min^{-1}) and rats (V_T = 1.71 mL, f = 181 min^{-1}). The f reported by Kuehl et al. (2012) for mice are similar to those of restrained mice in Table 4-1. Neither Raabe et al. (1988) nor Snipes et al. (1983) reported breathing patterns. On average, Cuddihy et al. (1969) reported a V_T of 164 mL and f of 12 min^{-1} in dogs. However, there was considerable within dog variability among the aerosol exposures in the Cuddihy et al. (1969) study, with V_T ranging from 130 to 200 mL and f ranging from 8 to 20 min^{-1}. The human data are for a male with resting breathing pattern (V_T = 625 mL, f = 12 min^{-1}) as predicted by the ICRP (1994) Human Respiratory Tract Model. There are some limited scintigraphic regional deposition data for three baboons (10−14 kg; 6.3 ± 0.5 years of age) from Albuquerque-Silva et al. (2014). Similar to data in Figure 4-10, the baboon data showed increasing extrathoracic deposition with increasing particle size from 0.23 to 2.8 μm (activity median aerodynamic diameter).

Despite the within and between species differences, some trends become apparent from this figure. First, the ET fraction generally increases with decreasing species size and increasing particle size. Second, the pulmonary fraction generally decreases with decreasing species size and increasing particle size. Third, the TB fraction is a small component of the overall deposition. With respect to this third observation, however, it should be noted that due to relatively small surface area of the TB region, delivered surface doses can be quite high.

4.2.4 Factors Modulating Deposition

4.2.4.1 Physical Activity

The activity level of an individual is well recognized to affect their minute ventilation and route of breathing. Changes in minute ventilation during exercise are accomplished by increasing both V_T and f (Table 4-2). As discussed in Section 4.1.3, route of breathing generally changes from the nose when at rest to increasingly through the mouth with increasing activity level. There is considerable variability in both the route by which people breathe and is affected by sex, age, nasal resistance, and upper airway infection and inflammation.

Table 4-2. Breathing patterns with activity level in adult human male.

Activity	Awake Rest[a]	Slow Walk[a]	Light Exertion[a]	Moderate Exertion[a]	Heavy Exertion[b]
Breaths/min	12	16	19	28	26
Tidal volume, mL	625	813	1,000	1,429	1,923
Minute ventilation, L/min	7.5	13	19	40	50

[a]de Winter-Sorkina and Cassee (2002).
[b]ICRP (1994).

When individuals increase their ventilation with activity the total number of particles inhaled per unit time (i.e., exposure rate) increases, but the fractional deposition of particles in each breath also changes with breathing pattern. Figure 4-11 illustrates the particle deposition at two breathing patterns in both a human and mouse. During exercise, both V_T and *f* increase. Fractional deposition for all particles increases with increased V_T. Increasing the *f*, however, decreases the fractional deposition of $PM_{2.5}$ and UFPs due to decreased time for gravitational and diffusive deposition. For particles of larger than a d^{ae} of roughly 3 μm, increasing *f* can increase the deposition fraction due to increased impaction in the extrathoracic and TB airways. Thus, it should be expected that the change in deposition fraction with activity will vary among individuals depending on the relative influences of these two variables (i.e., V_T and *f*) in a given subject and the particle size to which they are exposed.

Experimentally, the lung deposition fractions of fine particles during moderate exercise and mouth breathing are unchanged between rest and exercise (Bennett et al., 1985; Morgan et al., 1984). Löndahl et al. (2007) also found no difference in deposition fractions of particles (hygroscopic and hydrophobic; 0.013–0.290 μm mobility diameter of dry particles) between rest ($V_T = 0.72 \pm 0.15$ L; $f = 12 \pm 2$ min^{-1}) and exercise ($V_T = 2.1 \pm 0.5$ L; $f = 17 \pm 4$ min^{-1}). Kim (2000) evaluated differences in deposition of 1, 3, and 5 μm particles under varying breathing patterns (simulating breathing conditions of sleep, resting, and mild exercise). Total lung deposition increased with increasing V_T at a given flow rate and with increasing flow rate at a given breathing period. These experimental studies suggest that the total deposited dose rate (i.e., deposition per unit time) of particles will generally increase in direct proportion to the increase in minute ventilation associated with exercise.

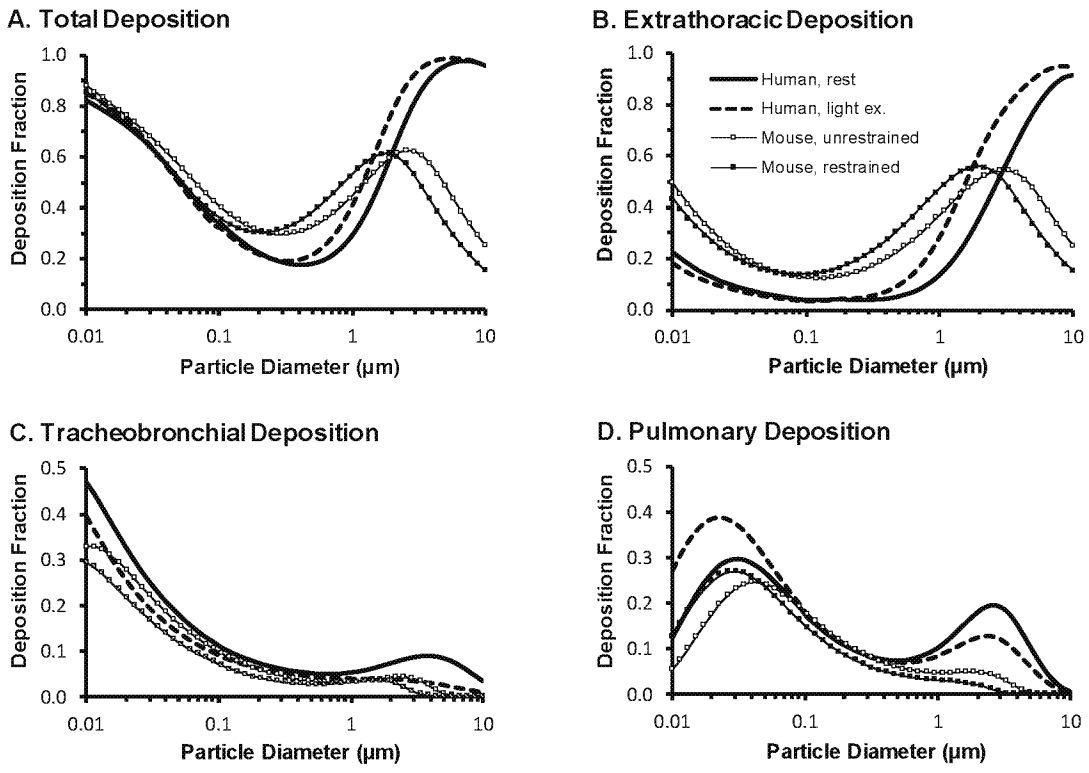

Source: Permission pending, Deposition fractions estimated using MPPD (Version 3.04) model.

Figure 4-11. Effect of increasing minute ventilation on total and regional deposition. Human, rest (V_T, 625 mL; *f*, 12 min^{-1}); Human, light exercise (V_T, 1,000 mL; *f*, 19 min^{-1}); Mouse, unrestrained (V_T, 0.19 mL; *f*, 145 min^{-1}); Mouse, restrained (V_T, 0.22 mL; *f*, 290 min^{-1}).

The changes in ventilation, i.e., breathing pattern and flow rate, may also alter the regional deposition of particles. Coarse particle deposition increases in the TB and ET regions during exercise due to the increased flow rates and associated impaction. A rapid-shallow breathing pattern during exercise may result in more bronchial airway versus alveolar deposition, while a slow-deep pattern will shift deposition to deeper lung regions (Valberg et al., 1982). Bennett et al. (1985) showed for 2.6 µm particles that moderate exercise shifted deposition from the lung periphery towards ET and larger, bronchial airways. Similarly, Morgan et al. (1984) showed that even for fine particles (0.7 µm) TB deposition was enhanced with exercise. This shift in deposition toward the bronchial airways results in a much greater dose per unit surface area of tissue in those regions. Morgan et al. (1984) also found that the apical-to-basal distribution of fine particles increased with exercise, i.e., a shift towards increased deposition in the lung apices. This shift may be less likely for larger particles, however, whose deposition

in large airway bifurcations may preclude their transport to these more apical regions (Bennett et al., 1985).

4.2.4.2 Age

Airway structure and respiratory conditions vary with age, and these variations may alter the amount and site of particle deposition in the respiratory tract. It was concluded in the 2004 PM AQCD (U.S. EPA, 2004) that significant differences between adults and children had been predicted by mathematical models and observed in experimental studies. Modeling studies generally indicated that ET and TB deposition was greater in children and that children received greater doses of particles per lung surface area than adults. Experimental studies show lower nasal particle deposition in children than adults (see Figure 4-9). Relative to adults, children also tend to breathe more through their mouth (see Section 4.1.3 Route of Breathing) which is less efficient for removing inhaled particles than the nose (see Section 4.1.6 Thoracic and Respirable Particles). For typical activity levels and route of breathing, the 50% cut-size for the thoracic fraction is at an aerodynamic diameter of around 3 μm in adults and 5 μm in children. These findings suggest that the lower respiratory tract of children may receive a higher intake dose of ambient PM compared to adults. Recent experimental studies suggest increased lower respiratory tract deposition fraction of particles in children relative to adults, but this may be an artifact of the methodology.

As discussed in the last PM ISA (U.S. EPA, 2009), during oral breathing on a mouthpiece, Bennett and Zeman (1998) measured the deposition fraction of inhaled, fine particles (2 μm d_{ae}) in children (age 7–14 years, n = 16), adolescents (age 14–18 years, n = 11), and adults (age 19–35 years, n = 12) as they breathed the aerosol with their natural, resting breathing pattern. The deposition fraction of particles was not significantly different among age groups. Among the children, variation in deposition fractions was highly dependent on inter-subject variation in V_T, but not height which is a predictor of lung volume. However, there was no difference in deposition fractions between children and adults for these fine particles. This finding and the modeling predictions (Hofmann et al., 1989) are explained, in part, by the smaller V_T and faster breathing rate of children relative to adults for natural breathing conditions. Bennett et al. (2008) also reported measures of fine particle (1 and 2 μm) deposition at ventilation rates typical of rest and light exercise in children (age 6–10 years, n = 12) and adults (age 18–27 years, n = 11). This study also found that the deposition of 2 μm d_{ae} particles during oral breathing and under conditions of rest and light exercise did not differ significantly between children and adults. However, the DF of 1 μm d_{ae} particles during oral breathing was significantly increased in adults relative to children for both breathing rates. The authors attributed increased DF in adults to mixing of inhaled aerosol with reserve air. Deposition during nasal inhalations, were significantly increased in adults relative to children for the 2 μm particles at both breathing patterns (rest and light exercise) and for the 1 μm particles during light exercise. Across all children and adults, the deposition of both 1 and 2 μm particles was generally a function of residences time within the lungs and depth of breathing. Because children breathe at higher

minute ventilations relative to their lung volumes, the rate of deposition of fine particles normalized to lung surface area may be greater in children versus adults (Bennett and Zeman, 1998).

Rissler et al. (2017a) also measured deposition in children and adults, but who were spontaneous breathing on a mouthpiece. On average, across all particle sizes (15 nm to 5 μm), the deposition fraction tended to be greater by 11% (1-DF_{child}/DF_{adult}) in children (n = 7; 7–12 years; V_T, 0.51 ± 0.13 L; *f*, 16 ± 3 min^{-1}) than adults (n = 60; 20–67 years; V_T, 0.73 ± 0.22 L; *f*, 11 ± 3 min^{-1}). Absolute difference in the deposition fractions between children and adults were 5% for 15 nm to 50 nm particles; 3–4% for 50 nm to 1.9 μm particles; 6–10% for 1.9 μm to 5 μm particles. Generally consistent with Bennett and Zeman (1998) and Bennett et al. (2008), stepwise regression showed the best predictors of deposition for prespecified size ranges (e.g., 15–30 nm and 1.3–1.9 μm) to be V_T, time of breathing cycle, anatomic dead space, and a measure of airway resistance. For most particle sizes, deposition decreased increasing anatomic dead space; deposition increased with increasing V_T, time of breathing cycle, and airway resistance.

Olvera et al. (2012) measured hygroscopic particle deposition during spontaneous breathing on a mouthpiece in healthy men (n = 5; age, 26 ± 7 years; V_T, 0.66 ± 0.34 L; *f*, 13 ± 2 min^{-1}), healthy boys (n = 8; age, 13 ± 2 years; V_T, 0.37 ± 0.20 L; *f*, 18 ± 10 min^{-1}), and boys with asthma (n = 9; age, 12 ± 3 years; V_T, 0.38 ± 0.20 L; *f*, 16 ± 5 min^{-1}). The authors estimated a total deposition fraction for a polydisperse UFPs (median, 40 nm; GSD, 1.9) of 0.48 for the healthy children and 0.54 for the asthmatic children, the latter of which was significantly ($p = 0.002$) greater than 0.36 for the adults.

The tendencies for increased deposition in healthy children versus healthy adults in the Rissler et al. (2017a) and Olvera et al. (2012) studies could, in large part, be due to spontaneous breathing on a mouthpiece. Spontaneous breathing on a mouthpiece generally results in increases in V_T and decreases in *f* (long breathing period) relative to natural unencumbered breathing (Bennett et al., 1996). Both of these changes in breathing pattern (i.e., the increase in V_T and decrease in *f*) cause increases in deposition by diffusion and sedimentation. If these changes were equivalently affecting both children and adults, then a comparison of the relative deposition fractions may be unaffected. For natural breathing, Bennett et al. (2008) found that V_T as a fraction of resting lung volume (i.e., $V_T/(FRC + V_T)$) was not different between adults and children (0.14 ± 0.03 vs. 0.16 ± 0.04, respectively); whereas, for spontaneous breathing on a mouthpiece in the Rissler et al. (2017a) study, the different between adults and children (0.21 ± 0.16 vs. 0.25 ± 0.05, respectively) is statistically significant by a two-tailed *t*-test ($p = 0.011$) based on data in supplemental materials (Rissler et al., 2017b). Spontaneous breathing on a mouthpiece resulted in an increase in V_T relative to lung volume that was larger for children than adults which in and of itself may have led to the tendency for greater deposition in children versus adults.

In 62 healthy adults with normal lung function aged 18–80 years, Bennett et al. (1996) showed there was no effect of age on the whole lung deposition fractions of 2-μm particles under natural breathing conditions. Across all subjects, the deposition fractions were found to be independent of age, depending on breathing period ($r = 0.58$, $p < 0.001$) and airway resistance ($r = 0.46$, $p < 0.001$). In the

same adults breathing with a fixed pattern (360 mL V_T, 3.4 s breathing period), there was a mild decrease in deposition with increasing age, which could be attributed to increased peripheral airspace dimensions in the elderly.

4.2.4.3 Sex

Males and females differ in body size, conductive airway size, and ventilatory parameters; therefore, sex differences in deposition might be expected. In some of the controlled studies, however, the men and women were constrained to breathe at the same V_T and *f*. Since women are generally smaller than men, the increased minute ventilation of women compared to their normal ventilation could affect deposition patterns. This may help explain why sex related effects on deposition have been observed in some studies. As discussed in Section 4.1.3, females have a greater nasal breathing contribution than males across all ages. This reduces exposure and deposition of particles in the lower respiratory tract of females relative to males under normal breathing conditions.

(Kim and Hu, 1998) assessed the regional deposition patterns of 1-, 3-, and 5-μm particles in healthy adult males and females using controlled breathing on a mouthpiece. The total fractional deposition in the lungs was similar for both sexes with the 1-μm particle size, but was greater in women for the 3- and 5-μm particles. Deposition also appeared to be more localized in the lungs of females compared to those of males. Kim and Jaques (2000) measured deposition in healthy adults using sizes in the ultrafine mode (0.04–0.1 μm). Total fractional lung deposition was greater in females than in males for 0.04- and 0.06-μm particles. The region of peak fractional deposition was shifted closer to the mouth and peak height was slightly greater for women than for men for all exposure conditions. The total lung deposition data for these ultrafine aerosols in men and women are illustrated in Figure 4-6 in Section 4.2.2.1, data for the coarse particles are form a different study (Kim and Hu, 2006) than discussed above. As illustrated in Figure 4-6, difference between males and females were relatively well predicted by the MPPD model. These differences can generally be attributed to the smaller size of the upper airways, particularly of the laryngeal structure, and smaller airways in the lungs of females than males.

In another study by Bennett et al. (1996), the total respiratory tract deposition of 2-μm particles was examined in adult males and females aged 18–80 years who breathed with a normal resting pattern. There was a tendency for a greater deposition fractions in females compared to males. However, since males had greater minute ventilation, the deposition rate (i.e., deposition per unit time) was greater in males than in females. Bennett and Zeman (2004) found no difference in the deposition of 2-μm particles in boys versus girls aged 6–13 years (n = 36).

4.2.4.4 Body Mass Index

Bennett and Zeman (2004) expanded their measures of fine particle deposition during resting breathing to a larger group of healthy children (6–13 years; 20 boys, 16 girls) and found again that the variation in total deposition, was best predicted by V_T ($r = 0.79$, $p < 0.001$). But both V_T and resting minute ventilation increased with both height and body mass index (BMI) of the children. Interestingly, these data suggest that for a given height and age, children with higher BMI have larger minute ventilations and V_T at rest than those with lower BMI. These differences in breathing patterns as a function of BMI translated into increased deposition of fine particles in the heaviest children. The rate of deposition (i.e., particles depositing per unit time) in the overweight children was 2.8 times that of the leanest children ($p < 0.02$). Among all children, the rate of deposition was significantly correlated with BMI ($r = 0.46$, $p < 0.004$). Some of the increase in deposition fractions of heavier children may be due to their elevated V_T, which was well correlated with BMI ($r = 0.72$, $p < 0.001$).

Consistent with the findings of Bennett and Zeman (2004), ventilation rates are increased in overweight individuals compared to those of normal weight (Brochu et al., 2014). For example, median daily ventilation rates (m^3/d) are about 1.2 times greater in overweight (>85th percentile body mass index [BMI]) than normal weight children (5–10 years of age). In 35–45-year-old adult males and females, ventilation rates are 1.4 times greater in overweight (BMI $\geq$ 25 kg/m^2) than normal weight (18.5 to <25 kg/m^2 BMI) individuals. Across all ages, overweight/obese individuals respire greater amounts of air and associated pollutants than age matched normal weight individuals. As discussed in Section 4.1.3 (Route of Breathing), some studies suggest that obese children may breathe a higher fraction through the mouth than normal weight children. Increased minute ventilation, a potentially lower nasal breathing fraction, and increased DF with increasing BMI would all lead to greater rates of deposition in the lung as well.

4.2.4.5 Anatomical Variability

Anatomical variability, even in the absence of respiratory disease, can affect deposition throughout the respiratory tract. The ET region is the first exposed to inhaled particles and, therefore, deposition within this region would reduce the amount of particles available for deposition in the lungs. Variations in relative deposition within the ET region will, therefore, propagate through the rest of the respiratory tract, creating differences in calculated doses among individuals.

The influence of variations in nasal airway geometry on particle deposition has been investigated. Cheng et al. (1996) examined nasal airway deposition in healthy adults using particles ranging in size from 0.004 to 0.15 μm and at two constant inspiratory flow rates, 167 and 333 mL/s. Interindividual variability in deposition was correlated with the wide variation of nasal dimensions; in that, greater surface area, smaller cross-sectional area, and increasing complexity of airway shape were all associated

with enhanced deposition. Bennett and Zeman (2005) have also shown that nasal anatomy influences the efficiency of particle uptake in the noses of adults. For light exercise breathing conditions in adults, their study demonstrated that nasal deposition efficiencies for both 1 and 2 μm monodisperse particles were significantly less in African Americans versus Caucasians. The lesser nasal efficiencies in African-Americans were associated with both lower nasal resistance and less elliptical nostrils compared to Caucasians.

Within the lungs, the branching structure of the airways may also differ between individuals. Zhao et al. (2009) examined the bronchial anatomy of the left lung in patients (132 M, 84 W; mean age 47 years) who underwent conventional thoracic computed tomography scans for various reasons. At the level of the segmental bronchus in the upper and lower lobes, a bifurcation occurred in the majority of patients. A trifurcation, however, was observed in 23% of the upper and 18% of the lower lobes. Other more unusual findings were also reported such as four bronchi arising from the left upper lobe bronchus.

Anatomic variability is also seen in other species. Miller et al. (2014) provide noticeably differing TB morphologies between two Sprague-Dawley rats of quite similar weight and lung volume. Although the patterns of depositing between lung regions were nearly identical, the morphometric differences in the TB airways caused slightly increased deposition (1−4% absolute difference) of 1 to 3 μm in this region of one rat relative to the other. However, across rat strains, Miller et al. (2014) found large differences in deposition patterns across all particle sizes (0.01−10 μm) with Sprague-Dawley having increased TB and decreased PU particle deposition relative to a Long-Evans rat. For example, with endotracheal exposure the deposition fractions in the TB region for 0.03 and 3 μm particles were 30 and 80% (respectively) in the Sprague-Dawley, whereas they were only 10 and 30% (for 0.03 and 3 μm, respectively) in the Long-Evans rat. However, the PU deposition was much greater for particles <0.1 and >1 μm in the Long-Evans than the Sprague-Dawley rat. More interesting, for the case of an endotracheal exposure, particles >3 μm were able to penetrate through the TB airways to deposit in the PU region of the Long-Evans rat, whereas the PU deposition was effectively zero by 4 μm in the Sprague-Dawley.

As described in Section 4.2.2.4, deposition can be highly localized near the carinal ridge of bifurcations. The effect of a bifurcation versus other branching patterns on airflow patterns and particle deposition has not been described in the literature. Martonen et al. (1994) showed that a wide blunt carinal ridge shape dramatically affected the flow stream lines relative to a narrower and more rounded ridge shape. Specifically, there were high flow velocities across the entire area of the blunt carinal ridge versus a smoother division of the airstream in the case of the narrow-rounded ridge shape. The implication may be that localized particle deposition on the carinal ridge would increase with ridge width. A similar situation might be expected for a trifurcation versus a bifurcation. These differences in branching patterns provide a clear example of anatomical variability among individuals that might affect both air flow patterns and sites of particle deposition.

4.2.4.6 Ventilation Distribution

Regional deposition in excess of regional ventilation to poorly ventilated areas has been reported for aerosols in the 0.5 to 1.0 μm size range and attributed to increased residence time in obstructed areas (Susskind et al., 1986; Trajan et al., 1984). However, others show increasing deposition with increasing ventilation. For instance, a significant association of increased aerosol (1.2 μm) deposition in better ventilated regions has been observed in lung transplant patients with bronchiolitis obliterans (O'Riordan et al., 1995). The trend for increased aerosol (0.78 μm) deposition with increasing ventilation has also been reported in normal individuals and asymptomatic smokers (Chamberlain et al., 1983). Other studies using similar sized aerosols, have found no association between ventilation distribution and particle deposition (O'Riordan and Smaldone, 1994; Smaldone et al., 1991). All of these studies compared regional ventilation to the regional particle deposition using scintigraphic methods. The mixed results in these studies may be due to deposition not having a simple monotonic relationship with ventilation.

Brown et al. (2001) examined the relationship of 5 μm particles in healthy adults (n = 11) and patients with cystic fibrosis (n = 12) using scintigraphic techniques. Deposition of particles in the TB airways followed the pattern of ventilation in the healthy individuals, whereas it was inversely related to ventilation in the patients. This is consistent with Kim et al. (1983) who found the pattern of particle deposition (3.0 μm) followed ventilation distribution in a three generation model, but was enhanced in the vicinity of obstructions. Consistent with Brown et al. (2001) data in healthy individuals, Verbanck et al. (2016) recently found experimentally and using CFD modeling that the regional deposition of coarse particles (6 μm) followed regional ventilation in a human airway cast which extended out to the fifth airway generation at inspiratory flows mimicking light and heavy exercise.

In the alveolar region, Brown et al. (2001) found deposition very strongly associated with ventilation distribution in the patients, i.e., the well-ventilated regions received increased alveolar deposition of particles relative to poorly ventilated regions. A similar trend was observed in the healthy individuals, but a more uniform pattern of ventilation lead to smaller differences in ventilation and deposition between lung regions. The recent experimental study of healthy adults (n = 7) by Sá et al. (2017) supports that alveolar deposition of coarse particles (5 μm) is directory proportional ventilation. As extreme example of no regional ventilation in patients with mild-to-moderate asthma, (King et al., 1998) reported large wedge-shaped regions of the lung which were absent the deposition of 0.12 μm particles.

With regard to interpreting the above discussion of coarse particle (5−6 μm) deposition in the lungs, it should be stress that the experimental and modeling work done with oral breathing on a mouthpiece. Referring back to Section 4.1.6 and Figure 4-3, these coarse particles would not be expected to reach the lower respiratory tract during nasal breathing.

4.2.4.7 Respiratory Tract Disease

The presence of respiratory tract disease can affect airway structure and ventilatory parameters, thus altering deposition compared to that occurring in healthy individuals. The effect of airway diseases on deposition has been studied extensively, as described in the 1996 and 2004 PM AQCD (U.S. EPA, 2004, 1996) and the 2009 PM ISA (U.S. EPA, 2009). Studies described therein showed that people with chronic obstructive pulmonary disease (COPD) had very heterogeneous deposition patterns and differences in regional deposition compared to healthy individuals. People with obstructive pulmonary diseases tended to have greater deposition in the TB region than did healthy people. Furthermore, there tended to be an inverse relationship between bronchoconstriction and the extent of deposition in the alveolar region, whereas total respiratory tract deposition generally increased with increasing degrees of airway obstruction. There are some limited new data available for children with asthma.

Olvera et al. (2012) measured hygroscopic particle deposition during spontaneous breathing on a mouthpiece in healthy men (n = 5; age, 26 ± 7 years; V_T, 0.66 ± 0.34 L; *f*, 13 ± 2 min^{-1}), healthy boys (n = 8; age, 13 ± 2 years; V_T, 0.37 ± 0.20 L; *f*, 18 ± 10 min^{-1}), and boys with asthma (n = 9; age, 12 ± 3 years; V_T, 0.38 ± 0.20 L; *f*, 16 ± 5 min^{-1}). The children with asthma had about 2–4% (absolute difference) greater deposition than healthy children for particles between 10–90 nm, and above this size the data converged. Across all particles sizes, the children with asthma had 8% (absolute difference) greater deposition than adults, this difference ranged from 3% for 11 nm particles to 10% for 200 nm particles. The authors estimated a total deposition fraction for a polydisperse UFPs (median, 40 nm; GSD, 1.9) of 0.48 for the healthy children and 0.54 for the asthmatic children, the latter of which was significantly ($p = 0.002$) greater than 0.36 for the adults. As discussed in Section 4.2.4.2, spontaneous breathing on a mouthpiece may have resulted in an increase in V_T relative to lung volume that was larger for children than adults which may have led to the tendency for greater deposition in children versus adults. It is not clear if asthma additionally affected breathing patterns. A prior study of adults using a fixed breathing pattering showed a greater deposition fraction of 1 μm particles in individuals with asthma relative to healthy adults (22 vs. 14%, respectively) (Kim and Kang, 1997).

The vast majority of deposition studies in individuals with respiratory disease have been performed during controlled breathing, i.e., all subjects breathed with the same V_T and *f*. However, although resting V_T is similar or elevated in people with COPD compared to healthy individuals, the former tend to breathe at a faster rate, resulting in higher than normal tidal peak flow and resting minute ventilation. Thus, given that breathing patterns differ between healthy and obstructed individuals, particle deposition data for controlled breathing may not be appropriate for estimating respiratory doses or dose rates from ambient PM exposures.

Bennett et al. (1997) measured the fractional deposition of insoluble 2 μm particles in moderate-to-severe COPD patients (n = 13; mean age 62 years) and healthy older adults (n = 11; mean age 67 years) during natural resting breathing. COPD patients had about a 1.6-times greater deposition fraction and a 1.5-times greater resting minute ventilation relative to the healthy adults. As a result, the

patients had an average deposition rate of about 2.4-times that of healthy adults. Similar to previously reviewed studies (U.S. EPA, 2004, 1996), these investigators observed an increase in deposition with an increase in airway resistance, suggesting that deposition increased with the severity of airway disease. Across a broad range of obstructive disease severity using a fixed breathing pattern, Kim and Kang (1997) previously reported the deposition of 1 μm particles to be well associated with several measures of lung function.

Brown et al. (2002) measured the deposition of UFPs (CMD = 0.033 μm) during natural resting breathing in 10 patients with moderate-to-severe COPD (mean age 61 years) and nine healthy adults (mean age 53 years). The COPD group consisted of seven patients with chronic bronchitis and three patients with emphysema. The total deposition fraction in the bronchitic patients (DF, 0.67) was significantly ($p < 0.02$) greater than in either the patients with emphysema (DF, 0.48) or the healthy subjects (DF, 0.54). Minute ventilation increased with disease severity (healthy, 5.8 L/min; chronic bronchitic, 6.9 L/min; emphysema, 11 L/min). Relative to the healthy subjects, the average dose rate was significantly ($p < 0.05$) increased by 1.5 times in the COPD patients, whereas the average deposition fraction only tended to be increased by 1.1 times. These data further demonstrate the need to consider dose rates (which depend on minute ventilation) rather than just deposition fractions when evaluating the effect of respiratory disease on particle deposition and dose.

Most of the available literature on particle deposition in the diseased lung have considered obstructive lung disease. There are some limited data showing ultrafine and fine particle (0.02–0.25 μm) deposition fractions are similar between healthy adults and those with restrictive lung disease (Anderson et al., 1990). However, individuals with restrictive lung disease have an increased minute ventilation relative to individuals with normal lungs (Tobin et al., 1983b). Thus, as described above for individuals with obstructive disease, it should be expected that dose rate for particulate matter would be increased in individuals with restrictive lung disease due to their increased ventilation rates comparted to individuals free of lung disease.

4.2.4.8 Particle Hygroscopicity

In an individual during controlled breathing (V_T = 0.75–1.0 L; f = 15 min^{-1}), Tu and Knutson (1984) found minimal deposition in the range of 0.06 to 0.09 μm for hygroscopic particles, whereas it was in the range 0.3 to 0.6 μm for hydrophobic particles. The deposition curves for hygroscopic and hydrophobic particles intersected at approximately 0.15 μm in the Tu and Knutson (1984) study. This implies that hygroscopic growth reduced diffusive deposition below 0.15 μm and increased aerodynamic deposition above this particle size. Nonhygroscopic particles around 0.3 μm have minimal intrinsic mobility and low total deposition in the lungs. Hygroscopic 0.3 μm (dry diameter) salt particles will grow to nearly 2 μm in the respiratory tract and deposit to a far greater extent than hydrophobic 0.3 μm particles (Anselm et al., 1990).

Löndahl et al. (2007) measured particle deposition in 29 individuals (20 M, 9 F; median age, 25 years) who inhaled hygroscopic and hydrophobic particles between 0.013 and 0.290 μm (mobility diameter of dry particles) by mouth during spontaneous breathing (not their natural breathing pattern measured prior to being on a mouthpiece) while engaged in rest ($V_T = 0.72 \pm 0.15$ L; $f = 12 \pm 2$ min^{-1}) or exercise ($V_T = 2.1 \pm 0.5$ L; $f = 17 \pm 4$ min^{-1}). Deposition fractions for each particle type were minimally affected by sex or activity. The prior study by Tu and Knutson (1984) found the deposition curves for hygroscopic and hydrophobic particles were also generally unaffected by route of breathing. Figure 4-12 illustrates deposition curves for hygroscopic and hydrophobic particles inhaled during rest in the Löndahl et al. (2007) study. From this figure, it is seen that the growth of 0.02 to 0.03 μm hygroscopic particles lowers their diffusive deposition to that of 0.07 μm hydrophobic particles. Deposition of the hygroscopic particles reached a minimum in the range of 0.1 to 0.14 μm. Hygroscopic growth reduced diffusive deposition below 0.2 μm and increased aerodynamic deposition above this particle size.

Olvera et al. (2012) also measured hygroscopic particle deposition during spontaneous breathing on a mouthpiece in five healthy men (age, 26 ± 7 years; V_T, 0.66 ± 0.34 L; f, 13 ± 2 min^{-1}), eight healthy boys (age, 13 ± 2 years; V_T, 0.37 ± 0.20 L; f, 18 ± 10 min^{-1}), and nine boys with asthma (age, 12 ± 3 years; V_T, 0.38 ± 0.20 L; f, 16 ± 5 min^{-1}). The data for the adult males appear in Figure 4-12 for comparison with the data by Löndahl et al. (2007).

Ferron et al. (2013) provide a model for hygroscopic particle deposition in the rat lung and compare with the predicted deposition in humans (adult male only). The paper illustrates the effect of particle size on the time required to its equilibrium size in the respiratory tract. As particle size is increased from 0.05 to 0.5 and to 2.0 μm, the time to reach equilibrium increased from 0.01 s to 1 s and to 10 s, respectively. The effect of varied hygroscopicity on particle equilibrium size and deposition were also provided. For example, given the same inhaled particle size, sodium chloride grows to about twice as large as zinc sulfate. Relative to hydrophobic particles, total deposition decreased for sodium chloride particles <0.3 μm and decreased for zinc sulfate particles <0.4 μm due to the reduction in diffusivity with increasing size due to particle growth. Above these sizes (i.e., 0.3 to 0.4 μm), total deposition increased due to the increase in inertial properties relative to hydrophobic particles. The reduction in diffusive deposition and increase in inertial deposition were more pronounced for sodium chloride than zinc sulfate relative to hydrophobic particles. For relaxed, resting breathing, Ferron et al. (2013) predicted that hygroscopic growth would affect deposition mainly for particles between 0.02 and 5 μm in the rat and between 0.02 and 6 μm in adult human males.

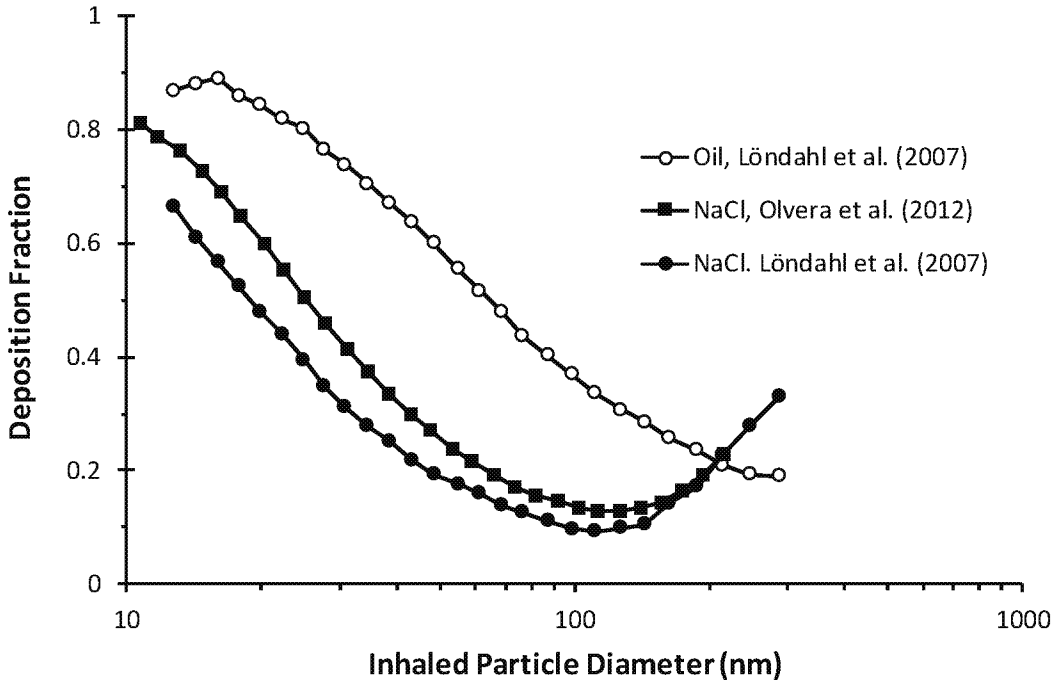

Source: Permission pending, Adapted from Löndahl et al. (2007) and Olvera et al. (2012).

Figure 4-12. Total deposition fraction of hygroscopic sodium chloride (NaCl) and hydrophobic diethylhexylsebacate oil aerosols in adults during oral breathing at rest as a function of dry particle diameter.

4.2.5 Summary

Particle deposition in the respiratory tract occurs predominantly by diffusion, impaction, and sedimentation. Deposition is minimal for particle diameters in the range of 0.1 to 1.0 μm, where particles are small enough to have minimal sedimentation or impaction and sufficiently large so as to have minimal diffusive deposition. In humans, total respiratory tract deposition approaches 100% for particles of roughly 0.01 μm due to diffusive deposition and for particles of around 10 μm due to the efficiency of sedimentation and impaction.

The first line of defense for protecting the lower respiratory tract from inhaled particles is the nose and mouth. Nasal deposition approaches 100% in the average human for 10 μm particles. Experimental studies show lower nasal particle deposition in children than adults. Relative to adults, children also tend to breathe more through their mouth which is less efficient for removing inhaled particles than the nose. These findings suggest that the lower respiratory tract of children may receive a higher dose of ambient PM compared to adults. Since children breathe at higher minute ventilations

relative to their lung volumes, the rate of particle deposition normalized to lung surface area may be further increased relative to adults.

People with COPD generally have greater total deposition and more heterogeneous deposition patterns compared to healthy individuals. The observed increase in deposition correlates with increases in airway resistance, suggesting that deposition increases with the severity of airway obstruction. Destruction of peripheral airspaces, such as with emphysema, can decrease particle deposition on a breath by breath basis. However, COPD patients also have an increased resting minute ventilation relative to the healthy adults. This demonstrates the need to consider dose rates (which depend on minute ventilation) rather than just deposition fractions when evaluating the effect of respiratory disease on particle deposition and dose.

Modeling studies indicate that, for particles greater than ~0.01 μm, some cells located near the carinal ridge of bronchial bifurcations may receive hundreds to thousands of times the average dose (particles per unit surface area) of the parent and daughter airways. The inertial impaction of particles ≥1 μm at the carinal ridge of large bronchi increases with increasing inspiratory flows. Airway constriction can further augment the overall deposition efficiency of coarse particles at downstream bifurcations. These findings suggest that substantial doses of particles may be justified for in vitro studies using tracheobronchial epithelial cell cultures.

Our ability to extrapolate between species has improved since the 2009 ISA (U.S. EPA, 2009). However, some considerations related to coarse particles warrant comment. The inhalability of particles having of 2.5, 5, and 10 μm is 80, 65, and 44% in rats, respectively, whereas it remains near 100% for 10 μm particles in humans. In most laboratory animal species (rat, mouse, hamster, guinea pig, and dogs), deposition in the extrathoracic region is near 100% for particles greater than 5 μm. By contrast, in humans, nasal deposition approaches 100% for 10 μm particles. Oronasal breathing versus obligate nasal breathing further contributes to greater penetration of coarse particles into the lower respiratory tract of humans than rodents.

4.3 Particle Clearance

This section discusses the clearance and translocation of poorly soluble particles that have deposited in the respiratory tract. The term "clearance" is used here to refer to the processes by which deposited particles are removed by mucociliary action or phagocytosis from the respiratory tract. "Translocation" is used here mainly to refer to the movement of free particles across cell membranes and to extrapulmonary sites. In the literature, translocation may also refer to the extra and intracellular dissolution of particles and the subsequent transfer of dissociated material to the blood through extra and intracellular fluids and across the various cell membranes and lung tissues.

A basic overview of biological mechanisms and clearance pathways from various regions of the respiratory tract are presented in the following sections. Then regional kinetics of particle clearance are addressed. Subsequently, an update on interspecies patterns and rates of particle clearance is provided. The translocation of UFPs is also discussed. Finally, information on biological factors that may modulate clearance is presented.

4.3.1 Clearance Mechanisms

For any given particle size, the deposition pattern of poorly soluble particles influences clearance by partitioning deposited material between lung regions. Tracheobronchial clearance of poorly soluble particles in humans, with some exceptions, is thought (in general) to be complete within 24–48 hours through the action of the mucociliary escalator. Clearance of poorly soluble particles from the alveolar region is a much slower process which may continue from months to years.

4.3.1.1 Extrathoracic Region

Particles deposited in either the nasal or oral passages are cleared by several mechanisms. Particles depositing in the mouth may generally be assumed to be swallowed or removed by expectoration. Particles deposited in the posterior portions of the nasal passages are moved via mucociliary transport towards the nasopharynx and swallowed. Mucus flow in the most anterior portion of the nasal passages is forward, toward the vestibular region where removal occurs by sneezing, wiping, or nose blowing.

Smith et al. (2014) updates the extrathoracic clearance portion of the ICRP (1994) human respiratory tract model. Deposition in the extrathoracic regions is considered as divided among the anterior and posterior nasal passage, oropharynx, and, depending on route of breathing, the mouth. Regardless of inhaled particle size, deposition in the nasal passages is portioned to have 65% in the anterior and 35% in the posterior nose. Of the deposition in the anterior nose, 29% is cleared by nose blowing, 71% is cleared to the posterior nose from which nearly all is cleared to the gastro-intestinal (GI) tract with only 0.05% sequestered in the nose. This new model was based on a study of nasal clearance in healthy adults (8 M, 1 F; 43 ± 10 years) who inhaled ^{111}In-labeled particles of 1.5, 3, or 6 μm under conditions of rest and light exercise (Smith et al., 2011).

4.3.1.2 Tracheobronchial Region

Mucociliary clearance in the TB region has generally been considered to be a rapid process that is relatively complete by 24–48 hours post-inhalation in humans. Mucociliary clearance is frequently

modeled as a series of "escalators" moving material proximally from one generation to the next. As such, the removal rate of particles from an airway generation increases with increasing tracheal mucus velocity. Assuming continuity in the amount of mucus between airway generations, mucus velocities decrease and transit times within an airway generation increase with distal progression. Although clearance from the TB region is generally rapid, experimental evidence discussed in the 1996 and 2004 PM AQCD (U.S. EPA, 2004, 1996), showed that a fraction of material deposited in the TB region is retained much longer.

The slow-cleared TB fraction (i.e., the fraction of particles deposited in the TB region that are subject to slow clearance) was thought to increase with decreasing particle size. For instance, Roth et al. (1993) showed approximately 93% retention of UFPs (30 nm median diameter) thought to be deposited in the TB region at 24 hours post-inhalation. The slow phase clearance of these UFPs continued with an estimated half-time ($t_{1/2}$) of around 40 days. Using a technique to target inhaled particles (monodisperse 4.2 μm MMAD) to the conducting airways, Möller et al. (2004) observed that 49 ± 9% of particles cleared rapidly ($t_{1/2}$ of 3.0 ± 1.6 hours), whereas the remaining fraction cleared considerably slower ($t_{1/2}$ of 109 ± 78 days). The ICRP (1994) human respiratory tract model assumes particles ≤2.5 μm (physical diameter) to have a slow-cleared TB fraction of 50%. The slow-cleared fraction assumed by the ICRP (1994) decreases with increasing particle size to <1% for 9 μm particles. Considering the UFP data of Roth et al. (1993) in addition to data considered by the ICRP (1994), Bailey et al. (1995) estimated a slow-cleared TB fraction of 75% for UFPs. At that time, they (Bailey et al., 1995) also estimated the slow-cleared fraction to decrease with increasing particle size to 0% for particles ≥6 μm. Experimental evidence from the same group (Smith et al., 2008) showed no difference in TB clearance among humans for particles with geometric sizes of 1.2 μm versus 5 μm, but the same d_{ae} (5 μm) so as to deposit similarly in the TB airways. For at least micron-sized particles, these findings do not support the particle size dependence of a slow-cleared TB fraction. As discussed further below, much of the apparent slow-cleared TB fraction may be accounted for by differences in deposition patterns, i.e., greater deposition in the alveolar region than expected based on symmetric, bulk flow into the lungs without longitudinal mixing.

A portion of the slow cleared fraction from the TB region appears to be associated with the smaller, more distal bronchioles. For large particles (d_{ae} = 6.2 μm) inhaled at a very slow rate to theoretically deposit mainly in small ciliated airways, 50% had cleared by 24 hours post-inhalation. Of the remaining particles, 20% cleared with a $t_{1/2}$ of 2.0 days and 80% with a $t_{1/2}$ of 50 days (Falk et al., 1997). Using the same techniques, Svartengren et al. (2005) also reported the existence of long-term clearance in humans from the small airways. It should be noted that the clearance rates for the slow-cleared TB fraction still exceeds the clearance rate of the alveolar region in humans. Kreyling et al. (1999) targeted inhaled particle (2.5 μm) deposition to the TB airways of adult beagle dogs and subsequently quantified particle retention using scintigraphic and morphometric analyses. Despite the use of shallow aerosol bolus inhalation to a volumetric lung depth of less than the anatomic dead space, 25% of inhaled particles deposited in alveoli. At 24 and 96 hours post-inhalation, more than 50% of the retained particles were in alveoli. However, 40% of particles present at 24 and 96 hours were localized to

small bronchioles of between 0.3 and 1 mm in diameter. Collectively, these studies suggest that although mucociliary clearance is fast and effective in healthy bronchi and larger bronchioles, it is less effective and sites of longer retention exist in smaller bronchioles.

The underlying sites and mechanisms of long-term retention in the bronchioles remain largely unknown. Several factors may contribute to the existence or experimental artifact of slow clearance from the smaller TB airways. Even when inhaled to very shallow lung volumes, some particles reach the alveolar region (Kreyling et al., 1999). Therefore, experiments utilizing bolus techniques to target inhaled particle deposition to the TB airways may have had some deposition in the alveolar region. This may occur due to variability in path length and the number of generations to the alveoli (Asgharian et al., 2001) and/or differences in regional ventilation (Brown and Bennett, 2004). Nonetheless, the experimentally measured clearance rates measured for the slow cleared TB fraction are faster than that of the alveolar region in both humans and canines. Thus, although experimental artifacts likely occur, they do not discount the existence of a slow cleared TB fraction. To some extent, it is possible that the slow cleared TB fraction may be due to distal bronchioles that do not have a continuous ciliated epithelium as in the larger bronchi and more proximal bronchioles. Neither path length, ventilation distribution, nor a discontinuous ciliated epithelium explains an apparently slow cleared TB fraction with decreasing particle size below 0.1 μm. As discussed in Section 4.3.3 on Particle Translocation, UFPs cross cell membranes by mechanisms different from larger (~1 μm) particles. Based on that body of literature, particles smaller than a micron may enter epithelial cells resulting in their prolonged retention, particularly in the bronchioles where the residence time is longer and distances necessary to reach the epithelium are shorter compared to that in the bronchi.

4.3.1.3 Alveolar Region

The primary alveolar clearance mechanism is macrophage phagocytosis and migration to terminal bronchioles where the cells are cleared by the mucociliary escalator. Alveolar macrophages originate from bone marrow, circulate briefly as monocytes in the blood, and then become pulmonary interstitial macrophages before migrating to the luminal surfaces. Under normal conditions, a small fraction of ingested particles may also be cleared through the lymphatic system. This may occur by transepithelial migration of alveolar macrophage following particle ingestion or free particle translocation with subsequent uptake by interstitial macrophages. Snipes et al. (1997) have also demonstrated the importance of neutrophil phagocytosis in clearance of particles from the alveolar region. Rates of alveolar clearance of poorly soluble particles vary between species and are briefly discussed in Section 4.3.2. The translocation of particles from their site of deposition is discussed in Section 4.3.3. The effect particle dissolution on retention in the alveolar region was recently reviewed by Oberdörster and Kuhlbusch (2018).

The efficiency of macrophage phagocytosis is thought to be greatest for particles between 1.5 and 3 μm (Oberdörster, 1988). The decreased efficiency of alveolar macrophage for engulfing UFPs increases the time available for these particles to be taken up by epithelial cells and moved into the inter-stitium (Ferin et al., 1992). Consistent with this supposition (i.e., translocation increases with time), an increase in titanium dioxide (TiO_2) particle transport to lymph nodes has been reported following inhalation of a cytotoxin to macrophages (Greenspan et al., 1988). Interestingly, the long-term clearance kinetics of the poorly soluble ultrafine (15−20 nm CMD) iridium (Ir) particles were found to be similar to the kinetics reported in the literature for micrometer-sized particles (Semmler-Behnke et al., 2007; Semmler et al., 2004). For rats, Semmler-Behnke et al. (2007) concluded that ultrafine Ir particles are less phagocytized by alveolar macrophage than larger particles, but are effectively removed from the airway surface into the inter-stitium. Particles are then engulfed by interstitial macrophages which then migrate to the airway lumen and are removed by mucociliary clearance to the larynx. The major role of macrophage-mediated clearance was supported by lavage of relatively few free particles versus predominantly phagocytized particles at time-points of up to 6 months. It is also possible that some free UFP as well as particle-laden macrophage were carried from interstitial sites via the lymph flow to bronchial and bronchiolar sites, including bronchial-associated lymphatic tissue, where they were excreted again into the airway lumen (Semmler-Behnke et al., 2007; Brundelet, 1965). In addition to macrophage phagocytosis and migration to the ciliated airways, these studies suggest that alveolar particle clearance via interstitial translocation and uptake into the lymphatics may be an important clearance pathway for UFP.

There is evidence that particle aggregates may disassociate once deposited in the lungs. This disassociation makes inhaled aggregate size the determinant of deposition amount and site, but primary particle size the determinant of subsequent clearance (Bermudez et al., 2002; Ferin et al., 1992; Takenaka et al., 1986). Following disaggregation, the ultrafine TiO_2 particles are cleared more slowly and cause a greater inflammatory response (neutrophil influx) than fine TiO_2 particles (Bermudez et al., 2002; Oberdorster et al., 2000; Oberdörster et al., 1994a; Oberdörster et al., 1994b; Ferin et al., 1992). (Balasubramanian et al., 2013) also suggested that disaggregation of following inhalation lead to differential organ concentration of 7 nm versus 20 nm gold particles. The differences in inflammatory effects and possibly lymph burdens between fine and ultrafine TiO_2 in many studies appear related to lung burden in terms of particle surface area and not particle mass or number (Oberdorster et al., 2000; Tran et al., 2000; Oberdorster, 1996; Oberdörster et al., 1992). There is some uncertainty related to these conclusions since the crystal form of TiO_2, anatase versus rutile, may have affected some results. Others have noted that particle surface area is not an appropriate metric across all particle types (Warheit et al., 2006). Surface characteristics such as roughness can also affect protein binding and potentially clearance kinetics, with smoother TiO_2 surfaces being more hydrophobic (Sousa et al., 2004).

4.3.2 Interspecies Clearance and Retention

There are differences between species in both the rates of particle clearance from the lung and manner in which particles are retained in the lung. For instance, based on models of mucociliary clearance from undiseased airways, >95% of particles deposited in the tracheobronchial airways of rats are predicted to be cleared by 5 hours post deposition, whereas it takes nearly 40 hours for comparable clearance in humans (Hofmann and Asgharian, 2003). As noted in Section 4.3.1.2, however, there is some evidence that a sizeable fraction of particles deposited at the bronchiolar level of the ciliated airways in humans (as well as canines) are cleared at a far slower rate. Some evidence suggests that the slow cleared TB fraction increases with decreasing particle size.

From interspecies comparisons of alveolar clearance, the path length from alveoli to ciliated terminal bronchioles may affect the particle transport rate (Kreyling and Scheuch, 2000). The average path length from alveoli to ciliated terminal bronchioles is longer in humans, monkeys, and dogs, than in sheep, rats, hamsters, and mice. Transport time and hence retention times may increase with path length. This hypothesis fits with all species in this comparison, except guinea pigs, which have a short path length yet particle retention that is nearly as long as in humans, monkeys, and dogs. However, sheep have a short path length and particle transport as fast as rodents. In general, alveolar clearance rates appear to increase with increasing path length from the alveoli to ciliated airways. This supports the important role of particle laden macrophage migration from the alveolar region to the ciliated airways with subsequent clearance from the lungs.

There are also distinct differences in the normal sites of particle retention that affect clearance pathways between species. Large mammals retain particles in interstitial tissues under normal conditions, whereas rats retain particles on epithelial surfaces and in alveolar macrophages (Snipes, 1996). The influence of exposure concentration on the pattern of particle retention in rats (exposed to diesel soot) and humans (exposed to coal dust) was examined by Nikula et al. (2001). In rats, the diesel particles were found to be primarily in the lumens of the alveolar duct and alveoli; whereas in humans, retained dust was found primarily in the interstitial tissue within the respiratory acini. With chronic high doses, there is a shift in rat's pattern of dust accumulation and response from that observed at lower doses in the lungs (Snipes, 1996; Vincent and Donaldson, 1990). Rats chronically exposed to high concentrations of insoluble particles experience a reduction in their alveolar clearance rates and an accumulation of interstitial particle burden (Bermudez et al., 2004; Bermudez et al., 2002; Warheit et al., 1997; Oberdörster et al., 1994a; Oberdörster et al., 1994b; Ferin et al., 1992). Even at lower acute doses of particles, the temporary impairment of alveolar clearance results in increased movement of particles into the interstitial tissues of rats (Snipes et al., 1997). However, the results of Semmler-Behnke et al. (2007) and other older studies (Brundelet, 1965; Gross and Westrick, 1954) suggest that alveolar particle clearance via interstitial translocation and uptake into the lymphatics may be an important clearance pathway for UFP.

Following transport of particles from the alveolar epithelium via macrophages or as free particles into interstitial tissues, fluid flow can draw particles into pulmonary lymphatics. Whether it is free particles that enter the inter-stitium and lymphatics or whether macrophage emigrate from pulmonary capillaries into the alveoli and then immigrate back into the inter-stitium after phagocyting particles has been debated since the 1870s (Gross and Westrick, 1954). Gross and Westrick (1954) demonstrated that free particles themselves can enter interstitial tissues and migrate to peribronchial (possibly via the lymphatics) and perivascular positions. Pulmonary particle clearance of via lymphatics has generally been considered minimal and its importance debated (Oberdörster, 1988). Particle transport in the pulmonary lymphatics is typically considered to terminate in lymph nodes (Stober and McClellan, 1997). Semmler-Behnke et al. (2007) concluded that, in rats, ultrafine Ir particles are less phagocytized by alveolar macrophage than larger particles, but are effectively removed from the airway surface into the inter-stitium. They further suggested that some free particles as well as particle-laden macrophage are carried from interstitial sites via the lymph flow to bronchial and bronchiolar sites, including bronchial-associated lymphatic tissue, where they are excreted again into the airway lumen.

4.3.3 Particle Translocation

Mucociliary and macrophage mediated clearance of poorly soluble particles from the respiratory tract was discussed in Section 4.3.1. There is growing evidence that a small fraction of particles may cross cell membranes and move from their site of deposition by other mechanisms. The following subsections discuss the movement of particles from the olfactory mucosa to the brain and from the luminal surfaces of the alveolar region into lung tissues and other organs. The clearance and distribution of soluble particles and soluble components of particles are also considered. There are pathways that particles could reach extrapulmonary organs by means other than direct translocation from the alveoli into the blood. For example, mucociliary clearance moves particles proximally until they are eventually swallowed. Recognizing this, the organ distribution of particles following gastrointestinal and intravenous delivery are also discussed. Finally, there are a few recent studies examining particle translocation to the fetus that are discussed.

In the last PM ISA (U.S. EPA, 2009) it was concluded that olfactory transport to the brain was likely unimportant in humans, it was not clear what portion of inhaled nanoparticles reached extrapulmonary sites via the lung's air-blood barrier versus clearance to the gastrointestinal tract with subsequent absorption and distribution to the organs, and there were data supporting translocation of poorly soluble particles from the human lung. It is now concluded that olfactory transport may be important in humans as well as rodents. A comparison of particle translocation following instillation versus ingestion also shows translocation of particles from the lungs occurs in a size dependent manner and that GI absorption of particles cleared from the respiratory tract is relatively minor route into circulation. A new human study shows that following inhalation, a small fraction of gold nanoparticles enters circulation.

4.3.3.1 Olfactory Delivery

Studies reviewed in the last PM ISA (U.S. EPA, 2009) demonstrated the translocation of soluble solutions (manganese chloride and sulfate, zinc) and poorly soluble particles (hureaulite, manganese oxide and tetroxide, silver, titanium dioxide, iridium) from the olfactory mucosa via axons to the olfactory bulb of the brain. Translocation via the axon to the olfactory bulb was observed for numerous compounds of varying composition, particle size, and solubility. Studies showed that the rate of translocation was rapid, less than an hour. The vast majority of these studies were conducted by instillation in rodents. However, DeLorenzo (1970) also observed the rapid (within 30–60 min) movement of 50 nm silver-coated colloidal gold particles instilled on the olfactory mucosa to the olfactory bulb of squirrel monkeys. Information on transport from the olfactory bulb to the olfactory tubercle, stratum, or other brain regions is limited.

Based on the diameter of the axon, the transport of insoluble particles from the olfactory mucosa via axons to the olfactory bulb should be limited to particles of less than about 200 nm (Griff et al., 2000; Plattig, 1989; De Lorenzo, 1957). These thin olfactory axons bundle into thicker filaments (aka fila olfactoria or olfactory nerves) and pass directly into the olfactory bulb through numerous foramina in the cribriform plate of the ethmoid bone (Plattig, 1989; De Lorenzo, 1957). Analysis of 40 skulls of known age and sex by Kalmey et al. (1998) showed a reduction in the area of the foramina in the cribriform plate with increasing age that did not differ significantly between the sexes. The reduction of the foramina area with aging has been postulated as a cause of a reduced sense of smell with aging and would suggest that olfactory translocation may also decrease with age.

A number of inhalation studies have investigated the transport of soluble and poorly soluble manganese compounds to the brain of rats. While most of this discussion and the available literature focuses on transport from the olfactory mucosa, it should be noted that Lewis et al. (2005) reported an accumulation of manganese in the trigeminal ganglia in rats following a 10-day inhalation exposure to soluble manganese chloride particles. Following a 13-week inhalation exposure to 0.1 mg Mn/m^3, relative to air controls, more soluble manganese sulfate reached the olfactory bulb of rats than was observed for the less soluble manganese phosphate in the form of hureaulite (Dorman et al., 2004). Manganese concentration in the olfactory bulb increased 2.3-times with exposure to Mn sulfate and only 1.5-times with exposure to hureaulite (Dorman et al., 2004). As part of this same study, exposures to 0.01 and 0.5 mg Mn/m^3 of Mn sulfate resulted in olfactory bulb concentrations of 1.3-times and 3.5-times relative to air control, respectively. Since the inhaled hureaulite particles were 1.0–1.1 μm (physical diameter) and so not likely due to their size to move along axons, these data suggest that around 20–30% of the hureaulite was solubilized to reach the olfactory bulb. However, insufficient hureaulite was solubilized find increased Mn in the striatum as occurred following the Mn sulfate exposures of 0.1 and 0.5 mg Mn/m^3.

Using smaller sized particles, a 2-day inhalation exposure to poorly soluble manganese oxide (~30 nm) with the right nostril blocked showed an accumulation of the Mn oxide in the left olfactory bulb

(Elder et al., 2006). This study demonstrates neuronal uptake and translocation of UFPs following inhalation without particle dissolution and in the absence of mucosal injury that may occur with instillation. For a longer 12-day inhalation exposure to poorly soluble manganese oxide (~30 nm) with both nostrils patent, Elder et al. (2006) also found Mn concentration was significantly increased in several brain regions (striatum, 1.6×; frontal cortex, 1.4×; cortex, 1.2× cerebellum, 1.2×), but most notably increased in the olfactory bulb (3.4×). Additionally, following nasal instillation of particles, similar amounts of Mn were found in the left olfactory bulb of rats instilled with soluble manganese chloride (8.2 ± 3.6% of instilled) and small poorly soluble particles (30 nm; 1.5% dissolution per day) of manganese oxide (8.2 ± 0.7% of instilled) at 24 hours post instillation. This finding supports the conclusion that poorly soluble manganese particles, if of a sufficiently small size, do not need to be solubilized to reach the olfactory bulb. The slow solubilization process would have resulted lesser amounts of the manganese oxide than manganese chloride in the brain by 24 hours similar to the finding by Dorman et al. (2004) following 13 week inhalation exposures to manganese sulfate versus less soluble hureaulite described in the preceding paragraph.

Leavens et al. (2007) modeled the transport of Mn from soluble and poorly soluble particles to the olfactory bulb and stratum based on the experimental studies by Brenneman et al. (2000) and Dorman et al. (2002), respectively. In both of these experimental studies rats were exposed to Mn-aerosol for a single 90 minute period. Leavens et al. (2007) estimated that 92–93% Mn from soluble particles reached the striatum via the blood with the additional 6–8% arriving via the olfactory transport. However, only small amount of Mn reaching the olfactory bulb from the inhaled soluble Mn chloride (0.1%) and poorly soluble Mn phosphate (3.3%) particles was estimated to reach the striatum. That is, Mn reached the olfactory bulb, but generally did not proceed to the adjacent stratum. The transport of Mn to the stratum from the olfactory bulb was estimated based on data from animals where one nostril was plugged while the other was left patent. Thus, the olfactory transport of Mn to the stratum only occurs on the side of the animal with a patent nostril. Mn in that stratum on the plugged side of the animal is presumably derived from the blood. At least two issues affect the interpretation of these data. First, rats having a plugged nostril reduce their minute ventilation by about 50% (Brenneman et al., 2000), this lowers the signal to noise ratio in these studies versus animals with fully patent nostrils. Second, rather large sized particles were delivered to the rats in these studies, 2.51 μm MMAD (GSD 1.17) by Brenneman et al. (2000) and 1.68 μm MMAD (GSD 1.42) (Dorman et al., 2002). Referring back to Figure 4-4 and Figure 4-5, only a small fraction of these sized particles are expected to penetrate through the head to reach the lower respiratory tract. The majority of deposition occurs in the extrathoracic airways, in this case, the nasal passages of the rat. Although Leavens et al. (2007) attributed all Mn in the blood as derived from the lungs, Mn reaching circulation through areas such as the turbinates following nasal particle deposition should not be ignored.

More recently, Kreyling (2016) determined the fraction of iridium-192 (^{192}Ir) nanoparticles reaching the brain via transport from the upper versus the lower respiratory tract. Female Wistar-Kyoto rats (8–10 weeks old, 270-300 g body weight) were exposed to aerosols (20 nm; GSD, 1.6) via nose-only

inhalation or intratracheal inhalation. Estimates of particle translocation at 24 hours post inhalation excluded activity of particles on the skin or rapidly cleared to the gut and feces. Of the delivered particles (excluding skin and rapidly cleared), at 24 hours post inhalation, 0.012% of what deposited in the upper respiratory tract and 0.0014% of what deposited in the lower respiratory tract reached the brain. That is, there was 9-times more in the brain derived from the upper than the lower respiratory tract. The predicted deposition was 3-times higher in the alveolar region than in the upper respiratory tract for the nose-only exposure. These results suggest that olfactory transport to the brain was 27-times (i.e., 9×3) greater than translocation from the alveolar region. This work, however, does not indicate what brain regions contained particles or how those brain regions differed between the exposures.

Antonini et al. (2009) exposed rats to welding fumes (0.31 μm MMAD) via inhalation or filtered air for 10 days. The poorly soluble particles (soluble/insoluble ratio, 0.0139 in water) were composed primarily of iron (80.6%), manganese (14.7%), silicon (2.75%), and copper (1.79%). The welding fume was reported to be highly insoluble in water (pH, 7.4; 37°C) with dissolution of 1.4% in 24 hours. The most marked increases in iron, manganese, and copper relative to control were found in the lungs. There was no evidence of pulmonary inflammation or injury despite exposure to 40 mg/m^3 of welding fume. Consistent with studies described in Section 4.3.3.2 on translocation from the lungs, there was a slight increase in iron and manganese concentrations in the liver, heart, kidney, and spleen at 1-day post-exposure relative to controls. Metal content was also assessed in seven brain regions: hippocampus, cerebellum, striatum, thalamus, cortex, olfactory bulb, and midbrain. Manganese concentrations, but not iron or copper, were significantly increased relative to controls in the cortex (1.3×) and cerebellum (1.2×), and especially the olfactory bulb (2.2×). Of the brain regions examined, only the thalamus showed a slight insignificant reduction in manganese relative to controls. Interestingly, although there was only a tendency for a small increase in Mn concentrations within the striatum (1.1×), proinflammatory chemokines and cytokines were significantly increased by about 1.5 times in the striatum. The lower relative increase in the olfactory bulb in this study as compared to the Elder et al. (2006) study (2.2× vs. 3.4×, respectively) may, in part, be due to the larger inhaled particle size with only around 30−40% (assuming log-normal particle size distribution with a GSD of 2−4) of the welding fume being less than 200 nm, the particle size necessary for olfactory translocation, whereas all the particles in the Elder et al. (2006) study were well under 200 nm. Less than 5% of the welding fume would be smaller than the 30 nm particles used by Elder et al. (2006). Given the distribution of manganese among brain regions, the Antonini et al. (2009) study supports the transport of manganese from welding fume particles depositing on the olfactory mucosa to the olfactory bulb. However, finding increased Mn concentrations but not other metals in the brain, suggests the differential solubilization and mobilization of the Mn rather than the movement of particles themselves along axons to the brain.

New modeling studies contradict the conclusion in the 2009 PM ISA that between species differences may predispose rats, more so than humans, to deposition of particles in the olfactory region with subsequent particle translocation to the olfactory bulb. The 2009 conclusion was based on two main differences between rodents and primates. First, the olfactory mucosa covers approximately 50% of the

nasal epithelium in rodents versus only about 5% in primates (Aschner et al., 2005). Second, a greater portion of inhaled air passes through the olfactory region of rats relative to primates (Kimbell, 2006). More recently, Garcia et al. (2015) provided CFD simulations of total ultrafine nasal deposition as well as that in the olfactory region of humans and compared to prior simulations (Garcia and Kimbell, 2009) for rats. Rats were predicted to have greater total and olfactory deposition than humans. However, due the much higher ventilation rate of humans than rats, humans were predicted to experience greater dose rate to the olfactory mucosa for particles between 1 and 13 nm, above this size the dose rate was slightly greater in rats than humans (Section 4.2.2.2 and Figure 4-7). Schroeter et al. (2015) provided experimental replica cast data and CFD simulations for total and regional deposition of particles between 2.6 and 14.3 μm. The olfactory region was assumed to be 14% of the nasal surface area. For 5 μm to 11 μm particles inhaled during light activity (flow = 30 L/min), greater than 1% deposition in the olfactory region was predicted with a maximum of 6% predicted for 8 μm particles. During a resting inhalation (flow = 15 L/min), the predicted olfactory deposition exceeded 1% for particles between 9 and 19 μm, with a maximum of 8% for 13 μm particles. Although the larger particles would not themselves be expected to move along to axon from the olfactory region of the nose to the olfactory bulb, soluble materials associated with large particles could be solubilized and pass along the axon to the olfactory bulb. Greater particle deposition was predicted to occur in the turbinates than the olfactory region by Schroeter et al. (2015), soluble materials could also move into the blood from this well perfused area and reach the brain. These newer modeling studies suggest that ultrafine particle translocation as well as soluble components associated with all sized particles could reach the olfactory bulb of humans as well as rodents in a measurable amount depending on the exposure concentration.

Human autopsy data are becoming available that also suggest the importance of translocation of material from the olfactory mucosa to the olfactory bulb. Although their source is unknown, the presence of UFP in the olfactory bulb was reported in 2 of 35 Mexico City residents (Calderon-Garciduenas et al., 2010). Presumably metal components of urban PM, statistically significant increases in manganese, nickel, and chromium have been reported in the frontal lobe of Mexico City residents relative to lower air pollution areas (Calderón-Garcidueñas et al., 2013). More recently, Maher et al. (2016) examined magnetite particles in the frontal lobes from subjects that lived in Mexico City and Manchester, U.K. The magnetite (Fe_3O_4) particles were found in two forms: smooth spherical particles and, more rarely, as angular cuboctahedrons. The authors attributed the presence of the smooth spherical particles to inhaled ambient combustion-related particles, whereas the angular cuboctahedral particles were attributed to endogenous formation. The spherical particles showed a median diameter around 14−18 nm with a maximum size of about 150 nm, sizes that can be transported to the olfactory bulb from the olfactory mucosa. As discussed in Section 4.3.3.2, some of these particles may have also reached the brain via the circulation following deposition in the alveolar region of the lung. The combined literature for animal toxicological studies, CFD modeling studies, and human autopsy data support the existence of olfactory translocation in animals and suggest its relevance in humans. Although olfactory translocation is rapid with particles appearing in the olfactory bulb within an hour following instillation on the olfactory mucosa, the relative amount of particles translocated is relatively small. For example, based on Garcia et

al. (2015) only 0.001% of 20 nm particles would potentially deposit on the olfactory mucosa in humans at rest or 0.03% in rats. Based on Elder et al. (2006), around 10% of the particles on the olfactory mucosa would translocate to the olfactory bulb. Thus, only a small fraction of poorly soluble particles inhaled through the nose might be expected to reach the olfactory bulb via the axons in humans or rats. However, absolute number of particles potentially reaching the olfactory bulb over time can be considerable (see Figure 4-7).

4.3.3.2 Pulmonary Delivery

4.3.3.2.1 Membrane Translocation

It was first demonstrated by Gross and Westrick (1954) that free particles can enter interstitial tissues and migrate to peribronchial (possibly via the lymphatics) and perivascular positions. Both in vitro and in vivo studies support the rapid (≤1 hour) translocation of free ultrafine TiO_2 particles across cell membranes (Geiser et al., 2005; Churg et al., 1998; Ferin et al., 1992). Geiser et al. (2005) conducted a detailed examination of the disposition of inhaled ultrafine TiO_2 in 20 healthy adult rats. They found that distributions of particles among lung tissue compartments appeared to follow the volume fraction of the tissues and did not significantly differ between 1 and 24 hours post-inhalation. Averaging 1 and 24-hour data, 79.3 ± 7.6% of particles were on the luminal side of the airway surfaces, 4.6 ± 2.6% were in epithelial or endothelial cells, 4.8 ± 4.5% were in connective tissues, and 11.3 ± 3.9% were within capillaries. Particles within cells were not membrane bound. It is not clear why the fraction of particles identified in compartments such as the capillaries did not differ between 1 and 24 hours post-inhalation. These findings were consistent with the smaller study of five rats by Kapp et al. (2004) who reported identifying TiO_2 aggregates in a Type II pneumocyte; a capillary close to the endothelial cells; and within the surface-lining layer close to the alveolar epithelium immediately following a 1 hour exposure. These studies effectively demonstrate that some inhaled ultrafine TiO_2 particles, once deposited on the pulmonary surfaces, can rapidly (≤1 hour) translocate beyond the epithelium and potentially into the vasculature.

A few studies have characterized differences in the behavior of fine and UFPs in vitro. Geiser et al. (2005) found that both ultrafine and fine (0.025 μm gold, 0.078 μm TiO_2, and 0.2 μm TiO_2) particles cross cellular membranes by nonendocytic (i.e., not involving vesicle formation) mechanisms such as adhesive interactions and diffusion, whereas the phagocytosis of larger 1 μm TiO_2 particles is ligand-receptor mediated. Gross and Westrick (1954) surmised that free particle translocation from the alveolar surface to interstitial tissues may be limited to smaller fine particles (<0.5 μm). Edetsberger et al. (2005) found that UFPs (0.020 μm polystyrene) translocated into cells by first measurement (~1 min after particle application). Intracellular agglomerates of 88−117 nm were seen by 15−20 min and of 253−675 nm by 50−60 min after particle application. These intracellular aggregates were thought to result

from particle incorporation into endosomes or similar structures since Genistein or Cytochalasin treatment generally blocked aggregate formation. Interestingly, particles did not translocate into dead cells, rather they attached to the outside of the cell membrane. Amine- or carboxyl-modified surfaces (46 nm polystyrene) did not affect translocation across cultures of human bronchial epithelial cells with about 6% regardless of the surface characteristics (Geys et al., 2006).

4.3.3.2.2 Extrapulmonary Distribution

Soluble material can move rapidly from the alveolar surface into the blood, but poorly soluble particles generally remain in the lung for an extended period of time. A number of human studies are available confirming that the majority of poorly soluble UFP deposited in the alveolar region undergo slow clearance and do not rapidly enter circulation. However, animal studies (primarily of rats) show that UFPs cross cell membranes by mechanisms different from larger (~1 μm) particles and that a small fraction of these particles enter capillaries and distribute systemically. Some evidence suggests that a small degree of pulmonary inflammation increases interstitial hydraulic pressure sufficiently to exceed pulmonary capillary pressure, resulting in a flux of fluid and any associated particles or fibers into pulmonary capillaries (Miserocchi et al., 2008). This is consistent with the presence of airway inflammation in a variety of airway diseases (e.g., asthma, fibrosis, ARDS, pulmonary edema, inflammation from smoking) and altered epithelial integrity, allowing more rapid movement of solutes into the bloodstream [see Section 4.4.2 of U.S. EPA (2009)]. In general, increased alveolar permeability to ^{99m}Tc-DTPA is associated with any lung syndrome characterized by pulmonary edema. Fluid flow and particle migration would be from the alveolar surface into the inter-stitium as inflammation and edema resolve.

Several human studies have investigated the pulmonary retention of radiolabeled UFPs (Wiebert et al., 2006a; Brown et al., 2002; Roth et al., 1994) or fine aggregates of UFPs (Möller et al., 2008; Mills et al., 2006; Wiebert et al., 2006b; Roth et al., 1997; Burch et al., 1986). All of these studies used technician-99m (^{99m}Tc; $t_{1/2}$ = 0.25 days; pure gamma emitter) labeled carbon, except for Roth et al. (1994) who used indium-111 (^{111}In; $t_{1/2}$ = 2.8 days; pure gamma emitter) oxide. All of these studies reported ≥80% pulmonary retention of particles at 24 hours post-inhalation. However, of the fraction cleared from the lungs in the studies using ^{99m}Tc-labeled particles, it is not entirely clear how much was deposited in the ciliated airways and cleared versus how much of the radiolabel leached from the particles and was cleared in its soluble pertechnetate form. Highly soluble in normal saline, pertechnetate clears rapidly from the lung with a $t_{1/2}$ of ~10 min and accumulates most notably in the bladder, stomach, thyroid, and salivary glands (Isawa et al., 1995; Monaghan et al., 1991). Wiebert et al. (2006a) were able to reduce leaching of the ^{99m}Tc-labeled carbon (35 nm CMD inhaled) and found effectively 100% retention at 24 hours post-inhalation. Similarly, Wiebert et al. (2006b) minimized leaching of ^{99m}Tc-labeled carbon (87 nm CMD inhaled) and found negligible particle clearance from the lungs by 70 hours post-inhalation. Using the longer half-life ^{111}In-oxide aerosol (18 nm CMD), Roth et al. (1994) found 93% retention in the

human lung at 24 hours and 80% retention at 9 days post inhalation. ^{111}In-oxide is poorly soluble and as such was not expected to move into circulation as pertechnetate does. The 7% clearance of the 18 nm ^{111}In-oxide versus near 0% clearance of the 35 nm ^{99m}Tc-labeled carbon may be, in part, caused by a more proximal deposition pattern of the smaller particles (see Figure 4-5C). These human data show that the majority of poorly soluble UFP remain in the lung.

Miller et al. (2017) investigated the translocation of gold nanoparticles having primary particle sizes of approximately 4–5 nm and 34 nm in a series of two separate inhalation experiments involving young healthy adults. In experiment one, 14 young healthy adult males inhaled (3.8 nm primary particle size) 18.7 nm agglomerates (1.5 GSD) via a face mask for 2 hours with intermittent exercise (exercise target of 25 L/min/m^2 body surface area, BSA). By 15 minutes post-exposure, gold was identified in the blood of three subjects. Gold was found in the blood of 12 subjects at 6 hours, 11 subjects at 24 hours, and 7 subjects at 3 months post-exposure.[45] Gold was also identified in the urine in an unspecified number of subjects at 24 hours and 3 months post-exposure. In experiment two, groups of healthy adult males inhaled gold nanoparticles with primary particle sizes of 4.1 nm (n = 10 subjects) and 34 nm (n = 9 subjects) as agglomerates of 17.8 nm (GSD, 1.2) and 52.4 nm (GSD, 1.4). The authors observed higher gold concentrations in the blood following inhalation of the smaller than larger primary sized particles. However, relative to the larger particles, the aerosol concentration of the smaller sized particles was, on average, 1.3 times higher (192 vs. 146 μg/m^3) and the predicted deposition is about double (total deposition fractions are 72 and 35% for smaller and larger agglomerates, respectively), leading to an estimated 2.7 times greater dose of the smaller sized particles.[46] This difference in delivered dose may have been adequate to account for differences in the amounts of gold in the blood out to 7 days post-exposure, but not necessarily at the 28 day time point. The authors also observed gold in urine for the smaller particles, but gold in urine was below the limit of detection for the larger particles. The relatively small estimated difference in delivered doses does not appear sufficient to large differences in gold in urine by 28 days post-exposure. This study demonstrates the presence of gold in the blood and urine of humans following the inhalation of gold nanoparticles.

The finding of material in the blood in this human study, Miller et al. (2017), but not prior human studies described above may, in part, be a matter of an increased signal to noise afforded in this new work and/or an indication that there is a difference in particle translocation from the lung depending on the inhaled particle type. There is uncertainty related to the actual fraction of the deposited dose that translocated from the lungs and interpretation of study results. Using data from experiment one (described above), based on the concentration of gold in urine (35 ng/L) at 24 hours and average urinary volume of

[45] The number having detectable gold in blood is based on Figure 1C of Miller et al. (2017).

[46] Deposition estimated using the MPPD model (Version 3.04) for exposure to 17.8 nm (GSD, 1.2) or 52.4 nm (GSD, 1.4) particle agglomerates during two hours of intermittent exercise with 15-minute periods of exposure at rest (V_T, 0.800 L; f, 15 min^{-1}) and 15-minute periods of exposure during exercise (V_T = 1.923 L; f = 26 min^{-1}) and default airway morphology for an adult male (i.e., Yeh/Schum symmetric morphology, FRC of 3.3 L, and upper respiratory tract volume of 0.05 L). A BSA of 2.0 m^2 was assumed (not provided by authors). The breathing pattern for rest was selected to have a minute ventilation of 6 L/min per m^2 BSA based on Mcdonnell et al. (2012). The heavy exercise breathing pattern was selected from ICRP (1994).

2.4 L, it can be estimated that about 84 ng gold was excreted from the body. This can be used as a lower end estimate of translocation from the lungs since (as described below) there is evidence from animal studies of particle accumulation in various organs. Based on the exposure concentration of 116 μg/m^3 and the ventilation rates of 12 L/min at rest and 50 L/min during exercise, the total amount of aerosol inhaled was 430 μg gold. The estimated total deposition fraction of the 18.7 nm (GSD 1.5) agglomerates is 60%.[47] The alveolar deposition fraction during periods of rest and exercise are about 30 and 40%, respectively, giving combined volume-weighted alveolar deposition fraction of 38% of the inhaled aerosol. Based on total deposition, about 0.03% translocation may have occurred given the urinary excretion at 24 hours (i.e., 0.084/256). It may be more appropriate to consider deposition in the alveolar region since the movement of particles from the gastrointestinal tract into circulation is minimal by comparison to that from the alveolar region (Kreyling et al., 2014). Translocation from the alveolar deposition to urinary excretion at 24 hours is estimated to be around 0.05% (i.e., 0.084/163). Based on the log-log plot in Figure 3i of Kreyling et al. (2014), excretion via urine as a percent of material in the lungs not cleared in 24 hours by mucus clearance in rats is about 0.42% for 2.8 nm particles and 0.006% for 5 nm particles, which provides an estimate of 0.05% for 3.8 nm particles by linear interpolation on log-log scale. The comparisons developed herein place the urinary elimination by 24 hours of 3.8 nm gold particles in humans by Miller et al. (2017) as nearly identical to those obtained in rats by Kreyling et al. (2014).

A greater amount of information on particle translocation from the lungs is available from animal studies. These studies fairly consistently show that a small portion (generally <1%) of particles delivered to the lungs via inhalation or instillation are translocated from the pulmonary surfaces to extrapulmonary organs. For example, as reviewed in the last PM ISA (U.S. EPA, 2009), extrapulmonary translocation was described for poorly soluble ultrafine gold and Ir particles. In male Wistar-Kyoto rats exposed by inhalation to ultrafine gold particles (5–8 nm), Takenaka et al. (2006) reported a low, but significant, fraction (0.03 to 0.06% of lung concentration) of gold in the blood from 1 to 7 days post inhalation. Semmler et al. (2004) also found small but detectable amounts of poorly soluble Ir particle (15 and 20 nm CMD) translocation from the lungs of female Wistar-Kyoto rats to secondary target organs like the liver, spleen, brain, and kidneys. Each of these organs contained about 0.2% of deposited Ir. The peak levels in these organs were found 7 days post inhalation. The translocated particles were largely cleared from extrapulmonary organs by 20 days and Ir levels were near background at 60 days post inhalation. Particles may have been distributed systemically via the gastrointestinal tract. Immediately after the 6-hour inhalation exposure, 18 ± 5% of the deposited Ir particles had already cleared into the gastrointestinal tract. After 3 weeks, 31 ± 5% of the deposited particles were retained in the lung. By 2 and 6 months post inhalation, lung retention was 17 ± 3 and 7 ± 1%, respectively. The particles appeared

[47] For 18.7 nm (GSD 1.5) using MPPD (Version 3.04) with intermittent exercise as described for Experiment Two. Although the authors provided a BSA of 2.76 m^2 in their Table S1, a BSA of 2.0 m^2 was assumed as a more reasonable value for males being 180 cm height and 79 kg mass. Breathing patterns used for Experiment Two were used again here.

to be cleared predominantly from the peripheral lung via the mucociliary escalator into the GI tract and were found in feces.

A considerable number of new studies have become available since the last PM ISA (U.S. EPA, 2009). Studies continue to show the translocation of a small fraction of particles following inhalation or instillation increases with decreasing particle size (Kreyling et al., 2014; Kreyling et al., 2009). However, the dissolution of poorly soluble particles increases with decreasing pH and decreasing particle size (Kreyling et al., 2002; Kreyling and Scheuch, 2000; Kreyling, 1992). Dissolution and absorption of UFPs in the gastrointestinal tract subsequent to clearance from the respiratory tract cannot be fully discounted as contributing to organ concentrations of inhaled or instilled particles. The organ distribution of particles may differ depending on the route by which they are reaching circulation. For example, in humans, the liver receives about 6.5% of arterial blood flow and all blood flow coming from the GI tract (ICRP, 2002). Additionally, the proteins that particles may encounter and potentially bind to will vary depending on the route by which they entered circulation. Recognizing such issues, a series of experiments have been conducted to quantify translocation using a ^{198}Au gamma-spectrometry[48] in female Wistar-Kyoto rats (8−10 weeks old, 250 g body weight) of negatively charged gold nanoparticles of 1.4, 2.8, 5, 18, 80, and 200 nm primary particle size and positively charged 2.8 nm primary particle size following intratracheal instillation (Kreyling et al., 2014), ingestion (Schleh et al., 2012), and intravenous delivery (Hirn et al., 2011). Although additional studies have become available since the last PM ISA, the primary focus will be on the careful comparison across these routes of delivery.

Following particle instillation, Kreyling et al. (2014) measured translocation from the lungs as a function of peripheral lung dose (i.e., ignoring particles found in the trachea, GI tract, and feces). Translocation from the lung by 24 hours of particles with a negative surface charge decreased from 5.6% for 1.4 nm particles, to 3.2% for 2.8 nm, to 0.22% for 5 nm, to 0.12% for 18 nm, to only 0.06% for 80 nm, and 0.2% for 200 nm particles.[49] Most of the translocation from the lungs appears to have occurred within 1−3 hours post-instillation, but continued up to 24 hours for the largest, 200 nm particles. The estimated translocation excluded the fraction of particles found in the trachea, GI tract and feces by 24 hours post-instillation, which was 30% (averaged across all particle sizes) of the instilled dose.[50] Potential GI tract absorption was considered negligible since a prior study by Schleh et al. (2012) of particle ingestion found only a small fraction of particles entered circulation (0.37% for 1.4 nm particles, 0.37% for 2.8 nm, 0.05% for 5 nm, 0.12% for 18 nm, 0.03% for 80 nm, and 0.01% for 200 nm particles).[51] Considering the fraction of instilled particles found in GI tract and feces and GI absorption of particles, about 4% (median of all particle sizes) to 7% (mean of all particle sizes) of the apparent translocation from the lung may have derived from the GI tract (i.e., 93−96% of the particles appearing in

[48] Gamma-spectrometry is a highly sensitive technique relative to inductively coupled plasma mass spectrometry.
[49] Values from Figures 2B and 6A of Kreyling et al. (2014) for the 24-hour time point.
[50] Data from Supplement Table S1 of Kreyling et al. (2014) for the 24-hour time point.
[51] Data estimated from Table III of Schleh et al. (2012).

circulation were derived from the lung).[52] For both instillation and ingestion, less positively charged than negatively charged 2.8 nm particles entered circulation. The organ distribution of particles following intravenous administration differed greatly from instillation. At 24 hours post intravenous delivery, 51% of 1.4 nm particles, 82% of 2.8 nm particles, and 92–97% of 5–200 nm particles were found in the liver (Hirn et al., 2011). Of the material translocating from the lungs following instillation, independent of particle size, only about 10% of particles are found in the liver with the majority (43% of 1.4 nm; 55% of 7 nm; 71% of 18 nm; 96% of 80 nm) of translocated particles found in the carcass (skeleton, soft tissues, and fat) (Kreyling et al., 2014). This difference in organ distribution following intravenous versus instillation was attributed to the proteins that particles may have encountered and bound with in the lungs prior to entering circulation. This series of studies shows that translocation of particles from the lungs occurs in a size-dependent manner, that GI absorption of particles cleared from the respiratory tract is a relatively minor route into circulation, and that organ distribution can vary depending on how particles are delivered to animals.

Following translocation from the lung or intravenous injection, particles appear to be rather rapidly cleared from the blood. This clearance from the blood occurs due to accumulation in extrapulmonary organs and elimination from the body. The blood concentrations of the smallest gold nanoparticles studied (1.4 nm) are 46% cleared in rats by one-hour post-injection and by 93% at 24 hours post-injection.[53] By 24 hours, about 10% of 1.4 nm particles had moved, in roughly equal portions, into feces and urine. Larger nanoparticles (18 and 80 nm) were roughly 99% cleared from blood by one-hour post-injection. By 24 hours post-injection, most of the organ retention, 92–97% for 5–200 nm particles, is in the liver (Hirn et al., 2011). Of these larger particles eliminated (0.1 to 1%) by 24 hours post-injection, most is via the feces.[54] Others have also reported similar dependence of organ accumulation of particle size in mice, with smaller gold nanoparticles (1.5–5 nm) persisting more in blood and excreted via urine than larger (30–70 nm) nanoparticles (Miller et al., 2017; Yang et al., 2014). This was similarly demonstrated in humans with 4.1 nm particles found in urine, but not 34.3 nm particles (Miller et al., 2017). A limited number of studies have shown the continued existence in the blood at 28 days post-delivery of inhaled gold nanoparticles (4.1 and 34.3 nm) in humans and instilled TiO_2 (70 nm) in rats (Kreyling et al., 2017b; Miller et al., 2017). It is likely that the particles in the blood at 28 days post-delivery were due to additional movement/clearance from the lungs.

The long-term health implications of translocation following acute or chronic PM exposures is uncertain. Heringa et al. (2018) recently reported the existence of TiO_2 in the livers and spleens of humans (9 F, 6 M; 84 ± 13 years) on autopsy. The average titanium content in was 40 μg/kg (TiO_2 mass/tissue mass) in the liver and 80 μg/kg in the spleen. Two of the subjects had received titanium implants, but had titanium content below the limit of detection in the liver and low amounts in the spleen

[52] Kreyling et al. (2017b) reported that at 24-hour post-instillation, 5% of TiO_2 (70 nm) reaching the blood was absorbed in the GI tract (i.e., 95% crossed the alveolar air-blood barrier). Due to long-term clearance of the lung, this percentage increased to 13% by 7 days post instillation and 21% at 28 days post instillation.
[53] Data from Table S1 of Semmler-Behnke et al. (2014).
[54] Data from Figure S4 of Semmler-Behnke et al. (2014).

relative to the other individuals. Titanium dioxide particles having diameters of 85–440 nm were identified. By count with a limit of detection at 85 nm, nearly 27% of the particles in the liver and 21% of the particles in the spleen were ≤100 nm. By count, about 75% of particles were ≤200 nm. Gamma-spectrometry studies of 70 nm TiO_2 particle translocation in rats show about 4% translocation into circulation following intratracheal instillation and about 0.6% following ingestion (Kreyling et al., 2017b; Kreyling et al., 2017c). As occurs for gold nanoparticles instillation, the translocated TiO_2 distribute around the body and accumulate in organs, but are found primarily (91% at 24-hour post instillation) in the carcass (skeleton, soft tissues, and fat). This differs from 24 hours post-intravenous injection where TiO_2 accumulates predominately (95.5%) in the liver (Kreyling et al., 2017a). Following rather high doses (25–30 mg/day) of ingested TiO_2 nanoparticles (10 nm) to rat dams from gestational day 2 to 21, pups sacrificed 1 day after birth have increased titanium content in the hippocampus (Mohammadipour et al., 2014). Quantification of translocation to fetuses is provided in Section 4.3.3.3. Particle accumulation in the liver and spleen of autopsied humans is consistent with accumulation in these organs in rodents following intratracheal instillation and ingestion of particles.

4.3.3.3 Transplacental Barrier Transport

A number of studies have become available since the last PM ISA (U.S. EPA, 2009) examining particle translocation to the fetus. The route of exposure in these studies is generally oral or intravenous delivery. These papers may be important regardless of the delivery method (with the exception of intraperitoneal) since they add biological plausibility for effects during pregnancy. However, as indicated in Section 4.3.3.2.2, the sites of accumulation differ greatly between intravenous delivery versus instillation into the lung and ingestion. Specifically, the majority of particles found in circulation following intravenous delivery accumulate in the liver, whereas as the majority of particles are found in the carcass (skeleton, soft tissues, and fat) following instillation and ingestion.

The primary focus herein is given to Semmler-Behnke et al. (2014). This study utilizes the highly sensitive ^{198}Au gamma-spectrometry technique and provides a mass balance for the full body and excrement. This study was also discussed in Section 4.3.3.2.2 and was conducted by the same German research group having many years of experience and numerous publications evaluating particle deposition, clearance, and translocation in humans and rodents. The principal finding of the Semmler-Behnke et al. (2014) study relevant to this section is the accumulation in rat fetuses following delivery of particles at gestational Day 18. This time point was selected because the nutrition of the fetus is primarily the dam's blood versus the yoke sac earlier in gestation. Following intravenous injection, 0.06% of 1.4 nm and 0.004% of 18 nm gold nanoparticles were found in fetuses. No 80 nm particles (<0.0004%, the detection limit) were found in fetuses. The authors attributed the decreasing translocation as a function of increasing particle size to the role of transtrophoblasitic channels (canaliculi of 20–25 nm in diameter) in transporting particles from the maternal blood to the fetuses. The organ distribution between pregnant and nonpregnant rats was generally similar. Yang et al. (2014) also reported similar organ distributions

between pregnant and nonpregnant animals at 5 hours post intravenous injection of gold nanoparticles (1.5, 4.5, 13, 30, and 70 nm diameter). Tsyganova et al. (2014) found increased gold content in liver and spleen of fetuses following intravenous injection of gold nanoparticles (5 and 30 nm) into pregnant rats. Following rather high doses (25−30 mg/day) of ingested TiO_2 nanoparticles (10 nm) to rat dams from gestational day 2 to 21, pups sacrificed 1 day after birth have increased titanium content in the hippocampus (Mohammadipour et al., 2014). Overall, these studies show that a small fraction of nanoparticles entering circulation may reach fetuses.

4.3.4 Factors Modulating Particle Clearance

4.3.4.1 Age

It was previously concluded that there appeared to be no clear evidence for any age-related differences in clearance from the lung or total respiratory tract, either from child to adult, or young adult to elderly (U.S. EPA, 2004, 1996). Studies showed either no change or some slowing in mucus clearance with age after maturity. Although some differences in alveolar macrophage function were reported between mature and senescent mice, no age-related decline in macrophage function had been observed in humans. A comprehensive review of the literature provided in the last PM ISA (U.S. EPA, 2009) supported a decrease in mucociliary clearance with increasing age beyond adulthood in humans and animals. Limited animal data also suggest macrophage-mediated alveolar clearance may also decrease with age. This evidence is briefly paraphrased below.

Ho et al. (2001) demonstrated that nasal mucociliary clearance rates were about 40% lower in old (age >40−90 years) versus young (age 11−40 years) men and women. Tracheal mucus velocities in elderly (or aged) humans and beagle dogs are about 50% that of young adults (Whaley et al., 1987; Goodman et al., 1978). Several human studies have demonstrated decreasing rates of mucociliary particle clearance from the large and small bronchial airways with increasing age (Svartengren et al., 2005; Vastag et al., 1985; Puchelle et al., 1979). Linear fits to the data show that rapid clearance (within 1 hour) from large bronchi and prolonged clearance (between 1−21 days) from the small bronchioles in an 80-year old is only about 50% of that in 20-year old (Svartengren et al., 2005; Vastag et al., 1985). One study reported that alveolar particle clearance rates decreased by nearly 40% in old versus young rats (Muhle et al., 1990). Another study has reported that older rats have an increased susceptibility to pulmonary infection due to altered alveolar macrophage function and slowed bacterial clearance (Antonini et al., 2001). Although data are somewhat limited, they consistently show a depression of clearance throughout the respiratory tract with increasing age from young adulthood in humans and laboratory animals.

4.3.4.2 Sex

Sex was not found to affect clearance rates in prior reviews (U.S. EPA, 2004, 1996). Studies included in the most recent review (U.S. EPA, 2009) also showed that human males and females have similar nasal mucus clearance rates (Ho et al., 2001), tracheal mucus velocities (Yeates et al., 1981), and large bronchial airway clearance rates (Vastag et al., 1985).

4.3.4.3 Respiratory Tract Disease

At the time of the last two reviews (U.S. EPA, 2004, 1996), it was well recognized that obstructive airways disease may influence both the site of initial deposition and the rate of mucociliary clearance from the airways. When deposition patterns are matched, mucociliary clearance rates are reduced in patients with COPD relative to healthy controls. The effects of acute bacterial/viral infections and cough on mucociliary clearance were briefly summarized in Section 10.4.2.5 (U.S. EPA, 1996) and Section 6.3.4.4 (U.S. EPA, 2004) of past reviews. While cough is generally a reaction to some inhaled stimulus, in some cases, especially respiratory disease, it can also serve to clear the upper bronchial airways of deposited substances by dislodging mucus from the airway surface. One of the difficulties in assessing effects on infection on mucociliary clearance is that spontaneous coughing increases during acute infections. Cough has been shown to supplement mucociliary clearance of secretions, especially in patients with obstructive lung disease and primary ciliary dyskinesia.

Using a bolus technique to target specific lung regions, Möller et al. (2008) examined particle clearance from the ciliated airways and alveolar region of healthy subjects, smokers, and patients with COPD. Airway retention after 1.5 hours was significantly lower in healthy subjects (89 ± 6%) than smokers (97 ± 3%) or COPD patients (96 ± 6%). At 24 and 48 hours, retention remained significantly higher in COPD patients (86 ± 6% and 82 ± 6%, respectively) than healthy subjects (75 ± 10% and 70 ± 9%, respectively). However, these findings are confounded by the more central pattern of deposition in the healthy subjects than in the smokers and COPD patients. Alveolar retention of particles was similar between the groups at 48 hours post-inhalation.

The effect of asthma on lung clearance of particles may depend on disease status. Lay et al. (2009) found significantly ($p < 0.01$) more rapid particle (0.22 μm) mucociliary clearance over a 2-hour period post-inhalation in mild asthmatics than in healthy volunteers. Although the pattern of deposition tended to be more central in the asthmatics, there was not a statistically significant difference from healthy controls ($p = 0.24$). The extent of central relative to peripheral airways deposition was well correlated with the lung retention at 2 hours post-inhalation in the subjects with asthma ($r = -0.78$, $p < 0.01$) but not the healthy subjects. In vivo uptake by airway macrophages in mild asthmatics was also enhanced relative to healthy volunteers ($p < 0.01$). In an ex vivo study, airway macrophages from individuals with more severe asthma had impaired phagocytic capacity relative to less severely affect

asthmatics and healthy volunteers (Alexis et al., 2001). Lay et al. (2009) concluded that enhanced uptake and processing of particulate antigens could contribute to the pathogenesis and progression of allergic airways disease in asthmatics and may contribute to an increased risk of exacerbations with particulate exposure.

Chen et al. (2006) investigated the effect of endotoxin on the disposition of particles. Healthy rats and those pretreated with endotoxin (12 hours before particle instillation) were instilled with ultrafine (56.4 nm) or fine (202 nm) particles. In healthy rats, there were no marked differences in lung retention or systemic distribution between the ultrafine and fine particles. In healthy animals, UFPs were primarily retained in lungs (72 ± 10% at 0.5–2 hours; 65 ± 1% at 1 day; 62 ± 5% at 5 days). Particles were also detected in the blood (2 ± 1% at 0.5–2 hours; 0.1 ± 0.1% at 5 days) and liver (3 ± 2% at 0.5–2 hours; 1 ± 0.1% at 5 days) of the healthy animals. At 1-day post-instillation, about 13% of the particles were excreted in the urine or feces of the healthy animals. In rats pretreated with endotoxin, by 2 hours post-instillation, the UFPs accessed the blood (5 vs. 2%) and liver (11 vs. 4%) to a significantly greater extent than fine particles. The endotoxin-treated rats also had significantly greater amounts of UFPs in the blood (5 vs. 2%) and liver (11 vs. 3%) relative to the healthy control rats. This study demonstrates that acute pulmonary inflammation caused by endotoxin increases the migration of UFPs into systemic circulation.

Adamson and Prieditis (1995) investigated the possibility that particle deposition into an already injured lung might affect particle retention and enhance the toxicity of "inert" particles. Bleomycin was instilled into mice to induce epithelial necrosis and subsequent pulmonary fibrosis. Instilled 3 days following bleomycin treatment, while epithelial permeability was compromised, carbon black particles in treated mice were translocated to the inter-stitium and showed increased pulmonary retention relative to untreated mice. When instilled at 4 weeks post bleomycin treatment, after epithelial integrity was restored, carbon black particle retention was similar between treated and untreated mice with minimal translocation to the inter-stitium. The instillation of carbon particles did not appear to increase lung injury in the bleomycin treated mice at either time point. This study shows that integrity of the epithelium affects particle retention and translocation into interstitial tissues.

4.3.4.4 Particle Overload

Unlike other laboratory animals, rats appear susceptible to "particle overload" effects due to impaired macrophage-mediated alveolar clearance. Numerous reviews have discussed this phenomenon and the difficulties it poses for the extrapolation of chronic effects in rats to humans (Oberdorster, 2002; ILRI Risk Science Institute, 2000; Miller, 2000; Oberdorster, 1995; Morrow, 1994). Large mammals have slow pulmonary particle clearance and retain particles in interstitial tissues under normal conditions, whereas rats have rapid pulmonary clearance and retain particles in alveolar macrophages (Snipes, 1996). With chronic high doses of PM there is a shift in the pattern of dust accumulation and response from that

observed at lower doses in rat lungs (Snipes, 1996; Vincent and Donaldson, 1990). Rats chronically exposed to high concentrations of insoluble particles experience a reduction in their alveolar clearance rates and an accumulation of interstitial particle burden (Bermudez et al., 2004; Bermudez et al., 2002; Warheit et al., 1997; Oberdörster et al., 1994a; Oberdörster et al., 1994b; Ferin et al., 1992). With continued exposure, some rats eventually develop pulmonary fibrosis and both benign and malignant tumors (Warheit et al., 1997; Lee et al., 1986; Lee et al., 1985a, b). Oberdorster (2002, 1996) proposed that high-dose effects observed in rats may be associated with two thresholds. The first threshold is the pulmonary dose that results in a reduction in macrophage-mediated clearance. The second threshold, occurring at a higher dose than the first, is the dose at which antioxidant defenses are overwhelmed and pulmonary tumors develop. Intrapulmonary tumors following TiO_2 exposures are exclusive to rats and are not found in mice or hamsters (Mauderly, 1997). Moreover, Lee et al. (1985a) noted that the squamous cell carcinomas observed with prolonged high concentration TiO_2 exposures developed from the alveolar lining cells adjacent to the alveolar ducts, whereas squamous cell carcinomas in humans which are generally linked with cigarette smoking are thought to arise from basal cells of the bronchial epithelium. Quoting Lee et al. (1986), "Since the lung tumors were a unique type of experimentally induced tumor under exaggerated exposure conditions and have not usually been seen in man or animals, their relevance to man in questionable."

4.3.5 Summary

For any given particle size, the pattern of particle deposition influences clearance by partitioning deposited material between regions of the respiratory tract. Particles depositing in the mouth may generally be assumed to be swallowed or removed by expectoration. About 80% of particles deposited in nasal passages and the majority deposited in the tracheobronchial airways move via mucociliary transport towards the nasopharynx and are swallowed. The primary alveolar clearance mechanism of poorly soluble particles is macrophage phagocytosis and migration to terminal bronchioles where the cells are cleared by the mucociliary escalator. Movement of particles into the lymphatics, both as free particles and in macrophages, also contributes to alveolar clearance. Clearance from both the tracheobronchial and alveolar region is more rapid in rodents than humans. Mucociliary and macrophage-mediated clearance decreases with age beyond adulthood.

A small fraction of nanoparticles (≤100 nm) depositing in the alveolar region translocate rapidly (≤1 hour) from the lungs in a size dependent manner. The fraction of nanoparticles translocating from the peripheral lung into circulation is generally low (less than a fraction of a percent) for larger nanoparticles (18−80 nm), but can approach several percent for extremely small particles (1.4−2.8 nm). Particle translocation has not been reported for particles larger than 200 nm. Translocation has now been reported in both a human study as well as numerous animal studies. Of particles found in circulation following delivery to the lung, the majority (~95%) arrive via the lung's air blood barrier with the remainder (~5%) coming from gastrointestinal absorption. These particles are cleared from circulation fairly rapidly (hours

to days) by accumulation predominately in the skeleton, soft tissues, and fat and secondarily by accumulation within the liver and spleen. Particles injected into circulation, however, accumulate predominately within the liver, suggesting a differing protein corona from those derived from the lung and gastrointestinal tract. Following nanoparticle inhalation or ingestion, particles may be identified in the blood out to a month post-delivery. This longer-term presence of particles in the blood is believed to result from continued particle clearance from the lung. Some limited new evidence in rodents suggests a small fraction of nanoparticles may also reach fetuses.

The translocation of particles from the olfactory mucosa via axons to the olfactory bulb has been reported in primates, rodents, and freshwater pike for numerous compounds of varying composition, particle size, and solubility. The rate of translocation is rapid, perhaps less than an hour. Axonal transport of poorly soluble particles is thought to be limited to those under 200 nm in diameter. It is unclear to what extent translocation to the olfactory bulb and other brain regions may occur. The most extensive study of olfactory translocation has been for manganese compounds. For manganese particles, most of the manganese found in brain regions beyond the olfactory bulb is believed to derive from the blood rather than from the olfactory bulb. New particle deposition modeling suggests that deposition on the olfactory mucosa with subsequent translocation to the olfactory bulb may be important in humans as well as rodents.

4.4 References

ACGIH (American Conference of Governmental Industrial Hygienists). (1985). Particle size-selective sampling in the workplace: Report of the ACGIH Technical Committee on Air Sampling Procedures. Cincinnati, OH.

ACGIH (American Conference of Governmental Industrial Hygienists). (2005). TLVs and BEIs: Based on the documentation of the threshold limit values for chemical substances and physical agents and biological exposure indices. Cincinnati, OH. http://www.acgih.org/Resources/press/TLV2005list.htm

Adamson, I; Prieditis, H. (1995). Response of mouse lung to carbon deposition during injury and repair. Environ Health Perspect 103: 72-76.

Albuquerque-Silva, I; Vecellio, L; Durand, M; Avet, J; Le Pennec, D; de Monte, M; Montharu, J; Diot, P; Cottier, M; Dubois, F; Pourchez, J. (2014). Particle deposition in a child respiratory tract model: in vivo regional deposition of fine and ultrafine aerosols in baboons. PLoS ONE 9: e95456. http://dx.doi.org/10.1371/journal.pone.0095456

Alessandrini, F; Semmler-Behnke, M; Jakob, T; Schulz, H; Behrendt, H; Kreyling, W. (2008). Total and regional deposition of ultrafine particles in a mouse model of allergic inflammation of the lung. Inhal Toxicol 20: 585-593. http://dx.doi.org/10.1080/08958370801949167

Alexander, DJ; Collins, CJ; Coombs, DW; Gilkison, IS; Hardy, CJ; Healey, G; Karantabias, G; Johnson, N; Karlsson, A; Kilgour, JD; McDonald, P. (2008). Association of Inhalation Toxicologists (AIT) working party recommendation for standard delivered dose calculation and expression in non-clinical aerosol inhalation toxicology studies with pharmaceuticals. Inhal Toxicol 20: 1179-1189. http://dx.doi.org/10.1080/08958370802207318

Alexis, N; Soukup, J; Nierkens, S; Becker, S. (2001). Association between airway hyperreactivity and bronchial macrophage dysfunction in individuals with mild asthma. Am J Physiol Lung Cell Mol Physiol 280: L369-L375.

Amirav, I; Borojeni, AA; Halamish, A; Newhouse, MT; Golshahi, L. (2014). Nasal versus oral aerosol delivery to the "lungs" in infants and toddlers. Pediatr Pulmonol 50: 276-283. http://dx.doi.org/10.1002/ppul.22999

Amis, TC; Pascoe, JR; Hornof, W. (1984). Topographic distribution of pulmonary ventilation and perfusion in the horse. Am J Vet Res 45: 1597-1601.

Anderson, PJ; Wilson, JD; Hiller, FC. (1990). Respiratory tract deposition of ultrafine particles in subjects with obstructive or restrictive lung disease. Chest 97: 1115-1120.

Anjilvel, S; Asgharian, B. (1995). A multiple-path model of particle deposition in the rat lung. Toxicol Sci 28: 41-50. http://dx.doi.org/10.1006/faat.1995.1144

Anselm, A; Heibel, T; Gebhart, J; Ferron, GA. (1990). In vivo studies of growth factors of sodium chloride particles in the human respiratory tract. J Aerosol Sci 21: S427-430.

Anthony, TR; Flynn, MR. (2006). Computational fluid dynamics investigation of particle inhalability. J Aerosol Sci 37: 750-765.

Antonini, JM; Roberts, JR; Clarke, RW; Yang, HM; Barger, MW; Ma, JYC; Weissman, DN. (2001). Effect of age on respiratory defense mechanisms: pulmonary bacterial clearance in Fischer 344 rats after intratracheal instillation of Listeria monocytogenes. Chest 120: 240-249.

Antonini, JM; Sriram, K; Benkovic, SA; Roberts, J. R.; Stone, S; Chen, BT; Schwegler-Berry, D; Jefferson, AM; Billig, BK; Felton, CM; Hammer, MA; Ma, F; Frazer, DG; O'Callaghan, JP; Miller, DB. (2009). Mild steel welding fume causes manganese accumulation and subtle neuroinflammatory changes but not overt neuronal damage in discrete brain regions of rats after short-term inhalation exposure. Neurotoxicology 30: 915-925. http://dx.doi.org/10.1016/j.neuro.2009.09.006

Asbach, C; Fissan, H; Stahlmecke, B; Kuhlbusch, TAJ; Pui, DYH. (2009). Conceptual limitations and extensions of lung-deposited Nanoparticle Surface Area Monitor (NSAM). J Nanopart Res 11: 101-109. http://dx.doi.org/10.1007/s11051-008-9479-8

Aschner, M; Erikson, KM; Dorman, DC. (2005). Manganese dosimetry: Species differences and implications for neurotoxicity [Review]. Crit Rev Toxicol 35: 1-32. http://dx.doi.org/10.1080/10408440590905920

Asgharian, B; Hofmann, W; Miller, FJ. (2001). Mucociliary clearance of insoluble particles from the tracheobronchial airways of the human lung. J Aerosol Sci 32: 817-832.

Asgharian, B; Kelly, JT; Tewksbury, EW. (2003). Respiratory deposition and inhalability of monodisperse aerosols in Long-Evans rats. Toxicol Sci 71: 104-111. http://dx.doi.org/10.1093/toxsci/71.1.104

Asgharian, B; Price, OT. (2007). Deposition of ultrafine (nano) particles in the human lung. Inhal Toxicol 19: 1045-1054. http://dx.doi.org/10.1080/08958370701626501

Asgharian, B; Price, OT; Oldham, M; Chen, LC; Saunders, EL; Gordon, T; Mikheev, VB; Minard, KR; Teeguarden, JG. (2014). Computational modeling of nanoscale and microscale particle deposition, retention and dosimetry in the mouse respiratory tract. Inhal Toxicol 26: 1-14. http://dx.doi.org/10.3109/08958378.2014.935535

Bailey, M; Dorrian, M; Birchall, A. (1995). Implications of airway retention for radiation doses from inhaled radionuclides. J Aerosol Med 8: 373-390.

Bailey, RS; Casey, KP; Pawar, SS; Garcia, GJ. (2017). Correlation of nasal mucosal temperature with subjective nasal patency in healthy individuals. JAMA Facial Plast Surg 19: 46-52. http://dx.doi.org/10.1001/jamafacial.2016.1445

Balashazy, I; Hofmann, W; Heistracher, T. (1999). Computation of local enhancement factors for the quantification of particle deposition patterns in airway bifurcations. J Aerosol Sci 30: 185-203.

Balasubramanian, SK; Poh, K; Ong, C; Kreyling, WG; Ong, W; Yu, LE. (2013). The effect of primary particle size on biodistribution of inhaled gold nano-agglomerates. Biomaterials 34: 5439-5452. http://dx.doi.org/10.1016/j.biomaterials.2013.03.080

Bastacky, J; Lee, CY; Goerke, J; Koushafar, H; Yager, D; Kenaga, L; Speed, TP; Chen, Y; Clements, JA. (1995). Alveolar lining layer is thin and continuous: Low-temperature scanning electron microscopy of rat lung. J Appl Physiol (1985) 79: 1615-1628.

Becquemin, MH; Swift, DL; Bouchikhi, A; Roy, M; Teillac, A. (1991). Particle deposition and resistance in the noses of adults and children. Eur Respir J 4: 694-702.

Becquemin, MM; Bertholon, JF; Bouchikhi, A; Malarbet, JL; Roy, M. (1999). Oronasal ventilation partitioning in adults and children: Effect on aerosol deposition in airways. Radiat Prot Dosimetry 81: 221-228.

Bennett, W; Messina, M; Smaldone, G. (1985). Effect of exercise on deposition and subsequent retention of inhaled particles. J Appl Physiol (1985) 59: 1046-1054.

Bennett, W; Zeman, K; Jarabek, A. (2003). Nasal contribution to breathing with exercise: Effect of race and gender. J Appl Physiol (1985) 95: 497-503. http://dx.doi.org/10.1152/japplphysiol.00718.2002

Bennett, WD; Brown, JS; Zeman, KL; Hu, SC; Scheuch, G; Sommerer, K. (2002). Targeting delivery of aerosols to different lung regions [Review]. J Aerosol Med 15: 179-188. http://dx.doi.org/10.1089/089426802320282301

Bennett, WD; Zeman, KL. (1998). Deposition of fine particles in children spontaneously breathing at rest. Inhal Toxicol 10: 831-842.

Bennett, WD; Zeman, KL. (2004). Effect of body size on breathing pattern and fine-particle deposition in children. J Appl Physiol (1985) 97: 821-826. http://dx.doi.org/10.1152/japplphysiol.01403.2003

Bennett, WD; Zeman, KL. (2005). Effect of race on fine particle deposition for oral and nasal breathing. Inhal Toxicol 17: 641-648. http://dx.doi.org/10.1080/08958370500188984

Bennett, WD; Zeman, KL; Jarabek, AM. (2008). Nasal contribution to breathing and fine particle deposition in children versus adults. J Toxicol Environ Health A 71: 227-237. http://dx.doi.org/10.1080/15287390701598200

Bennett, WD; Zeman, KL; Kim, C. (1996). Variability of fine particle deposition in healthy adults: effect of age and gender. Am J Respir Crit Care Med 153: 1641-1647.

Bennett, WD; Zeman, KL; Kim, C; Mascarella, J. (1997). Enhanced deposition of fine particles in COPD patients spontaneously breathing at rest. Inhal Toxicol 9: 1-14. http://dx.doi.org/10.1080/089583797198376

Bermudez, E; Mangum, JB; Asgharian, B; Wong, BA; Reverdy, EE; Janszen, DB; Hext, PM; Warheit, DB; Everitt, JI. (2002). Long-term pulmonary responses of three laboratory rodent species to subchronic inhalation of pigmentary titanium dioxide particles. Toxicol Sci 70: 86-97.

Bermudez, E; Mangum, JB; Wong, BA; Asgharian, B; Hext, PM; Warheit, DB; Everitt, JI. (2004). Pulmonary responses of mice, rats, and hamsters to subchronic inhalation of ultrafine titanium dioxide particles. Toxicol Sci 77: 347-357. http://dx.doi.org/10.1093/toxsci/kfh019

Bhaskar, KR; O'Sullivan, DD; Seltzer, J; Rossing, TH; Drazen, JM; Reid, LM. (1985). Density gradient study of bronchial mucus aspirates from healthy volunteers (smokers and nonsmokers) and from patients with tracheostomy. Exp Lung Res 9: 289-308. http://dx.doi.org/10.3109/01902148509057529

Bide, RW; Armour, SJ; Yee, E. (2000). Allometric respiration/body mass data for animals to be used for estimates of inhalation toxicity to young adult humans. J Appl Toxicol 20: 273-290. http://dx.doi.org/10.1002/1099-1263(200007/08)20:4<273::AID-JAT657>3.0.CO;2-X

Bourbon, J; Boucherat, O; Chailley-Heu, B; Delacourt, C. (2005). Control mechanisms of lung alveolar development and their disorders in bronchopulmonary dysplasia [Review]. Pediatr Res 57: 38R-46R. http://dx.doi.org/10.1203/01.PDR.0000159630.35883.BE

Brenneman, KA; Wong, BA; Buccellato, MA; Costa, ER; Gross, EA; Dorman, DC. (2000). Direct olfactory transport of inhaled manganese (54MnCl2) to the rat brain: toxicokinetic investigations in a unilateral nasal occlusion model. Toxicol Appl Pharmacol 169: 238-248. http://dx.doi.org/10.1006/taap.2000.9073

Briant, JK. (1990). Calculation of equivalent aerosol-particle mobility in different mixtures of gases used to study convective-transport in airways. J Aerosol Med 3: 221-232.

Brochu, P; Bouchard, M; Haddad, S. (2014). Physiological daily inhalation rates for health risk assessment in overweight/obese children, adults, and elderly. Risk Anal 34: 567-582. http://dx.doi.org/10.1111/risa.12125

Brochu, P; Brodeur, J; Krishnan, K. (2011). Derivation of physiological inhalation rates in children, adults, and elderly based on nighttime and daytime respiratory parameters. Inhal Toxicol 23: 74-94. http://dx.doi.org/10.3109/08958378.2010.543439

Brown, J; Bennett, W. (2004). Deposition of coarse particles in cystic fibrosis: Model predictions versus experimental results. J Aerosol Med 17: 239-248. http://dx.doi.org/10.1089/jam.2004.17.239

Brown, JS. (2005). Particle inhalability at low wind speeds. Inhal Toxicol 17: 831-837. http://dx.doi.org/10.1080/08958370500241296

Brown, JS. (2015). Deposition of particles. In RA Parent; R Schlesinger; D Costa; D Laksin; G Burleson (Eds.), Comparative biology of the normal lung (2nd ed.). Waltham, Massachusetts: Academic Press. http://store.elsevier.com/Comparative-Biology-of-the-Normal-Lung/isbn-9780124045774/

Brown, JS; Gordon, T; Price, O; Asgharian, B. (2013). Thoracic and respirable particle definitions for human health risk assessment. Part Fibre Toxicol 10: 12. http://dx.doi.org/10.1186/1743-8977-10-12

Brown, JS; Wilson, WE; Grant, LD. (2005). Dosimetric comparisons of particle deposition and retention in rats and humans. Inhal Toxicol 17: 355-385. http://dx.doi.org/10.1080/08958370590929475

Brown, JS; Zeman, KL; Bennett, WD. (2001). Regional deposition of coarse particles and ventilation distribution in healthy subjects and patients with cystic fibrosis. J Aerosol Med Pulm Drug Deliv 14: 443-454. http://dx.doi.org/10.1089/08942680152744659

Brown, JS; Zeman, KL; Bennett, WD. (2002). Ultrafine particle deposition and clearance in the healthy and obstructed lung. Am J Respir Crit Care Med 166: 1240-1247. http://dx.doi.org/10.1164/rccm.00205-399OC

Brundelet, PJ. (1965). Experimental study of the dust-clearance mechanism of the lung: I histological study in rats of the intra-pulmonary bronchial route of elimination. APMIS 175: 1-141.

Burch, WM; Sullivan, PJ; McLaren, CJ. (1986). Technegas--a new ventilation agent for lung scanning. Nucl Med Comm 7: 865-871.

Button, B; Cai, LH; Ehre, C; Kesimer, M; Hill, DB; Sheehan, JK; Boucher, RC; Rubinstein, M. (2012). A periciliary brush promotes the lung health by separating the mucus layer from airway epithelia. Science 337: 937-941. http://dx.doi.org/10.1126/science.1223012

Calderon-Garciduenas, L; Franco-Lira, M; Henriquez-Roldan, C; Osnaya, N; Gonzalez-Maciel, A; Reynoso-Robles, R; Villarreal-Calderon, R; Herritt, L; Brooks, D; Keefe, S; Palacios-Moreno, J; Torres-Jardon, R; Medina-Cortina, H; Delgado-Chavez, R; Aiello-Mora, M; Maronpot, RR; Doty, RL. (2010). Urban air pollution: influences on olfactory function and pathology in exposed children and young adults. Exp Toxicol Pathol 62: 91-102. http://dx.doi.org/10.1016/j.etp.2009.02.117

Calderón-Garcidueñas, L; Serrano-Sierra, A; Torres-Jardón, R; Zhu, H; Yuan, Y; Smith, D; Delgado-Chávez, R; Cross, JV; Medina-Cortina, H; Kavanaugh, M; Guilarte, TR. (2013). The impact of environmental metals in young urbanites' brains. Exp Toxicol Pathol 65: 503-511. http://dx.doi.org/10.1016/j.etp.2012.02.006

CEN (European Committee for Standardization). (1993). Workplace atmospheres-size fraction definitions for measurement of airborne particles. (BS EN 481:1993). London, England: European Committee for Standardization (CEN), British Standards Institute. http://legacy.library.ucsf.edu:8080/i/e/m/iem52d00/Siem52d00.pdf

Chadha, TS; Birch, S; Sackner, MA. (1987). Oronasal distribution of ventilation during exercise in normal subjects and patients with asthma and rhinitis. Chest 92: 1037-1041. http://dx.doi.org/10.1378/chest.92.6.1037

Chamberlain, MJ; Morgan, WK; Vinitski, S. (1983). Factors influencing the regional deposition of inhaled particles in man. Clin Sci (Lond) 64: 69-78.

Chen, J; Tan, M; Nemmar, A; Song, W; Dong, M; Zhang, G; Li, Y. (2006). Quantification of extrapulmonary translocation of intratracheal-instilled particles in vivo in rats: effect of lipopolysaccharide. Toxicology 222: 195-201. http://dx.doi.org/10.1016/j.tox.2006.02.016

Cheng, KH; Cheng, YS; Yeh, HC; Guilmette, RA; Simpson, SQ; Yang, YH; Swift, DL. (1996). In vivo measurements of nasal airway dimensions and ultrafine aerosol deposition in the human nasal and oral airways. J Aerosol Sci 27: 785-801.

Churg, A; Stevens, B; Wright, JL. (1998). Comparison of the uptake of fine and ultrafine TiO2 in a tracheal explant system. Am J Physiol 274: L81-L86.

Clary-Meinesz, C; Mouroux, J; Huitorel, P; Cosson, J; Schoevaert, D; Blaive, B. (1997). Ciliary beat frequency in human bronchi and bronchioles. Chest 111: 692-697. http://dx.doi.org/10.1378/chest.111.3.692

Crouse, U; Laine-Alava, MT; Warren, DW; Wood, CL. (1999). A longitudinal study of nasal airway size from age 9 to age 13. Angle Orthod 69: 413-418.

Cuddihy, RG; Kanapilly, GM; Raabe, OG. (1969). Relationship between particle size and respiratory deposition of 140La-labeled aerosols in the beagle dog. LF-41. 82-87.

Dai, YT; Juang, YJ; Wu, Y; Breysse, PN; Hsu, DJ. (2006). In vivo measurements of inhalability of ultralarge aerosol particles in calm air by humans. J Aerosol Sci 37: 967-973.

De Lorenzo, AJ. (1957). Electron microscopic observations of the olfactory mucosa and olfactory nerve. J Biophys Biochem Cytol 3: 839-850. http://dx.doi.org/10.1083/jcb.3.6.839

de Winter-Sorkina, R; Cassee, FR. (2002). From concentration to dose: Factors influencing airborne particulate matter deposition in humans and rats (pp. 1-36). (RIVM Report 650010031). Bilthoven, Netherlands: National Institute for Public Health and the Environment. http://www.rivm.nl/en/Documents_and_publications/Scientific/Reports/2003/februari/From_concentration_to_dose_factors_influencing_airborne_particulate_matter_deposition_in_humans_and_rats?sp=cml2bXE9ZmFsc2U7c2VhcmNoYmFzZT01MDI5MDtyaXZtcT1mYWxzZTs=&pagenr=5030

DeLorenzo, AJD. (1970). The olfactory neuron and the blood-brain barrier. In GEW Wolstenholme; J Knight (Eds.), Taste and Smell in Vertebrates: A Ciba Foundation symposium (pp. 151-175). London: Churchill Livingstone.

DeLorme, MP; Moss, OR. (2002). Pulmonary function assessment by whole-body plethysmography in restrained versus unrestrained mice. J Pharmacol Toxicol Methods 47: 1-10. http://dx.doi.org/10.1016/S1056-8719(02)00191-0

Dorman, DC; Brenneman, KA; McElveen, AM; Lynch, SE; Roberts, KC; Wong, BA. (2002). Olfactory transport: a direct route of delivery of inhaled manganese phosphate to the rat brain. J Toxicol Environ Health A 65: 1493-1511. http://dx.doi.org/10.1080/00984100290071630

Dorman, DC; McManus, BE; Parkinson, CU; Manuel, CA; McElveen, AM; Everitt, JI. (2004). Nasal toxicity of manganese sulfate and manganese phosphate in young male rats following subchronic (13-week) inhalation exposure. Inhal Toxicol 16: 481-488.

Dunnill, MS. (1962). Postnatal growth of the lung. Thorax 17: 329-333.

Dunster, KR; Friese, M; Fraser, JF; Cowin, GJ; Schibler, A. (2012). Ventilation distribution in rats: Part I--The effect of gas composition as measured with electrical impedance tomography. Biomed Eng Online 11: 64. http://dx.doi.org/10.1186/1475-925X-11-64

Edetsberger, M; Gaubitzer, E; Valic, E; Waigmann, E; Köhler, G. (2005). Detection of nanometer-sized particles in living cells using modern fluorescence fluctuation methods. Biochem Biophys Res Commun 332: 109-116. http://dx.doi.org/10.1016/j.bbrc.2005.04.100

Elder, A; Gelein, R; Silva, V; Feikert, T; Opanashuk, L; Carter, J; Potter, R; Maynard, A; Ito, Y; Finkelstein, J; Oberdorster, G. (2006). Translocation of inhaled ultrafine manganese oxide particles to the central nervous system. Environ Health Perspect 114: 1172-1178. http://dx.doi.org/10.1289/ehp.9030

Endes, S; Schaffner, E; Caviezel, S; Dratva, J; Stolz, D; Schindler, C; Künzli, N; Schmidt-Trucksäss, A; Probst-Hensch, N. (2017). Is physical activity a modifier of the association between air pollution and arterial stiffness in older adults: The SAPALDIA cohort study. Int J Hyg Environ Health 220: 1030-1038. http://dx.doi.org/10.1016/j.ijheh.2017.06.001

Falk, R; Philipson, K; Svartengren, M; Jarvis, N; Bailey, M; Camner, P. (1997). Clearance of particles from small ciliated airways. Exp Lung Res 23: 495-515.

Farkas, A; Balásházy, I. (2008). Quantification of particle deposition in asymmetrical tracheobronchial model geometry. Comput Biol Med 38: 508-518. http://dx.doi.org/10.1016/j.compbiomed.2008.01.014

Farkas, A; Balashazy, I; Szqcs, K. (2006). Characterization of regional and local deposition of inhaled aerosol drugs in the respiratory system by computational fluid and particle dynamics methods. J Aerosol Med 19: 329-343.

Ferin, J; Oberdorster, G; Penney, DP. (1992). Pulmonary retention of ultrafine and fine particles in rats. Am J Respir Cell Mol Biol 6: 535-542. http://dx.doi.org/10.1165/ajrcmb/6.5.535

Ferron, GA; Upadhyay, S; Zimmermann, R; Karg, E. (2013). Model of the deposition of aerosol particles in the respiratory tract of the rat. II. Hygroscopic particle deposition. J Aerosol Med Pulm Drug Deliv 26: 101-119. http://dx.doi.org/10.1089/jamp.2011.0965

Fissan, H; Neumann, S; Trampe, A; Pui, DYH; Shin, WG. (2007). Rationale and principle of an instrument measuring lung deposited nanoparticle surface area. J Nanopart Res 9: 53-59. http://dx.doi.org/10.1007/978-1-4020-5859-2_6

Fleming, S; Thompson, M; Stevens, R; Heneghan, C; Plüddemann, A; Maconochie, I; Tarassenko, L; Mant, D. (2011). Normal ranges of heart rate and respiratory rate in children from birth to 18 years of age: A systematic review of observational studies [Review]. Lancet 377: 1011-1018. http://dx.doi.org/10.1016/S0140-6736(10)62226-X

Garcia, GJ; Kimbell, JS. (2009). Deposition of inhaled nanoparticles in the rat nasal passages: dose to the olfactory region. Inhal Toxicol 21: 1165-1175. http://dx.doi.org/10.3109/08958370902882713

Garcia, GJ; Schroeter, JD; Kimbell, JS. (2015). Olfactory deposition of inhaled nanoparticles in humans. Inhal Toxicol 27: 394-403. http://dx.doi.org/10.3109/08958378.2015.1066904

Garcia, GJM; Tewksbury, EW; Wong, BA; Kimbell, JS. (2009). Interindividual variability in nasal filtration as a function of nasal cavity geometry. J Aerosol Med Pulm Drug Deliv 22: 139-155. http://dx.doi.org/10.1089/jamp.2008.0713

Geiser, M; Rothen-Rutishauser, B; Kapp, N; Schurch, S; Kreyling, W; Schulz, H; Semmler, M; Im Hof, V; Heyder, J; Gehr, P. (2005). Ultrafine particles cross cellular membranes by nonphagocytic mechanisms in lungs and in cultured cells. Environ Health Perspect 113: 1555-1560. http://dx.doi.org/10.1289/ehp.8006

Geiss, O; Bianchi, I; Barrero-Moreno, J. (2016). Lung-deposited surface area concentration measurements in selected occupational and non-occupational environments. J Aerosol Sci 96: 24-37. http://dx.doi.org/10.1016/j.jaerosci.2016.02.007

Geys, J; Coenegrachts, L; Vercammen, J; Engelborghs, Y; Nemmar, A; Nemery, B; Hoet, PHM. (2006). In vitro study of the pulmonary translocation of nanoparticles A preliminary study. Toxicol Lett 160: 218-226. http://dx.doi.org/10.1016/j.toxlet.2005.07.005

Goodman, RM; Yergin, BM; Landa, JF; Golinvaux, MH; Sackner, MA. (1978). Relationship of smoking history and pulmonary function tests to tracheal mucous velocity in nonsmokers, young smokers, ex-smokers, and patients with chronic bronchitis. Am Rev Respir Dis 117: 205-214.

Greenspan, BJ; Morrow, PE; Ferin, J. (1988). Effects of aerosol exposures to cadmium chloride on the clearance of titanium dioxide from the lungs of rats. Exp Lung Res 14: 491-499.

Griff, ER; Greer, CA; Margolis, F; Ennis, M; Shipley, MT. (2000). Ultrastructural characteristics and conduction velocity of olfactory receptor neuron axons in the olfactory marker protein-null mouse. Brain Res 866: 227-236.

Gross, P; Westrick, M. (1954). The permeability of lung parenchyma to particulate matter. Am J Pathol 30: 195-213.

Hankinson, JL; Odencrantz, JR; Fedan, KB. (1999). Spirometric reference values from a sample of the general US population. Am J Respir Crit Care Med 159: 179-187. http://dx.doi.org/10.1164/ajrccm.159.1.9712108

Heistracher, T; Hofmann, W. (1997). Flow and deposition patterns in successive airway bifurcations. Ann Occup Hyg 41: 537-542. http://dx.doi.org/10.1093/annhyg/41.inhaled_particles_VIII.537

Heringa, MB; Peters, RJB; Bleys, RLA, W; van der Lee, MK; Tromp, PC; van Kesteren, PCE; van Eijkeren, JCH; Undas, AK; Oomen, AG; Bouwmeester, H. (2018). Detection of titanium particles in human liver and spleen and possible health implications. Part Fibre Toxicol 15: 15. http://dx.doi.org/10.1186/s12989-018-0251-7

Herring, MJ; Putney, L; Wyatt, G; Finkbeiner, WE; Hyde, DM. (2014). Growth of alveoli during postnatal development in humans based on stereological estimation. Am J Physiol Lung Cell Mol Physiol 307: L338-L344. http://dx.doi.org/10.1152/ajplung.00094.2014

Hinds, W. (1999). Aerosol science and technology. New York: John Wiley and Sons.

Hirn, S; Semmler-Behnke, M; Schleh, C; Wenk, A; Lipka, J; Schäffler, M; Takenaka, S; Möller, W; Schmid, G; Simon, U; Kreyling, WG. (2011). Particle size-dependent and surface charge-dependent biodistribution of gold nanoparticles after intravenous administration. Eur J Pharm Biopharm 77: 407-416. http://dx.doi.org/10.1016/j.ejpb.2010.12.029

Ho, JC; Chan, KN; Hu, WH; Lam, WK; Zheng, L; Tipoe, GL; Sun, J; Leung, R; Tsang, KW. (2001). The effect of aging on nasal mucociliary clearance, beat frequency, and ultrastructure of respiratory cilia. Am J Respir Crit Care Med 163: 983-988.

Hoffman, EA; Ritman, EL. (1985). Effect of body orientation on regional lung expansion in dog and sloth. J Appl Physiol (1985) 59: 481-491.

Hofmann, W; Asgharian, B. (2003). The effect of lung structure on mucociliary clearance and particle retention in human and rat lungs. Toxicol Sci 73: 448-456. http://dx.doi.org/10.1093/toxsci/kfg075

Hofmann, W; Balashazy, I; Heistracher, T; Koblinger, L. (1996). The significance of particle deposition patterns in bronchial airway bifurcations for extrapolation modeling. Aerosol Sci Technol 25: 305-327.

Hofmann, W; Martonen, TB; Graham, RC. (1989). Predicted deposition of nonhygroscopic aerosols in the human lung as a function of subject age. J Aerosol Med 2: 49-68.

Hsu, DJ; Swift, DL. (1999). The measurements of human inhalability of ultralarge aerosols in calm air using mannikins. J Aerosol Sci 30: 1331-1343.

Hyde, DM; Blozis, SA; Avdalovic, MV; Putney, LF; Dettorre, R; Quesenberry, NJ; Singh, P; Tyler, NK. (2007). Alveoli increase in number but not size from birth to adulthood in rhesus monkeys. Am J Physiol Lung Cell Mol Physiol 293: L570-579. http://dx.doi.org/10.1152/ajplung.00467.2006

ICRP (International Commission on Radiological Protection). (1994). Human respiratory tract model for radiological protection: A report of a task group of the International Commission on Radiological Protection. ICRP Publication 66. New York, NY: Pergamon Press.

ICRP (International Commission on Radiological Protection). (2002). Basic anatomical and physiological data for use in radiological protection: Reference values (pp. 1-277). (ICRP Publication 89). New York, NY: Pergamon Press. http://dx.doi.org/10.1016/S0146-6453(03)00002-2

ILRI Risk Science Institute. (2000). The relevance of the rat lung response to particle overload for human risk assessment: A workshop consensus report [Review]. Inhal Toxicol 12: 1-17. http://dx.doi.org/10.1080/08958370050164833

Isawa, T; Teshima, T; Anazawa, Y; Miki, M; Mahmud, AM. (1995). Inhalation of pertechnegas: similar clearance from the lungs to that of inhaled pertechnetate aerosol. Nucl Med Comm 16: 741-746.

ISO (International Organization for Standardization). (2008). Nanotechnologies -- Terminology and definitions for nano-objects -- Nanoparticle, nanofibre and nanoplate. (Technical Specification (TS) 27687). Geneva, Switzerland.

James, DS; Stidley, CA; Lambert, WE; Chick, TW; Mermier, CM; Samet, JM. (1997). Oronasal distribution of ventilation at different ages. Arch Environ Occup Health 52: 118-123. http://dx.doi.org/10.1080/00039899709602874

Janz, A; Köckritz, A; Yao, L; Martin, A. (2010). Fundamental calculations on the surface area determination of supported gold nanoparticles by alkanethiol adsorption. Langmuir 26: 6783-6789. http://dx.doi.org/10.1021/la9041277

Jaques, PA; Kim, CS. (2000). Measurement of total lung deposition of inhaled ultrafine particles in healthy men and women. Inhal Toxicol 12: 715-731.

Jeffers, DE. (2005). Relative magnitudes of the effects of electrostatic image and thermophoretic forces on particles in the respiratory tract. Radiat Prot Dosimetry 113: 189-194. http://dx.doi.org/10.1093/rpd/nch456

Kalmey, JK; Thewissen, JG; Dluzen, DE. (1998). Age-related size reduction of foramina in the cribriform plate. Anat Rec 251: 326-329. http://dx.doi.org/10.1002/(SICI)1097-0185(199807)251:3<326::AID-AR7>3.0.CO;2-T

Kapp, N; Kreyling, W; Schulz, H; Im Hof, V; Gehr, P; Semmler, M; Geiser, M. (2004). Electron energy loss spectroscopy for analysis of inhaled ultrafine particles in rat lungs. Microsc Res Tech 63: 298-305. http://dx.doi.org/10.1002/jemt.20044

Kerr, WJ; McWilliam, JS; Linder-Aronson, S. (1989). Mandibular form and position related to changed mode of breathing--a five-year longitudinal study. Angle Orthod 59: 91-96.

Kim, CS. (2000). Methods of calculating lung delivery and deposition of aerosol particles. Respir Care 45: 695-711.

Kim, CS; Brown, LK; Lewars, GG; Sackner, MA. (1983). Deposition of aerosol particles and flow resistance in mathematical and experimental airway models. J Appl Physiol Respir Environ Exerc Physiol 55: 154-163.

Kim, CS; Hu, S, -C. (2006). Total respiratory tract deposition of fine micrometer-sized particles in healthy adults: empirical equations for sex and breathing pattern. J Appl Physiol (1985) 101: 401-412. http://dx.doi.org/10.1152/japplphysiol.00026.2006

Kim, CS; Hu, SC. (1998). Regional deposition of inhaled particles in human lungs: comparison between men and women. J Appl Physiol (1985) 84: 1834-1844.

Kim, CS; Iglesias, AJ. (1989). Deposition of inhaled particles in bifurcating airway models: I. Inspiratory deposition. J Aerosol Med 2: 1-14.

Kim, CS; Jaques, PA. (2000). Respiratory dose of inhaled ultrafine particles in healthy adults. Philos Transact A Math Phys Eng Sci 358: 2693-2705. http://dx.doi.org/10.1098/rsta.2000.0678

Kim, CS; Kang, TC. (1997). Comparative measurement of lung deposition of inhaled fine particles in normal subjects and patients with obstructive airway disease. Am J Respir Crit Care Med 155: 899-905.

Kim, J; Xi, J; Si, X; Berlinski, A; Su, WC. (2014). Hood nebulization: effects of head direction and breathing mode on particle inhalability and deposition in a 7-month-old infant model. J Aerosol Med Pulm Drug Deliv 27: 209-218. http://dx.doi.org/10.1089/jamp.2013.1051

Kimbell, JS. (2006). Nasal dosimetry of inhaled gases and particles: Where do inhaled agents go in the nose? Toxicol Pathol 34: 270-273. http://dx.doi.org/10.1080/01926230600695607

King, GG; Eberl, S; Salome, CM; Young, IH; Woolcock, AJ. (1998). Differences in airway closure between normal and asthmatic subjects measured with single-photon emission computed tomography and technegas. Am J Respir Crit Care Med 158: 1900-1906. http://dx.doi.org/10.1164/ajrccm.158.6.9608027

Kreyling, WG. (1992). Intracellular particle dissolution in alveolar macrophages. Environ Health Perspect 97: 121-126.

Kreyling, WG. (2016). Discovery of unique and ENM- specific pathophysiologic pathways: Comparison of the translocation of inhaled iridium nanoparticles from nasal epithelium versus alveolar epithelium towards the brain of rats. Toxicol Appl Pharmacol 299: 41-46. http://dx.doi.org/10.1016/j.taap.2016.02.004

Kreyling, WG; Blanchard, JD; Godleski, JJ; Haeussermann, S; Heyder, J; Hutzler, P; Schulz, H; Sweeney, TD; Takenaka, S; Ziesenis, A. (1999). Anatomic localization of 24- and 96-h particle retention in canine airways. J Appl Physiol (1985) 87: 269-284.

Kreyling, WG; Hirn, S; Möller, W; Schleh, C; Wenk, A; Celik, G; Lipka, J; Schäffler, M; Haberl, N; Johnston, BD; Sperling, R; Schmid, G; Simon, U; Parak, WJ; Semmler-Behnke, M. (2014). Air-blood barrier translocation of tracheally instilled gold nanoparticles inversely depends on particle size. ACS Nano 8: 222-233. http://dx.doi.org/10.1021/nn403256v

Kreyling, WG; Holzwarth, U; Haberl, N; Kozempel, J; Hirn, S; Wenk, A; Schleh, C; Schäffler, M; Lipka, J; Semmler-Behnke, M; Gibson, N. (2017a). Quantitative biokinetics of titanium dioxide nanoparticles after intravenous injection in rats: Part 1. Nanotoxicology 11: 434-442. http://dx.doi.org/10.1080/17435390.2017.1306892

Kreyling, WG; Holzwarth, U; Haberl, N; Kozempel, J; Wenk, A; Hirn, S; Schleh, C; Schäffler, M; Lipka, J; Semmler-Behnke, M; Gibson, N. (2017b). Quantitative biokinetics of titanium dioxide nanoparticles after intratracheal instillation in rats: Part 3. Nanotoxicology 11: 454-464. http://dx.doi.org/10.1080/17435390.2017.1306894

Kreyling, WG; Holzwarth, U; Schleh, C; Kozempel, J; Wenk, A; Haberl, N; Hirn, S; Schäffler, M; Lipka, J; Semmler-Behnke, M; Gibson, N. (2017c). Quantitative biokinetics of titanium dioxide nanoparticles after oral application in rats: Part 2. Nanotoxicology 11: 443-453. http://dx.doi.org/10.1080/17435390.2017.1306893

Kreyling, WG; Scheuch, G. (2000). Clearance of particles deposited in the lungs. In P Gehr; J Heyder (Eds.), Particle-lung Interactions (pp. 323-376). New York, NY: Marcel Dekker, Inc.

Kreyling, WG; Semmler-Behnke, M; Seitz, J; Scymczak, W; Wenk, A; Mayer, P; Takenaka, S; Oberdörster, G. (2009). Size dependence of the translocation of inhaled iridium and carbon nanoparticle aggregates from the lung of rats to the blood and secondary target organs. Inhal Toxicol 21 Suppl 1: 55-60. http://dx.doi.org/10.1080/08958370902942517

Kreyling, WG; Semmler, M; Erbe, F; Mayer, P; Takenaka, S; Schulz, H; Oberdorster, G; Ziesenis, A. (2002). Translocation of ultrafine insoluble iridium particles from lung epithelium to extrapulmonary organs is size dependent but very low. J Toxicol Environ Health A 65: 1513-1530. http://dx.doi.org/10.1080/00984100290071649

Kuehl, PJ; Anderson, TL; Candelaria, G; Gershman, B; Harlin, K; Hesterman, JY; Holmes, T; Hoppin, J; Lackas, C; Norenberg, JP; Yu, H; McDonald, JD. (2012). Regional particle size dependent deposition of inhaled aerosols in rats and mice. Inhal Toxicol 24: 27-35. http://dx.doi.org/10.3109/08958378.2011.632787

Kuuluvainen, H; Ronkko, T; Jarvinen, A; Saari, S; Karjalainen, P; Lande, T; Pirjola, L; Niemi, JV; Hillamo, R; Keskinen, J. (2016). Lung deposited surface area size distributions of particulate matter in different urban areas. Atmos Environ 136: 105-113. http://dx.doi.org/10.1016/j.atmosenv.2016.04.019

Lay, J; Alexis, N; Zeman, K; Peden, D; Bennett, W. (2009). In vivo uptake of inhaled particles by airway phagocytes is enhanced in patients with mild asthma compared with normal volunteers. Thorax 64: 313-320. http://dx.doi.org/10.1136/thx.2008.096222

Leavens, TL; Reo, D; Andersen, ME; Dorman, DC. (2007). Evaluating transport of manganese from olfactory mucosa to striatum by pharmacokinetic modeling. Toxicol Sci 97: 265-278. http://dx.doi.org/10.1093/toxsci/kfm061

Lee, KP; III, HN; Trochimowicz, HJ; Reinhardt, CF. (1986). Pulmonary response to impaired lung clearance in rats following excessive TiO2 dust deposition. Environ Res 41: 144-167.

Lee, KP; Trochimowicz, HJ; Reinhardt, CF. (1985a). Pulmonary response of rats exposed to titanium dioxide (TiO2) by inhalation for two years. Toxicol Appl Pharmacol 79: 179-192. http://dx.doi.org/10.1016/0041-008X(85)90339-4

Lee, KP; Trochimowicz, HJ; Reinhardt, CF. (1985b). Transmigration of titanium dioxide (TiO2) particles in rats after inhalation exposure. Exp Mol Pathol 42: 331-343.

Leiberman, A; Ohki, M; Forte, V; Fraschetti, J; Cole, P. (1990). Nose/mouth distribution of respiratory airflow in 'mouth breathing' children. Acta Otolaryngol 109: 454-460. http://dx.doi.org/10.3109/00016489009125169

Leiter, JC; Baker, GL. (1989). Partitioning of ventilation between nose and mouth: The role of nasal resistance. Am J Orthod Dentofacial Orthop 95: 432-438. http://dx.doi.org/10.1016/0889-5406(89)90305-3

Lewin, G; Hurtt, ME. (2017). Pre- and postnatal lung development: An updated species comparison [Review]. Birth Defects Res 109: 1519-1539. http://dx.doi.org/10.1002/bdr2.1089

Lewis, J; Bench, G; Myers, O; Tinner, B; Staines, W; Barr, E; Divine, KK; Barrington, W; Karlsson, J. (2005). Trigeminal uptake and clearance of inhaled manganese chloride in rats and mice. Neurotoxicology 26: 113-123.

Lindemann, J; Leiacker, R; Rettinger, G; Keck, T. (2002). Nasal mucosal temperature during respiration. Clin Otolaryngol Allied Sci 27: 135-139.

Löndahl, J; Massling, A; Pagels, J; Swietlicki, E; Vaclavik, E; Loft, S. (2007). Size-resolved respiratory-tract deposition of fine and ultrafine hydrophobic and hygroscopic aerosol particles during rest and exercise. Inhal Toxicol 19: 109-116. http://dx.doi.org/10.1080/08958370601051677

Maher, BA; Ahmed, IA; Karloukovski, V; MacLaren, DA; Foulds, PG; Allsop, D; Mann, DM; Torres-Jardón, R; Calderon-Garciduenas, L. (2016). Magnetite pollution nanoparticles in the human brain. Proc Natl Acad Sci USA 113: 10797-10801. http://dx.doi.org/10.1073/pnas.1605941113

Martonen, TB; Yang, Y; Xue, ZQ. (1994). Effects of carinal ridge shapes on lung airstreams. Aerosol Sci Technol 21: 119-136. http://dx.doi.org/10.1080/02786829408959702

Mauderly, JL. (1979). Effect of age on pulmonary structure and function of immature and adult animals and man. FASEB J 38: 173-177.

Mauderly, JL. (1997). Relevance of particle-induced rat lung tumors for assessing lung carcinogenic hazard and human lung cancer risk [Review]. Environ Health Perspect 105 (Suppl 5): 1337-1346.

Mauderly, JL; Kritchevsky, J. (1979). Respiration of unsedated Fischer 344 rats and the effect of confinement in exposure tubes. In Inhalation Toxicology Research Institute annual report 1978-1979 (pp. 475-478). (LMF-69). Albuquerque, NM: U.S. Department of Energy, Lovelace Biomedical and Environmental Research Institute.

Mcdonnell, WF; Stewart, PW; Smith, MV; Kim, CS; Schelegle, ES. (2012). Prediction of lung function response for populations exposed to a wide range of ozone conditions. Inhal Toxicol 24: 619-633. http://dx.doi.org/10.3109/08958378.2012.705919

Ménache, MG; Miller, FJ; Raabe, OG. (1995). Particle inhalability curves for humans and small laboratory animals. Ann Occup Hyg 39: 317-328.

Mendez, LB; Gookin, G; Phalen, RF. (2010). Inhaled aerosol particle dosimetry in mice: A review [Review]. Inhal Toxicol 22: 15-20. http://dx.doi.org/10.3109/08958378.2010.541337

Milic-Emili, J; Henderson, JAM; Dolovich, MB; Trop, D; Kaneko, K. (1966). Regional distribution of inspired gas in the lung. J Appl Physiol (1985) 21: 749-759.

Miller, FJ. (2000). Dosimetry of particles in laboratory animals and humans in relationship to issues surrounding lung overload and human health risk assessment: a critical review [Review]. Inhal Toxicol 12: 19-57. http://dx.doi.org/10.1080/089583700196536

Miller, FJ; Asgharian, B; Schroeter, JD; Price, O. (2016). Improvements and additions to the Multiple Path Particle Dosimetry model. J Aerosol Sci 99: 14-26. http://dx.doi.org/10.1016/j.jaerosci.2016.01.018

Miller, FJ; Asgharian, B; Schroeter, JD; Price, O; Corley, RA; Einstein, DR; Jacob, RE; Cox, TC; Kabilan, S; Bentley, T. (2014). Respiratory tract lung geometry and dosimetry model for male Sprague-Dawley rats. Inhal Toxicol 26: 524-544. http://dx.doi.org/10.3109/08958378.2014.925991

Miller, FJ; Gardner, DE; Graham, JA; Lee, RE, Jr; Wilson, WE; Bachmann, JD. (1979). Size considerations for establishing a standard for inhalable particles. J Air Waste Manag Assoc 29: 610-615.

Miller, MR; Raftis, JB; Langrish, JP; McLean, SG; Samutrtai, P; Connell, SP; Wilson, S; Vesey, AT; Fokkens, PHB; Boere, AJF; Krystek, P; Campbell, CJ; Hadoke, PWF; Donaldson, K; Cassee, FR; Newby, DE; Duffin, R; Mills, NL. (2017). Inhaled nanoparticles accumulate at sites of vascular disease. ACS Nano 11: 4542-4552. http://dx.doi.org/10.1021/acsnano.6b08551

Mills, NL; Amin, N; Robinson, SD; Anand, A; Davies, J; Patel, D; de la Fuente, JM; Cassee, FR; Boon, NA; Macnee, W; Millar, AM; Donaldson, K; Newby, DE. (2006). Do inhaled carbon nanoparticles translocate directly into the circulation in humans? Am J Respir Crit Care Med 173: 426-431. http://dx.doi.org/10.1164/rccm.200506-865OC

Miserocchi, G; Sancini, G; Mantegazza, F; Chiappino, G. (2008). Translocation pathways for inhaled asbestos fibers [Review]. Environ Health 7: 4. http://dx.doi.org/10.1186/1476-069X-7-4

Mohammadipour, A; Fazel, A; Haghir, H; Motejaded, F; Rafatpanah, H; Zabihi, H; Hosseini, M; Bideskan, AE. (2014). Maternal exposure to titanium dioxide nanoparticles during pregnancy; impaired memory and decreased hippocampal cell proliferation in rat offspring. Environ Toxicol Pharmacol 37: 617-625. http://dx.doi.org/10.1016/j.etap.2014.01.014

Möller, W; Felten, K; Sommerer, K; Scheuch, G; Meyer, G; Meyer, P; Haussinger, K; Kreyling, WG. (2008). Deposition, retention, and translocation of ultrafine particles from the central airways and lung periphery. Am J Respir Crit Care Med 177: 426-432. http://dx.doi.org/10.1164/rccm.200602-301OC

Möller, W; Haussinger, K; Winkler-Heil, R; Stahlhofen, W; Meyer, T; Hofmann, W; Heyder, J. (2004). Mucociliary and long-term particle clearance in the airways of healthy nonsmoker subjects. J Appl Physiol (1985) 97: 2200-2206.

Möller, W; Meyer, G; Scheuch, G; Kreyling, WG; Bennett, WD. (2009). Left-to-right asymmetry of aerosol deposition after shallow bolus inhalation depends on lung ventilation. J Aerosol Med Pulm Drug Deliv 22: 333-339. http://dx.doi.org/10.1089/jamp.2009.0749

Monaghan, P; Provan, I; Murray, C; Mackey, DW; Van der Wall, H; Walker, BM; Jones, PD. (1991). An improved radionuclide technique for the detection of altered pulmonary permeability. J Nucl Med 32: 1945-1949.

Morgan, W; Ahmad, D; Chamberlain, M; Clague, H; Pearson, M; Vinitski, S. (1984). The effect of exercise on the deposition of an inhaled aerosol. Respir Physiol 56: 327-338.

Morrow, PE. (1994). Mechanisms and significance of "particle overload". In U Mohr (Ed.), Toxic and Carcinogenic Effects of Solid Particles in the Respiratory Tract (pp. 17-25). Washington, DC: ILSI Press.

Muhle, H; Creutzenberg, O; Bellmann, B; Heinrich, U; Mermelstein, R. (1990). Dust overloading of lungs: investigations of various materials, species differences, and irreversibility of effects. J Aerosol Med 1: S111-S128.

Narayanan, M; Owers-Bradley, J; Beardsmore, CS; Mada, M; Ball, I; Garipov, R; Panesar, KS; Kuehni, CE; Spycher, B; Williams, SE; Silverman, M. (2012). Alveolarization continues during childhood and adolescence: New evidence from helium-3 magnetic resonance. Am J Respir Crit Care Med 185: 186-191. http://dx.doi.org/10.1164/rccm.201107-1348OC

Ng, AW; Bidani, A; Heming, TA. (2004). Innate host defense of the lung: effects of lung-lining fluid pH [Review]. Lung 182: 297-317. http://dx.doi.org/10.1007/s00408-004-2511-6

Niinimaa, V; Cole, P; Mintz, S; Shephard, RJ. (1981). Oronasal distribution of respiratory airflow. Respir Physiol 43: 69-75. http://dx.doi.org/10.1016/0034-5687(81)90089-X

Nikula, KJ; Vallyathan, V; Green, FHY; Hahn, FF. (2001). Influence of exposure concentration or dose on the distribution of particulate material in rat and human lungs. Environ Health Perspect 109: 311-318.

NRPB (National Radiological Protection Board (UK)). (2004). Particle deposition in the vicinity of power lines and possible effects on health: Report of an independent advisory group on non-ionising radiation and its ad hoc group on corona ions. Oxfordshire, England: National Radiological Protection Board.

O'Riordan, TG; Iacono, A; Keenan, RJ; Duncan, S. R.; Burckart, GJ; Griffith, BP; Smaldone, GC. (1995). Delivery and distribution of aerosolized cyclosporine in lung allograft recipients. Am J Respir Crit Care Med 151: 516-521. http://dx.doi.org/10.1164/ajrccm.151.2.7842214

O'Riordan, TG; Smaldone, GC. (1994). Regional deposition and regional ventilation during inhalation of pentamidine. Chest 105: 396-401. http://dx.doi.org/10.1378/chest.105.2.396

Oberdorster, G. (1995). Lung particle overload: implications for occupational exposures to particles [Review]. Regul Toxicol Pharmacol 27: 123-135. http://dx.doi.org/10.1006/rtph.1995.1017

Oberdorster, G. (1996). Significance of particle parameters in the evaluation of exposure-dose-response relationships of inhaled particles [Review]. Inhal Toxicol 8 Supplement: 73-89. http://dx.doi.org/10.1080/02726359608906690

Oberdorster, G. (2002). Toxicokinetics and effects of fibrous and nonfibrous particles [Review]. Inhal Toxicol 14: 29-56. http://dx.doi.org/10.1080/089583701753338622

Oberdörster, G. (1988). Lung clearance of inhaled insoluble and soluble particles. J Aerosol Med 1: 289-330.

Oberdörster, G; Ferin, J; Gelein, R; Soderholm, SC; Finkelstein, J. (1992). Role of the alveolar macrophage in lung injury: Studies with ultrafine particles. Environ Health Perspect 97: 193-199.

Oberdörster, G; Ferin, J; Lehnert, BE. (1994a). Correlation between particle size, in vivo particle persistence, and lung injury. Environ Health Perspect 102: 173-179.

Oberdörster, G; Ferin, J; Soderholm, S; Gelein, R; Cox, C; Baggs, R; Morrow, PE. (1994b). Increased pulmonary toxicity of inhaled ultrafine particles: due to lung overload alone? Ann Occup Hyg 38: 295-302.

Oberdorster, G; Finkelstein, JN; Johnston, C; Gelein, R; Cox, C; Baggs, R; Elder, ACP. (2000). Acute pulmonary effects of ultrafine particles in rats and mice. (Report Number 96). Boston: Health Effects Institute.

Oberdörster, G; Kuhlbusch, TAJ. (2018). In vivo effects: Methodologies and biokinetics of inhaled nanomaterials [Review]. NanoImpact 10: 38-60. http://dx.doi.org/10.1016/j.impact.2017.10.007

Olvera, HA; Perez, D; Clague, JW; Cheng, YS; Li, WW; Amaya, MA; Burchiel, SW; Berwick, M; Pingitore, NE. (2012). The effect of ventilation, age, and asthmatic condition on ultrafine particle deposition in children. Pulm Med 2012: 736290. http://dx.doi.org/10.1155/2012/736290

Pan, Y; Neuss, S; Leifert, A; Fischler, M; Wen, F; Simon, U; Schmid, G; Brandau, W; Jahnen-Dechent, W. (2007). Size-dependent cytotoxicity of gold nanoparticles. Small 3: 1941-1949.

Peters, TM; Vanderpool, RW; Wiener, RW. (2001). Design and calibration of the EPA PM25 well impactor ninety-six (WINS). Aerosol Sci Technol 34: 389-397.

Phalen, RF; Oldham, MJ. (1983). Tracheobronchial airway structure as revealed by casting techniques. Am Rev Respir Dis 128: S1-S4.

Phalen, RF; Oldham, MJ; Wolff, RK. (2008). The relevance of animal models for aerosol studies [Review]. J Aerosol Med Pulm Drug Deliv 21: 113-124. http://dx.doi.org/10.1089/jamp.2007.0673

Piccione, G; Caola, G; Mortola, JP. (2005). Scaling the daily oscillations of breathing frequency and skin temperature in mammals. Comp Biochem Physiol A Mol Integr Physiol 140: 477-486. http://dx.doi.org/10.1016/j.cbpb.2005.02.010

Plattig, KH. (1989). Electrophysiology of taste and smell [Review]. Clin Phys Physiol Meas 10: 91-126. http://dx.doi.org/10.1088/0143-0815/10/2/001

Puchelle, E; Zahm, JM; Bertrand, A. (1979). Influence of age on bronchial mucociliary transport. Scand J Respir Dis 60: 307-313.

Raabe, OG; Al-Bayati, MA; Teague, SV; Rasolt, A. (1988). Regional deposition of inhaled monodisperse, coarse, and fine aerosol particles in small laboratory animals. In Inhaled particles VI: Proceedings of an international symposium and workshop on lung dosimetry. Cambridge, U.K.: Pergamon Press.

Rissler, J; Gudmundsson, A; Nicklasson, H; Swietlicki, E; Wollmer, P; Löndahl, J. (2017a). Deposition efficiency of inhaled particles (15-5000nm) related to breathing pattern and lung function: an experimental study in healthy children and adults. Part Fibre Toxicol 14: Article #10. http://dx.doi.org/10.1186/s12989-017-0190-8

Rissler, J; Gudmundsson, A; Nicklasson, H; Swietlicki, E; Wollmer, P; Löndahl, J. (2017b). Supplement: Deposition efficiency of inhaled particles (15-5000nm) related to breathing pattern and lung function: an experimental study in healthy children and adults. Part Fibre Toxicol 14: 10.

Rooney, D; Friese, M; Fraser, JF; Dunster, KR; Schibler, A. (2009). Gravity-dependent ventilation distribution in rats measured with electrical impedance tomography. Physiol Meas 30: 1075-1085. http://dx.doi.org/10.1088/0967-3334/30/10/008

Roth, C; Kreyling, WG; Scheuch, G; Busch, B; Stahlhofen, W. (1997). Deposition and clearance of fine particles in the human respiratory tract. Ann Occup Hyg 41: 503-508.

Roth, C; Scheuch, G; Stahlhofen, W. (1993). Clearance of the human lungs for ultrafine particles. J Aerosol Sci 24: S95-S96. http://dx.doi.org/10.1016/0021-8502

Roth, C; Scheuch, G; Stahlhofen, W. (1994). Clearance measurements with radioactively labelled ultrafine particles. Ann Occup Hyg 38: 101-106.

Sá, RC; Zeman, KL; Bennett, WD; Prisk, GK; Darquenne, C. (2017). Regional ventilation is the main determinant of alveolar deposition of coarse particles in the supine healthy human lung during tidal breathing. J Aerosol Med Pulm Drug Deliv 30: 322-331. http://dx.doi.org/10.1089/jamp.2016.1336

Scheuch, G; Gebhart, J; Roth, C. (1990). Uptake of electrical charges in the human respiratory tract during exposure to air loaded with negative ions. J Aerosol Sci 21: S439-S442.

Schleh, C; Semmler-Behnke, M; Lipka, J; Wenk, A; Hirn, S; Schäffler, M; Schmid, G; Simon, U; Kreyling, WG. (2012). Size and surface charge of gold nanoparticles determine absorption across intestinal barriers and accumulation in secondary target organs after oral administration. Nanotoxicology 6: 36-46. http://dx.doi.org/10.3109/17435390.2011.552811

Schramel, J; Nagel, C; Auer, U; Palm, F; Aurich, C; Moens, Y. (2012). Distribution of ventilation in pregnant Shetland ponies measured by Electrical Impedance Tomography. Respir Physiol Neurobiol 180: 258-262. http://dx.doi.org/10.1016/j.resp.2011.11.018

Schroeter, JD; Tewksbury, EW; Wong, BA; Kimbell, JS. (2015). Experimental measurements and computational predictions of regional particle deposition in a sectional nasal model. J Aerosol Med Pulm Drug Deliv 28: 20-29. http://dx.doi.org/10.1089/jamp.2013.1084

Schwab, RJ; Kim, C; Bagchi, S; Keenan, BT; Comyn, FL; Wang, S; Tapia, IE; Huang, S; Traylor, J; Torigian, DA; Bradford, RM; Marcus, CL. (2015). Understanding the anatomic basis for obstructive sleep apnea syndrome in adolescents. Am J Respir Crit Care Med 191: 1295-1309. http://dx.doi.org/10.1164/rccm.201501-0169OC

Semmler-Behnke, M; Lipka, J; Wenk, A; Hirn, S; Schaeffler, M; Tian, F; Schmid, G; Oberdoerster, G; Kreyling, WG. (2014). Size dependent translocation and fetal accumulation of gold nanoparticles from maternal blood in the rat. Part Fibre Toxicol 11: 33. http://dx.doi.org/10.1186/s12989-014-0033-9

Semmler-Behnke, M; Takenaka, S; Fertsch, S; Wenk, A; Seitz, J; Mayer, P; Oberdörster, G; Kreyling, WG. (2007). Efficient elimination of inhaled nanoparticles from the alveolar region: evidence for interstitial uptake and subsequent reentrainment onto airways epithelium. Environ Health Perspect 115: 728-733. http://dx.doi.org/10.1289/ehp.9685

Semmler, M; Seitz, J; Erbe, F; Mayer, P; Heyder, J; Oberdorster, G; Kreyling, WG. (2004). Long-term clearance kinetics of inhaled ultrafine insoluble iridium particles from the rat lung, including transient translocation into secondary organs. Inhal Toxicol 16: 453-459. http://dx.doi.org/10.1080/08958370490439650

Smaldone, GC; Fuhrer, J; Steigbigel, RT; McPeck, M. (1991). Factors determining pulmonary deposition of aerosolized pentamidine in patients with human immunodeficiency virus infection. Am Rev Respir Dis 143: 727-737. http://dx.doi.org/10.1164/ajrccm/143.4_Pt_1.727

Smith, JR; Bailey, MR; Etherington, G; Shutt, AL; Youngman, MJ. (2008). Effect of particle size on slow particle clearance from the bronchial tree. Exp Lung Res 34: 287-312. http://dx.doi.org/10.1080/01902140802093196

Smith, JR; Bailey, MR; Etherington, G; Shutt, AL; Youngman, MJ. (2011). An experimental study of clearance of inhaled particles from the human nose. Exp Lung Res 37: 109-129. http://dx.doi.org/10.3109/01902148.2010.518301

Smith, JR; Birchall, A; Etherington, G; Ishigure, N; Bailey, MR. (2014). A revised model for the deposition and clearance of inhaled particles in human extra-thoracic airways. Radiat Prot Dosimetry 158: 135-147. http://dx.doi.org/10.1093/rpd/nct218

Snipes, MB. (1996). Current information on lung overload in nonrodent mammals: contrast with rats. Inhal Toxicol 8: 91-109.

Snipes, MB; Boecker, BB; McClellan, RO. (1983). Retention of monodisperse or polydisperse aluminosilicate particles inhaled by dogs, rats, and mice. Toxicol Appl Pharmacol 69: 345-362.

Snipes, MB; Harkema, JR; Hotchkiss, JA; Bice, DE. (1997). Neutrophil involvement in the retention and clearance of dust intratracheally instilled into the lungs of F344/N rats. Exp Lung Res 23: 65-84.

Soderholm, SC. (1985). Size-selective sampling criterial for inspirable mass fraction. In Particle size-selective sampling in the workplace : report of the ACGIH Technical Committee on Air Sampling Procedures. Cincinnati, Ohio: American Conference of Governmental Industrial Hygienists.

Song, Y; Namkung, W; Nielson, DW; Lee, JW; Finkbeiner, WE; Verkman, AS. (2009). Airway surface liquid depth measured in ex vivo fragments of pig and human trachea: Dependence on Na+ and Cl- channel function. Am J Physiol Lung Cell Mol Physiol 297: L1131-L1140. http://dx.doi.org/10.1152/ajplung.00085.2009

Soppa, VJ; Schins, RPF; Hennig, F; Nieuwenhuijsen, MJ; Hellack, B; Quass, U; Kaminski, H; Sasse, B; Shinnawi, S; Kuhlbusch, TAJ; Hoffmann, B. (2017). Arterial blood pressure responses to short-term exposure to fine and ultrafine particles from indoor sources - A randomized sham-controlled exposure study of healthy volunteers. Environ Res 158: 225-232. http://dx.doi.org/10.1016/j.envres.2017.06.006

Sousa, SR; Moradas-Ferreira, P; Saramango, B; Viseu, ML; Barbosa, MA. (2004). Human serum albumin adsorption on TiO2 from single protein solutions and from plasma. Langmuir 20: 9745-9754. http://dx.doi.org/10.1021/la049158d

Stober, W; McClellan, RO. (1997). Pulmonary retention and clearance of inhaled biopersistent aerosol particles: data-reducing interpolation models and models of physiologically based systems - a review of recent progress and remaining problems [Review]. Crit Rev Toxicol 27: 539-598.

Stone, KC; Mercer, RR; Gehr, P; Stockstill, B; Crapo, JD. (1992). Allometric relationships of cell numbers and size in the mammalian lung. Am J Respir Cell Mol Biol 6: 235-243. http://dx.doi.org/10.1165/ajrcmb/6.2.235

Suga, K; Nishigauchi, K; Kume, N; Koike, S; Takano, K; Matsunaga, N. (1995). Regional ventilatory evaluation using dynamic SPET imaging of xenon-133 washout in obstructive lung disease: an initial study. Eur J Nucl Med 22: 220-226. http://dx.doi.org/10.1007/BF01081516

Susskind, H; Brill, AB; Harold, WH. (1986). Quantitative comparison of regional distributions of inhaled Tc-99m DTPA aerosol and Kr-81m gas in coal miners' lungs. Am J Physiol Imaging 1: 67-76.

Svartengren, M; Falk, R; Philipson, K. (2005). Long-term clearance from small airways decreases with age. Eur Respir J 26: 609-615.

Tabachnik, E; Muller, N; Toye, B; Levison, H. (1981). Measurement of ventilation in children using the respiratory inductive plethysmograph. J Pediatr 99: 895-899.

Takenaka, S; Dornhofer-Takenaka, H; Muhle, H. (1986). Alveolar distribution of fly ash and of titanium dioxide after long-term inhalation by Wistar rats. J Aerosol Sci 17: 361-364.

Takenaka, S; Karg, E; Kreyling, W; Lentner, B; Möller, W; Behnke-Semmler, M; Jennen, L; Walch, A; Michalke, B; Schramel, P. (2006). Distribution pattern of inhaled ultrafine gold particles in the rat lung. Inhal Toxicol 18: 733-740. http://dx.doi.org/10.1080/08958370600748281

Takezawa, J; Miller, FJ; O'Neil, JJ. (1980). Single-breath diffusing capacity and lung volumes in small laboratory mammals. J Appl Physiol (1985) 48: 1052-1059.

Thurlbeck, WM. (1982). Postnatal human lung growth. Thorax 37: 564-571. http://dx.doi.org/10.1136/thx.37.8.564

Tobin, MJ; Chadha, TS; Jenouri, G; Birch, SJ; Gazeroglu, HB; Sackner, MA. (1983a). Breathing patterns. 1. Normal subjects. Chest 84: 202-205. http://dx.doi.org/10.1378/chest.84.2.202

Tobin, MJ; Chadha, TS; Jenouri, G; Birch, SJ; Gazeroglu, HB; Sackner, MA. (1983b). Breathing patterns. 2. Diseased subjects. Chest 84: 286-294.

Todea, AM; Beckmann, S; Kaminski, H; Asbach, C. (2015). Accuracy of electrical aerosol sensors measuring lung deposited surface area concentrations. J Aerosol Sci 89: 96-109. http://dx.doi.org/10.1016/j.jaerosci.2015.07.003

Trajan, M; Logus, JW; Enns, EG; Man, SF. (1984). Relationship between regional ventilation and aerosol deposition in tidal breathing. Am Rev Respir Dis 130: 64-70. http://dx.doi.org/10.1164/arrd.1984.130.1.64

Tran, CL; Buchanan, D; Cullen, RT; Searl, A; Jones, AD; Donaldson, K. (2000). Inhalation of poorly soluble particles: II. Influence of particle surface area on inflammation and clearance. Inhal Toxicol 12: 1113-1126. http://dx.doi.org/10.1080/08958370050166796

Tsyganova, NA; Khairullin, RM; Terentyuk, GS; Khlebtsov, BN; Bogatyrev, VA; Dykman, LA; Erykov, SN; Khlebtsov, NG. (2014). Penetration of pegylated gold nanoparticles through rat placental barrier. Bull Exp Biol Med 157: 383-385. http://dx.doi.org/10.1007/s10517-014-2572-3

Tu, KW; Knutson, EO. (1984). Total deposition of ultrafine hydrophobic and hygroscopic aerosols in the human respiratory system. Aerosol Sci Technol 3: 453-465.

U.S. EPA (U.S. Environmental Protection Agency). (1982). Air quality criteria for particulate matter and sulfur oxides (final, 1982) [EPA Report]. (EPA 600/8-82/029a). Washington, DC: Environmental Criteria and Assessment Office. http://cfpub.epa.gov/ncea/cfm/recordisplay.cfm?deid=46205

U.S. EPA (U.S. Environmental Protection Agency). (1996). Air quality criteria for particulate matter, volume 1 of 3 [EPA Report]. (EPA/600/P-95/001aF). Washington, DC.

U.S. EPA (U.S. Environmental Protection Agency). (1997). National ambient air quality standards for particulate matter; final rule. Fed Reg 62: 38652-38752.

U.S. EPA (U.S. Environmental Protection Agency). (2004). Air quality criteria for particulate matter [EPA Report]. (EPA/600/P-99/002aF-bF). Research Triangle Park, NC: U.S. Environmental Protection Agency, Office of Research and Development, National Center for Environemntal Assessment- RTP Office. http://cfpub.epa.gov/ncea/cfm/recordisplay.cfm?deid=87903

U.S. EPA (U.S. Environmental Protection Agency). (2009). Integrated science assessment for particulate matter [EPA Report]. (EPA/600/R-08/139F). Research Triangle Park, NC: U.S. Environmental Protection Agency, Office of Research and Development, National Center for Environmental Assessment- RTP Division. http://cfpub.epa.gov/ncea/cfm/recordisplay.cfm?deid=216546

U.S. EPA (U.S. Environmental Protection Agency). (2011). Exposure factors handbook: 2011 edition (final) [EPA Report]. (EPA/600/R-090/052F). Washington, DC: U.S. Environmental Protection Agency, Office of Research and Development, National Center for Environmental Assessment. http://cfpub.epa.gov/ncea/cfm/recordisplay.cfm?deid=236252

Valberg, P; Brain, J; Sneddon, S; LeMott, S. (1982). Breathing patterns influence aerosol deposition sites in excised dog lungs. J Appl Physiol (1985) 53: 824-837.

Van As, A. (1977). Pulmonary airway clearance mechanisms: A reappraisal [Editorial]. Am Rev Respir Dis 115: 721-726.

Vastag, E; Matthys, H; Kohler, D; Gronbeck, L; Daikeler, G. (1985). Mucociliary clearance and airways obstruction in smokers, ex-smokers and normal subjects who never smoked. Eur J Respir Dis 139: 93-100.

Verbanck, S; Ghorbaniasl, G; Biddiscombe, MF; Dragojlovic, D; Ricks, N; Lacor, C; Ilsen, B; de Mey, J; Schuermans, D; Underwood, SR; Barnes, PJ; Vincken, W; Usmani, OS. (2016). Inhaled aerosol distribution in human airways: A scintigraphy-guided study in a 3d printed model. J Aerosol Med Pulm Drug Deliv 29: 525-533. http://dx.doi.org/10.1089/jamp.2016.1291

Vig, PS; Zajac, DJ. (1993). Age and gender effects on nasal respiratory function in normal subjects. Cleft Palate Craniofac J 30: 279-284. http://dx.doi.org/10.1597/1545-1569(1993)030<0279:AAGEON>2.3.CO;2

Vincent, JH; Donaldson, K. (1990). A dosimetric approach for relating the biological response of the lung to the accumulation of inhaled mineral dust. Br J Ind Med 47: 302-307.

Warheit, DB; Hansen, JF; Yuen, IS; Kelly, DP; Snajdr, SI; Hartsky, MA. (1997). Inhalation of high concentrations of low toxicity dusts in rats results in impaired pulmonary clearance mechanisms and persistent inflammation. Toxicol Appl Pharmacol 145: 10-22. http://dx.doi.org/10.1006/taap.1997.8102

Warheit, DB; Webb, TR; Sayes, CM; Colvin, VL; Reed, KL. (2006). Pulmonary instillation studies with nanoscale TiO2 rods and dots in rats: Toxicity is not dependent upon particle size and surface area. Toxicol Sci 91: 227-236. http://dx.doi.org/10.1093/toxsci/kfj140

Warren, DW; Hairfield, WM; Dalston, ET. (1990). Effect of age on nasal cross-sectional area and respiratory mode in children. Laryngoscope 100: 89-93. http://dx.doi.org/10.1288/00005537-199001000-00018

Whaley, SL; Muggenburg, BA; Seiler, FA; Wolff, RK. (1987). Effect of aging on tracheal mucociliary clearance in beagle dogs. J Appl Physiol (1985) 62: 1331-1334.

Widdicombe, JH. (2002). Regulation of the depth and composition of airway surface liquid [Review]. J Anat 201: 313-318. http://dx.doi.org/10.1046/j.1469-7580.2002.00098.x

Widdicombe, JH; Widdicombe, JG. (1995). Regulation of human airway surface liquid [Review]. Respir Physiol 99: 3-12. http://dx.doi.org/10.1016/0034-5687(94)00095-H

Wiebert, P; Sanchez-Crespo, A; Falk, R; Philipson, K; Lundin, A; Larsson, S; Möller, W; Kreyling, W; Svartengren, M. (2006a). No significant translocation of inhaled 35-nm carbon particles to the circulation in humans. Inhal Toxicol 18: 741-747. http://dx.doi.org/10.1080/08958370600748455

Wiebert, P; Sanchez-Crespo, A; Seitz, J; Falk, R; Philipson, K; Kreyling, WG; Moller, W; Sommerer, K; Larsson, S; Svartengren, M. (2006b). Negligible clearance of ultrafine particles retained in healthy and affected human lungs. Eur Respir J 28: 286-290. http://dx.doi.org/10.1183/09031936.06.00103805

Xi, J; Berlinski, A; Zhou, Y, ue; Greenberg, B; Ou, X. (2012). Breathing Resistance and Ultrafine Particle Deposition in Nasal-Laryngeal Airways of a Newborn, an Infant, a Child, and an Adult. Ann Biomed Eng 40: 2579-2595. http://dx.doi.org/10.1007/s10439-012-0603-7

Xi, J; Si, X; Zhou, Y; Kim, J; Berlinski, A. (2014). Growth of nasal and laryngeal airways in children: implications in breathing and inhaled aerosol dynamics. Respir Care 59: 263-273. http://dx.doi.org/10.4187/respcare.02568

Yaghi, A; Zaman, A; Cox, G; Dolovich, MB. (2012). Ciliary beating is depressed in nasal cilia from chronic obstructive pulmonary disease subjects. Respir Med 106: 1139-1147. http://dx.doi.org/10.1016/j.rmed.2012.04.001

Yang, H; Du, L; Tian, X; Fan, Z; Sun, C; Liu, Y; Keelan, JA; Nie, G. (2014). Effects of nanoparticle size and gestational age on maternal biodistribution and toxicity of gold nanoparticles in pregnant mice. Toxicol Lett 230: 10-18. http://dx.doi.org/10.1016/j.toxlet.2014.07.030

Yeates, DB; Gerrity, TR; Garrard, CS. (1981). Particle deposition and clearance in the bronchial tree. Ann Biomed Eng 9: 577-592. http://dx.doi.org/10.1007/BF02364772

Yeh, HC. (1980). Respiratory tract deposition models: Final report. Albuquerque, NM: Inhalation Toxicology Research Institute, Lovelace Biomedical and Environmental Research Institute.

Yu, CP. (1985). Theories of electrostatic lung deposition of inhaled aerosols. Ann Occup Hyg 29: 219-227.

Zeidler-Erdely, PC; Calhoun, WJ; Ameredes, BT; Clark, MP; Deye, GJ; Baron, P; Jones, W; Blake, T; Castranova, V. (2006). In vitro cytotoxicity of Manville Code 100 glass fibers: Effect of fiber length on human alveolar macrophages. Part Fibre Toxicol 28: 3:5.

Zhao, X; Ju, Y; Liu, C; Li, J; Huang, M; Sun, J; Wang, T. (2009). Bronchial anatomy of left lung: a study of multi-detector row CT. Surg Rad Anat 31: 85-91. http://dx.doi.org/10.1007/s00276-008-0404-8

Zhou, Y; Guo, M; Xi, J; Irshad, H; Cheng, YS. (2014). Nasal deposition in infants and children. J Aerosol Med Pulm Drug Deliv 27: 110-116. http://dx.doi.org/10.1089/jamp.2013.1039

Zhou, Y, ue; Xi, J; Simpson, J; Irshad, H; Cheng, YS. (2013). Aerosol deposition in a nasopharyngolaryngeal replica of a 5-year-old child. Aerosol Sci Technol 47: 275-282. http://dx.doi.org/10.1080/02786826.2012.749341

Zierenberg, B. (1999). Optimizing the in vitro performance of Respimat [Review]. J Aerosol Med 12: S19-S24. http://dx.doi.org/10.1089/jam.1999.12.Suppl_1.S-19

CHAPTER 5 RESPIRATORY EFFECTS

Summary of Causality Determinations for Short- and Long-Term Particulate Matter (PM) Exposure and Respiratory Effects

This chapter characterizes the scientific evidence that supports causality determinations for short- and long-term PM exposure and respiratory effects. The types of studies evaluated within this chapter are consistent with the overall scope of the ISA as detailed in the Preface (see Section 11P.3.1). In assessing the overall evidence, strengths and limitations of individual studies were evaluated based on scientific considerations detailed in the Appendix. The evidence presented throughout this chapter support the following causality determinations. More details on the causal framework used to reach these conclusions are included in the Preamble to the ISA (U.S. EPA, 2015).

Size Fraction	Causality Determinations
Short-term exposure	
$PM_{2.5}$	Likely to be causal
$PM_{10-2.5}$	Suggestive of, but not sufficient to infer
UFP	Suggestive of, but not sufficient to infer
Long-term exposure	
$PM_{2.5}$	Likely to be causal
$PM_{10-2.5}$	Inadequate
UFP	Inadequate

5.1 Short-Term $PM_{2.5}$ Exposure and Respiratory Effects

The 2009 PM ISA (U.S. EPA, 2009) concluded that a "causal relationship is likely to exist" between short-term $PM_{2.5}$ exposure and respiratory effects (U.S. EPA, 2009).[55] This conclusion was based mainly on epidemiologic evidence demonstrating associations between short-term $PM_{2.5}$ exposure and various respiratory effects. The more limited evidence from controlled human exposure and animal toxicological studies provided coherence and biological plausibility for a subset of respiratory effects for which $PM_{2.5}$-related associations were observed in epidemiologic studies. In addition, the 2009 PM ISA described epidemiologic evidence as consistently showing $PM_{2.5}$-associated increases in hospital

[55] As detailed in the Preface, risk estimates are for a 10 $\mu g/m^3$ increase in 24-hour average $PM_{2.5}$ concentrations unless otherwise noted.

admissions and emergency department (ED) visits for chronic obstructive pulmonary disease (COPD) and respiratory infection among adults or people of all ages, as well as increases in respiratory mortality. Epidemiologic evidence was inconsistent for hospital admissions or ED visits for asthma but supported associations with increased respiratory symptoms and decreases in lung function in children with asthma. Studies examining copollutant models showed that $PM_{2.5}$ associations with respiratory effects were robust to inclusion of CO or SO_2 in the model, but often were attenuated with inclusion of O_3 or NO_2. Evidence supporting an independent effect of $PM_{2.5}$ exposure on the respiratory system was provided by animal toxicological studies of $PM_{2.5}$ concentrated ambient particles (CAPs) demonstrating changes in some pulmonary function parameters, as well as inflammation, oxidative stress, injury, enhanced allergic responses, and reduced host defenses. Many of these effects have been implicated in the pathophysiology for asthma exacerbation, COPD exacerbation, or respiratory infection. Some of these effects were also observed with diesel exhaust (DE) or woodsmoke exposures; however, there was no attempt to attribute the effect to the particulate or gaseous components of the mixture. In the few controlled human exposure studies conducted in individuals with asthma or COPD, $PM_{2.5}$ exposure mostly had no effect on respiratory symptoms, lung function, or pulmonary inflammation. Short-term $PM_{2.5}$ exposure was not clearly related to respiratory effects in healthy people. Evidence integrated across scientific disciplines linked respiratory effects to several $PM_{2.5}$ components such as elemental carbon/black carbon (EC/BC), organic carbon (OC), and metals and $PM_{2.5}$ sources such as wildfires and traffic. However, there were few studies on any given component or source, and disparate outcomes were examined across studies and disciplines, complicating the overall interpretation of results. As a result, the 2009 PM ISA did not make a conclusion with respect to PM sources and components specifically for respiratory effects, but broadly concluded that "many [components] of PM can be linked with differing health effects and the evidence is not yet sufficient to allow differentiation of those components or sources that are more closely related to specific health outcomes" (U.S. EPA, 2009).

The following section on short-term $PM_{2.5}$ exposure and respiratory effects opens with a discussion of biological plausibility (Section 5.1.1) that provides background for the subsequent sections in which groups of related endpoints are presented in the context of relevant disease pathways. The organization of sections by outcome group aims to clearly characterize the extent of coherence among related endpoints (e.g., hospital admissions, symptoms, inflammation) and biological plausibility of $PM_{2.5}$ effects. These outcome groups include asthma exacerbation (Section 5.1.2), COPD exacerbation (Section 5.1.4), respiratory infection (Section 5.1.5), combinations of respiratory-related disease hospital admissions and ED visits (Section 5.1.6), and respiratory mortality (Section 5.1.9). New to this ISA are distinct discussions of allergy exacerbation (Section 5.1.3), respiratory effects in healthy populations (Section 5.1.7), and respiratory effects in populations with cardiovascular disease (Section 5.1.8). Section 5.1.10 comprises an integrated discussion of policy-relevant considerations across the epidemiologic studies evaluated within Section 5.1. The evaluation of whether there is evidence of differential associations by various $PM_{2.5}$ components and sources, compared to $PM_{2.5}$ mass, is detailed in Section 5.1.11.

5.1.1 Biological Plausibility

This section describes biological pathways that potentially underlie respiratory health effects resulting from short-term exposure to $PM_{2.5}$. Figure 5-1 graphically depicts the proposed pathways as a continuum of upstream events, connected by arrows, that may lead to downstream events observed in epidemiologic studies. This discussion of "how" short-term exposure to $PM_{2.5}$ may lead to respiratory health effects contributes to an understanding of the biological plausibility of epidemiologic results evaluated later in Section 5.1.

Once $PM_{2.5}$ deposits in the respiratory tract, it may be retained, cleared, or solubilized (see CHAPTER 4). Insoluble and soluble components of $PM_{2.5}$ may interact with cells in the respiratory tract, such as epithelial cells, inflammatory cells, and sensory nerve cells. One way in which this may occur is through reduction-oxidative (redox) reactions. As discussed in Section 2.3.3, PM may generate reactive oxygen species (ROS) and this capacity is termed "oxidative potential." Furthermore, cells in the respiratory tract may respond to the presence of PM by generating ROS. Further discussion of these redox reactions, which may contribute to oxidative stress, is found in Section 5.1.1 of the 2009 PM ISA (U.S. EPA, 2009). In addition, poorly soluble particles may translocate to the interstitial space beneath the respiratory epithelium and accumulate in the lymph nodes (see CHAPTER 4). Immune system responses due to the presence of particles in the interstitial space may contribute to respiratory health effects.

Evidence that short-term exposure to $PM_{2.5}$ may affect the respiratory tract generally informs two proposed pathways (Figure 5-1). The first pathway begins with injury, inflammation, and oxidative stress responses, which are difficult to disentangle. Inflammation generally occurs as a consequence of injury and oxidative stress, but it can also lead to further oxidative stress and injury due to secondary production of ROS by inflammatory cells. The second pathway begins with the activation of sensory nerves in the respiratory tract that can trigger local reflex responses and transmit signals to regions of the central nervous system that regulate autonomic outflow.

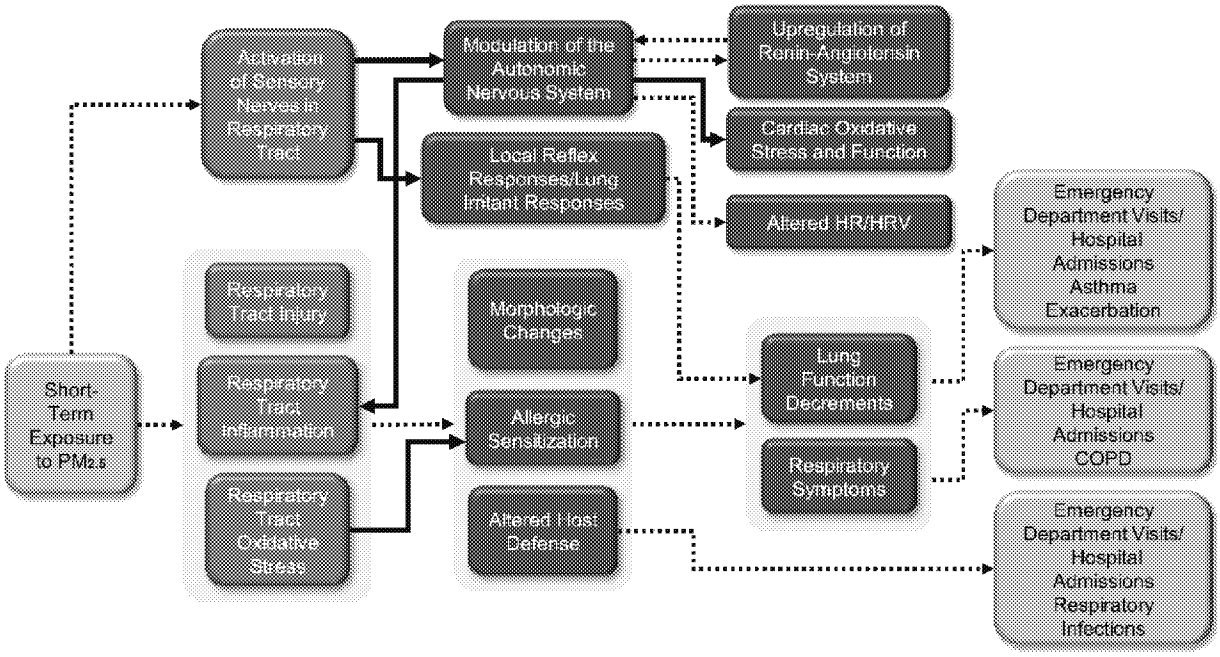

Note: The boxes above represent the effects for which there is experimental or epidemiologic evidence, and the dotted arrows indicate a proposed relationship between those effects. Solid arrows denote direct evidence of the relationship as provided, for example, by an inhibitor of the pathway or a genetic knock-out model used in an experimental study. Shading around multiple boxes denotes relationships between groups of upstream and downstream effects. Progression of effects is depicted from left to right and color-coded (gray, exposure; green, initial event; blue, intermediate event; orange, apical event). Here, apical events generally reflect results of epidemiologic studies, which often observe effects at the population level. Epidemiologic evidence may also contribute to upstream boxes. When there are gaps in the evidence, there are complementary gaps in the figure and the accompanying text below.

Figure 5-1 Potential biological pathways for respiratory effects following short-term $PM_{2.5}$ exposure.

Injury, Inflammation, and Oxidative Stress

Regarding the first pathway, a large body of evidence from controlled human exposure (Section 5.1.7.2) and animal toxicological studies (Section 5.1.7.3 and Section 5.1.8) found injury, inflammation, and oxidative stress responses in healthy individuals and animals. These responses are highly variable. In studies involving concentrated ambient particles (CAPs) exposure, variability may be due to differences in concentration and sources of $PM_{2.5}$ present in the airshed. Multiday exposures generally resulted in more robust responses than exposures of a few hours. Some studies in humans and animals that examined markers in bronchoalveolar lavage fluid (BALF) found increased numbers of macrophages and neutrophils. Animal toxicological studies examining responses in lung tissue found markers of injury and oxidative stress, such as increased lung water and protein carbonyl content (Rhoden et al., 2004; Gurgueira et al., 2002), and markers of inflammation such as recruitment of macrophage populations (Xu et al., 2013). Other studies found evidence of mild morphologic changes, such as hyperplasia of the bronchoalveolar duct (Batalha et al., 2002) and changes in the mucus content of the nasal epithelium (Yoshizaki et al., 2016), that could be downstream effects of inflammation following

inhalation of $PM_{2.5}$. Inflammation may lead to other downstream effects, such as lung function decrements. A decrease in maximal mid-expiratory flow coupled with a decrease in oxygen saturation, possibly indicating dysfunction of small peripheral airways, was observed in healthy humans following inhalation of $PM_{2.5}$ (Gong et al., 2005). It is not clear whether the decrement in lung function seen in this study was due to inflammation or to autonomic nervous system (ANS) responses, which are discussed below.

Some experimental evidence focuses on respiratory responses in specific disease states, such as asthma and COPD, in which inflammation is known to play an important role. In animal models of allergic airway disease, which share many phenotypic features with asthma in humans, short-term exposure to $PM_{2.5}$ led to morphologic changes due to allergic responses and airway remodeling (Section 5.1.2.4). These morphologic changes could lead to lung function decrements and respiratory symptoms, both of which are associated with $PM_{2.5}$ concentrations in epidemiologic panel studies of humans with asthma (Section 5.1.2.2 and Section 0). Further, evidence from epidemiologic panel studies in children with asthma linked $PM_{2.5}$ concentrations to the inflammatory marker leukotriene E4, asthma symptoms, medication use (Section 5.1.2.2 and Section 5.1.2.4) and decrements in lung function (Section 0). Overall, these results provide plausibility for epidemiologic findings of hospital admissions and ED visits for asthma (Section 5.1.2.1).

Injury and inflammatory responses to inhaled CAPs were more robust in animal models of COPD than in healthy animals (Saldiva et al., 2002; Kodavanti et al., 2000; Clarke et al., 1999). Lung function-related changes in oxygen saturation, FEV_1, and tidal volume were seen in controlled human exposure studies involving human subjects with COPD and in animal models of COPD following short-term exposure to $PM_{2.5}$ (Gong et al., 2005; Saldiva et al., 2002; Clarke et al., 1999) and provide plausibility for epidemiologic findings of exacerbation of COPD (Section 5.1.4). Whether these COPD-related changes in lung function were due to inflammation or to ANS responses, which are discussed below, is not clear.

In animal toxicological studies, inhalation of $PM_{2.5}$ resulted in additional effects on the immune system subsequent to respiratory tract inflammation and oxidative stress. Allergic sensitization occurred in one study using diesel exhaust particles (DEPs) (Whitekus et al., 2002). It was blocked by treatment with antioxidants (depicted by the solid line connecting oxidative stress and allergic sensitization in Figure 5-1), indicating a role for oxidative stress in mediating the response. Allergic sensitization is an early step in the development of an allergic phenotype, which could contribute to both lung function decrements and respiratory symptoms. Another study found altered macrophage function and increased susceptibility to an infectious following inhalation of CAPs (Zelikoff et al., 2003). This demonstration of impaired host defense provides plausibility for epidemiologic findings of respiratory infection (Section 5.2.6).

Activation of Sensory Nerves

Regarding the second pathway, activation of sensory nerves, animal toxicological studies described in the previous ISA and later in this chapter demonstrated changes in respiratory rate and lung volumes (i.e., rapid, shallow breathing) (Section 5.1.7 and Section 5.1.8). These responses are characteristic of lung irritant responses. Activation of sensory nerves in the respiratory tract can trigger local reflex responses resulting in lung irritation. Evidence that lung irritant responses are mediated by parasympathetic pathways involving the vagus nerve is provided by a study in which DEPs were intra-tracheally instilled into a rodent (Mcqueen et al., 2007) (depicted as a solid line connecting activation of sensory nerves and local reflex responses in Figure 5-1). In this study, pretreatment with atropine, an inhibitor of parasympathetic pathways, and vagotomy, which involves severing of the vagus nerve, blocked the irritant response to DEP. Lung irritation serves as an adaptive response to a noxious chemical that can potentially decrease exposure to that chemical. While some studies in humans and animals involving inhalation of $PM_{2.5}$ found FEV_1 changes, it is not clear whether this effect was mediated by lung irritant responses or by inflammation.

Activation of sensory nerves in the respiratory tract can also transmit signals to regions of the central nervous system that regulate autonomic outflow and influence all the internal organs, including the heart. Involvement of specific receptors on the sensory nerves, the transient receptor potential (TRP) sensory nerve receptors, was demonstrated by (Ghelfi et al., 2008), since TRP antagonists blocked downstream effects of exposure to $PM_{2.5}$ on the heart (depicted by the solid line connecting activation of sensory nerves and cardiac oxidative stress and function in Figure 5-1). In this study, modulation of the ANS resulted in altered autonomic outflow, which was manifest as a change in heart rate (see Section 8.1.1 and Section 6.1.1).

Furthermore, studies suggest connections between $PM_{2.5}$-mediated modulation of the ANS and other effects. A study in mice found that short-term exposure to $PM_{2.5}$ increased sympathetic nervous system (SNS) activity, as indicated by increased norepinephrine levels in lung and brown adipose tissue (Chiarella et al., 2014). Furthermore, inhalation of $PM_{2.5}$ increased BALF cytokine levels, an effect which was enhanced by β_2 adrenergic receptor agonists, which mimic the actions of norepinephrine. Using knock-out mice lacking the β_2 adrenergic receptor specifically in alveolar macrophage, it was demonstrated that inhalation of $PM_{2.5}$ enhanced cytokine release from alveolar macrophages. This involvement of the SNS in $PM_{2.5}$-mediated inflammatory responses is depicted by the solid line connecting modulation of the ANS and respiratory tract inflammation in Figure 5-1. The SNS is one arm of the ANS (the other arm being the parasympathetic nervous system). This is likely to represent a positive feed-back mechanism by which ANS responses may enhance inflammation. Another study found upregulation of the renin-angiotensin system (RAS), as indicated by an increase in mRNA for angiotensin receptor Type 1 and angiotensin converting enzyme, in the lung (Aztatzi-Aguilar et al., 2015). Angiotensin receptor Type 1 mediates the effects of angiotensin II, which is a potent vasoconstrictor and mediator in the vasculature. The SNS and the RAS are known to interact in a positive feedback fashion

(Section 8.1.2) with important ramifications in the cardiovascular system. However, it is not known whether SNS activation or some other mechanism mediated the changes in the RAS observed in the respiratory tract in this study.

Summary

As described here, there are two proposed pathways by which short-term exposure to $PM_{2.5}$ may lead to respiratory health effects. One pathway involves respiratory tract injury, inflammation, and oxidative stress that may lead to morphologic changes and lung function decrements, which are linked to asthma and COPD exacerbations. Respiratory tract inflammation may also lead to altered host defense, which is linked to increased respiratory infections. The second pathway involves the activation of sensory nerves in the respiratory tract leading to lung function decrements, which are linked to asthma and COPD exacerbations. While experimental studies involving animals or human subjects contribute most of the evidence of upstream effects, epidemiologic studies found associations between exposure to $PM_{2.5}$ and both respiratory tract inflammation and lung function decrements. Together, these proposed pathways provide biological plausibility for epidemiologic evidence of respiratory health effects and will be used to inform a causality determination, which is discussed later in the chapter (Section 5.1.12).

5.1.2 Asthma Exacerbation

Asthma is a chronic inflammatory lung disease characterized by reversible airway obstruction and increased airway responsiveness. Exacerbation of disease is associated with symptoms such as wheeze, cough, chest tightness, and shortness of breath. Symptoms may be treated with asthma medication, and uncontrollable symptoms may lead to seeking medical treatment. Previous findings linking short-term $PM_{2.5}$ exposure to asthma exacerbation, particularly from epidemiologic studies of children, comprised one line of evidence informing the determination of a likely to be causal relationship with respiratory effects. Some incoherence was noted in the evidence for children with asthma in that $PM_{2.5}$ concentrations were associated with respiratory symptoms and lung function decrements but inconsistently and imprecisely associated with hospital admissions and ED visits for asthma. However, the main uncertainty was whether $PM_{2.5}$ exposure had an effect independent of correlated copollutants. In the few epidemiologic studies that examined copollutant confounding, $PM_{2.5}$ associations with asthma-related effects did not always persist in models that included O_3, NO_2, CO, or SO_2. Further, in the 2009 PM ISA, coherence between evidence for allergic responses and epidemiologic findings for asthma exacerbation was not assessed for short-term $PM_{2.5}$ exposure. In controlled human exposure and animal toxicological studies, short-term $PM_{2.5}$ exposure induced allergic inflammation, which is part of the pathophysiology for allergic asthma. Allergic asthma is the most common asthmatic phenotype in children, and allergic inflammation could link $PM_{2.5}$ exposure and asthma exacerbation.

In characterizing the current state of the evidence, this section begins by considering the effects of short-term exposure to $PM_{2.5}$ on clinical indicators of asthma exacerbation (i.e., hospital admissions, ED visits, and physician visits for asthma) and then considers respiratory symptoms and asthma medication use in people with asthma. The evaluation follows with a consideration of the effects of short-term exposure to $PM_{2.5}$ on lung function, which may indicate airway obstruction and poorer control of asthma. The last section describes the evidence for subclinical effects such as pulmonary inflammation and oxidative stress resulting from short-term exposure to $PM_{2.5}$.

In addition to examining the relationship between short-term $PM_{2.5}$ exposure and asthma exacerbation, some epidemiologic studies often conduct analyses to assess whether the associations observed are due to chance, confounding, or other biases. As such, this evidence across epidemiologic studies is not discussed within this section, but evaluated in an integrative manner and focuses specifically on those analyses that address policy-relevant issues (Section 5.1.10), and includes evaluations of copollutant confounding (Section 5.1.10.1), model specification (Section 0), lag structure (Section 5.1.10.3), the role of season and temperature on $PM_{2.5}$ associations (Section 5.1.10.4), averaging time of $PM_{2.5}$ concentrations (Section 5.1.10.5), and concentration-response (C-R) and threshold analyses (Section 5.1.10.6). The studies that inform these issues and evaluated within these sections are primarily epidemiologic studies that conducted time-series or case-crossover analyses examining asthma hospital admissions and ED visits.

5.1.2.1 Hospital Admissions and Emergency Department (ED) Visits

The 2009 PM ISA reported inconsistent evidence of associations between short-term increases in $PM_{2.5}$ concentration and hospital admissions and ED visits for asthma in children, but generally consistent positive associations in studies focusing on adults and people of all ages combined (U.S. EPA, 2009). However, the evaluation of results from studies conducted in populations of children is complicated by the difficulty in reliably diagnosing asthma in children <5 years of age because young children often have transient wheeze (NAEPP, 2007). The inclusion of children <5 years of age may add some uncertainty to the results of studies focusing on all children, but the few studies that presented results in children older than 5 years did indicate $PM_{2.5}$-associated increases in asthma hospital admissions and ED visits. The examination of potential copollutant confounding was not thoroughly considered by the studies evaluated in the 2009 PM ISA but provided some evidence that $PM_{2.5}$-asthma hospital admission and ED visit associations are robust to the inclusion of gaseous pollutants in copollutant models. Across studies, associations were observed for a range of lags, with evidence that risk estimates for asthma hospital admissions and ED visits increased in magnitude for longer or cumulative lags.

Asthma hospital admissions and ED visit studies are evaluated separately because only a small percentage of asthma ED visits result in a hospital admission. As a result, asthma ED visits may represent less severe outcomes compared to asthma hospital admissions. For each of the studies evaluated in this